III. CHAPTER 3

Lymphomas associated with aberrant DNA rearrangements are suppressed by Mre11 mutation

Cheryl Jacobs Smith[1], Jeffrey Xie[2], and JoAnn M. Sekiguchi[1,3]

[1]Department of Human Genetics, [2]University of Michigan, [3]Internal Medicine, University of Michigan Medical School, Ann Arbor, MI 48109, USA

Smith (Jacobs) contribution: Figures 3.1-3.6; 3.10 Supplementary figures 3S11-3S16

In preparation

Abstract

A large number of lymphoid malignancies are characterized by specific chromosomal translocations, which are closely linked to the initial steps of pathogenesis. The hallmark of translocations that occur in lymphoid malignancies such as Burkitt's lymphoma, is the ectopic activation of a proto-oncogene through its relocation at the vicinity of an active regulatory element. Due to the unique feature of lymphoid cells to somatically rearrange and mutate antigen receptor genes, and to the corresponding strong activity of the immune enhancers/promoters at that stage of cell development, B- and T-cell differentiation represent propitious targets for chromosomal translocations and oncogene activation.

A specific lymphoid rearrangement, V(D)J recombination, utilizes the cNHEJ pathway to facilitate somatic rearrangements between numerous V, D, and J gene segments to create a V(D)J exon that expresses the variable region of the antigen receptor. Mutations in cNHEJ genes can alter the fate of DSBs and lead to chromosomal instability, including oncogenic translocations. Indeed, mouse models harboring inactivating mutations in *Ku70, Ku80, DNA-PKcs*, *Xrcc4, Lig4* and *Artemis* in the context of p53 mutation are predisposed to early onset pro-B lymphoma associated with oncogenic chromosomal translocations involving the immunoglobulin heavy chain locus and cellular oncogenes involving *c-myc* (and *n-myc* in *Artemis*$^{-/-}$*p53*$^{-/-}$ mice).

The cNHEJ nuclease, ARTEMIS*,* was initially discovered as mutated in a human radiosensitive severe combined immunodeficiency syndrome and is required for processing a subset of DNA ends during general DSB in addition to DSB intermediates during V(D)J recombination. Like ARTEMIS, MRE11 is a DNA nuclease that is critical to the repair of DSBs. The MRE11 nuclease functions within the context of the MRE11/RAD50/NBS1 complex (MRE11 complex). The MRE11 complex is required for homologous recombination and is

implicated in cNHEJ as well as a less well-defined, alternative NHEJ (aNHEJ) pathway where a subset of end joining events are mediated by sequence homology at the breakpoint (microhomology). The activities of the aNHEJ complex are implicated in the pro-B lymphomas that arise in cNHEJ/p53 double mutant mice as chromosomal translocations are mediated by sequence homology. Thus, we wanted to investigate the contribution of the MRE11 complex to pro-B lymphomas associated with chromosomal translocations mediated by sequence homology in cNHEJ/p53 double mutant mice using the *Aremis*$^{-/-}$*p53*$^{-/-}$ animal model. To this end I introduce *Mre11* mutations in *Artemis*$^{-/-}$ *p53*$^{-/-}$ B-cells taking advantage of the CD19 Cre recombinase transgene, which is expressed during early B-cell development and throughout B-cell differentiation. I observed that, in contrast to *Artemis*$^{-/-}$*p53*$^{-/-}$ mice that succumb primarily to pro-B lymphoma, *Artemis*$^{-/-}$*p53*$^{-/-}$ mice harboring B-cell specific mutation of the MRE11 complex, have a distinct tumor spectrum, and are devoid of pro-B lymphomas. Thus, the MRE11 complex facilitates pro-B lymphoma genesis in *Artemis*$^{-/-}$*p53*$^{-/-}$ mice. My findings have significant implications for the role of the MRE11 complex and its nuclease properties in promoting tumorigenesis associated with aberrant repair.

Introduction

Lymphoid malignancies are cancers of the immune system, which afflict both adults and children (1). For some lymphoid neoplasias, the intricacies of the pathogenic mechanism are related to the fundamental strategy of the immune system, in which gene rearrangement ensures diversity and optimal function of the B-cell receptor (BCR) and T-cell receptor (TCR) for the foreign antigens. Inadvertently, these mechanisms can cause chromosomal anomalies imposing a potential threat of malignant transformation through specific and recurrent chromosomal translocations (2). Unraveling the molecular mechanisms by which illegitimate events in the normal immune system can predispose to lymphoid cancer, and the role played by genetic factors are central to the development of diagnostic, preventive, therapeutic and disease monitoring programs of clinical significance.

During B-cell differentiation in the bone marrow and T-cell differentiation in the thymus, V(D)J recombination rearranges non-contiguous V (variable), D (diversity) and J (joining) gene segments, to form a complete V(D)J exon coding for the variable region of the immunoglobulin and T-cell receptor (3). This unique mechanism of site-specific somatic recombination generates the extraordinary diversity of the antigen receptors. This process requires a specialized recombinase activity, encoded by the recombination activating genes 1 and 2 (RAG1/2), the recognition of recombination signal sequences (RSSs) flanking each of the V, D and J gene segments, the generation of double strand breaks (DSBs) and the recruitment of proteins of the ubiquitous classical nonhomologous end joining (cNHEJ) pathway. It is clear that such a mechanism that relies on chromosomal DSBs between sequences sometimes located up to a megabase a part, must be regulated at the highest level. Indeed, V(D)J recombination is a highly orchestrated mechanism, regulated in a tissue-, lineage-, and developmental stage-specific manner (4).

Defects during the joining phase of V(D)J recombination can lead to immunodeficiency syndromes due to impaired lymphocyte development (5-15). Inappropriate joining of RAG1/2-generated DSBs can also result in chromosomal translocations involving the juxtaposition of rearranging antigen receptor loci and cellular oncogenes, which represent hallmark events associated with human lymphoid malignancies (2, 16, 17). Mutations in cNHEJ genes can alter the fate of DSBs and lead to oncogenic translocations and predisposition to lymphoid malignancy (18, 19). Indeed, hypomorphic mutations in cNHEJ factors such as *LIG4* and *DCLRE1C* (*ARTEMIS*) have been found in human patients with lymphoid malignancies (20, 21). Mouse models harboring inactivating mutations in cNHEJ genes in the context of p53 mutation are predisposed to early onset pro B-cell lymphomas characterized by translocations that result in complex genomic amplification involving immunoglobulins and cellular oncogenes such as *c-myc* and *n-myc* (22-28). Likewise, the RAG1/2 endonuclease has been implicated in suppressing tumorigenesis as both patient and murine mouse models harboring hypormorphic *RAG/Rag* mutations can predispose to lymphoma (8, 29, 30). Thus, V(D)J factors play critical roles in suppressing tumorigenesis.

The cNHEJ pathway is critical for the repair of RAG1/2-generated DSBs evidenced by the accumulation of RAG1/2-generated DSB in cNHEJ-deficient cells (31-33). Surprisingly, low levels of end joining remain in cNHEJ-deficient cells suggesting an alternative end joining mechanism. Rare junctions isolated from cNHEJ-deficient cells often bear features such as large deletions, small sequence homologies on either side of the junction (microhomologies), and occasional insertions of large DNA segments of unknown origin (34-37). This recurrent type of joining observed in cNHEJ-deficient cells became known as alternative NHEJ (aNHEJ). The characteristic joins within aNHEJ suggest the involvement of enzymes that promote end resection, proteins that can mediate joining using microhomology, nucleases capable of removing non-compatible 5' and 3' overhangs, and ligation. However, the factors involved and the

mechanism(s) underlying aNHEJ are poorly understood and is a major investigation of this chapter.

Observations of chromosomal translocation junctions in human tumors and *cNHEJ/p53*-deficient lymphomas revealed several features consistent with joining by the aNHEJ pathway such as microhomologies and extensive end resection, and led to the suggestion that aNHEJ mediates translocation formation (27, 38). Indeed, most chromosomal translocations in both cNHEJ-proficient and cNHEJ-deficient cells appear to be generated by aNHEJ (39-41). Consequently, pro-B lymphomas arising in *cNHEJ/p53* double deficient mice frequently contain translocations and gene amplification that result in the overexpression of C-MYC (and N-MYC for *Artemis/p53* double null mice) (22, 24, 25, 42-46). Therefore, the implication is that aNHEJ promotes chromosomal translocations that can lead to oncogene overexpression.

Activation of oncogenes is generally associated with the induction of an oncogene-induced DNA damage response (DDR), which acts as a barrier to tumor progression. Human cancers and pro-B lymphomas that arise in *cNHEJ/p53* double mutant overexpress the cellular oncogene, *c-myc*. C-*myc*-induced DNA damage can result in increased replication stress and genomic instability and lead to the activation of DNA repair factors critical to the DNA damage response such as ATM, CHK2, and p53 (47-49). Indeed, a number of chromosomal abnormalities including translocations, dicentric chromosomes and tetraploidy have been observed upon C-MYC overexpression (47). The oncogene-induced DDR emerges as an oncogene-inducible biological barrier against progression of cancer beyond its early stages. However, chronic activation of the oncogene-induced DDR possibly creates selective pressure that eventually favors outgrowth of malignant clones with mutations in the genome maintenance machinery, such as aberrations in the ATM–CHK2–p53 cascade or other DDR components. Thus, it is critical to understand the mechanisms by which DNA repair factors mediate the oncogene-induced DDR. This led us to study the MRE11 complex due to its role in the repair of replication associated damage and DSBs, in signaling to the DDR in a damage-dependent manner, its

association to V(D)J recombination intermediates, and its nuclease properties critical to the repair of DSBs. In the context of pro-B lymphomas that arise in *cNHEJ/p53* double mutant mice associated with complex chromosomal rearrangements involving the immunoglobulin heavy chain locus and *c-myc* or *n-myc*, we hypothesize that the MRE11 complex promote pro-B lymphoma genesis.

We use a well-characterized *cNHEJ/p53* mouse model, *Artemis/p53* double null mice, that succumb to pro-B lymphoma characterized by complex translocations mediated by microhomology involving the immunoglobulin heavy chain and *c-myc* or *n-myc*. We identify that deletion of the MRE11 complex suppresses pro-B lymphoma associated with aberrant V(D)J rearrangements involving the immunoglobulin heavy chain locus and *c-myc*/*n-myc*. This observation is dependent upon the nuclease properties of the MRE11 complex as *Artemis/p53* double null mice harboring the $Mre11^{H129N}$ allele are also devoid of pro-B lymphomas. These results suggest that the MRE11 complex may promote tumorigenesis via an error-prone pathway (perhaps aNHEJ) that promotes chromosomal translocations resulting in oncogene overexpression and, not mutually exclusive, tumor cell survival.

Results

CD19 Cre recombinase deletes MRE11 in B-lineage *Artemis/p53* lymphocytes

Homozygous *Mre11 null* and *Mre11*^{H129N} mutations result in early embryonic lethality in mouse models; therefore, we have obtained mice harboring the *Mre11* conditionally targeted null allele (*Mre11*^{C}) and the *Mre11*^{H129N} knock-in allele harboring the CD19 Cre recombinase transgene (50, 51). The CD19 promoter drives Cre expression in the pro-B cell lineage. The pro-B cells have little or no immunoglobulin rearrangement as a consequence of the initiation of RAG1/2 expression during pro-B cell commitment. With the initiation of RAG1/2 expression, D_H-to-J_H rearrangements commence at the immunoglobulin heavy chain locus. Thus CD19 Cre expression is concomitant with the initiation of RAG1/2 expression in B-cells and V(D)J recombination.

Previous work has shown that conversion of the *Mre11*^{C} allele to the *Mre11*$^{\Delta}$ allele, in a homozygous state, causes depletion of not only MRE11, but the entire MRE11 complex likely due to instability of the other components (51, 52). The *Mre11*^{H129N} allele abrogates the endo- and exonuclease activities of MRE11 without disrupting the MRE11 complex or its ability to sense DSBs (via its end bridging/tethering capabilities) and activate ATM (52). Thus, the *Mre11* mutant alleles are advantageous because we can distinguish between the nuclease activities of the MRE11 complex versus its role in checkpoint activation, end bridging/end tethering, and direct repair of DSBs (52-54).

We wanted to investigate the contribution of the MRE11 complex to pro-B lymphomagenesis in *Artemis/p53* double null mice. To this end, I introduced engineered *Mre11* mutant alleles into the *Artemis/p53* double null background through mouse breedings. CD19 Cre recombinase-mediated deletion of the *Mre11*^{C} allele to the *Mre11*$^{\Delta}$ allele was detected in pro-B cells (sorted from total

bone marrow) in *Mre11*$^{C/+}$*Artemis*$^{-/-}$*p53*$^{+/-}$;CD19 Cre mice and *Mre11*$^{C/+}$*Artemis*$^{-/-}$ *p53*$^{-/-}$;CD19 Cre mice (Figure 3.1); however, the deletion was incomplete. Despite the observation that a large proportion of pro B-cells retained the *Mre11* conditional allele, the cohort of mice harboring the CD19 Cre transgene was aged and monitored for tumorigenesis.

MRE11 deletion suppresses pro-B lymphoma when combined with *Artemis/p53* double nullizygosity

To examine the impact of loss of the MRE11 complex on the tumorigenesis phenotypes of *Artemis/p53* double null mice, I bred the *Mre11*^{C} allele harboring the CD19 Cre transgene to an *Artemis*/*p53* double null background to produce ***A****rtemis*$^{-/-}$***p****53*$^{-/-}$*Mre11*$^{C/-}$;CD19 Cre mice (referred to as *AP Mre11*$^{C/-}$ mice). Typically, *cNHEJ/p53* double deficient mice succumb to pro-B lymphoma between 8-12 weeks (22, 24, 25, 42-46) and thymic lymphoma between 14-16 weeks (55). Surprisingly, *AP Mre11*$^{C/-}$ mice did not become moribund between 8-12 weeks and it was not until after 16 weeks that I observed moribund mice (Figure 3.2A). *AP Mre11*$^{C/-}$ mice survived (average survival time: 18 weeks) significantly longer than *Artemis*$^{-/-}$*p53*$^{-/-}$;CD19 Cre mice (average survival time: 15 weeks) (***A****rtemis*$^{-/-}$***p****53*$^{-/-}$; CD19 Cre, referred to as *AP* mice) (log rank (Mantel-Cox) test, p=0.01) (Figure 3.2A).

Upon dissection of moribund *AP* mice I observed thymomegaly, splenomegaly, and lymphadenopathy that resulted in palpable lymph nodes. In contrast, dissection of *AP Mre11*$^{C/-}$ mice identified only thymomegaly and splenomegaly. The enlarged lymphoid tissues from each mouse were removed and dissociated into single cells for additional cellular and molecular analysis.

Flow cytometric analysis using cell surface markers expressed on B-cells identified that 6/10 of the tumors arising in *AP* mice were B220^{+}CD43^{+}IgM^{-} indicating they were pro-B lymphomas (Figure 3.2B and Figure 3.3). These findings parallel those of previous studies which found that 10/19 of the tumors arising in *Artemis*$^{-/-}$*p53*$^{-/-}$ were pro-B lymphomas (55). In contrast, flow cytometric analysis identified that 11/12 tumors isolated from *AP Mre11*$^{C/-}$ mice were B220^{-}

$CD43^-IgM^-$ indicating they were not pro-B lymphomas (Figure 3.2B and Figure 3.3).

We next investigated if $B220^-CD43^-IgM^-$ tumors expressed T-cell markers. *AP* tumors that did not express B-cell markers demonstrated they were $CD4^+CD8^+TCR\beta^-$ indicating they were thymic lymphomas of T-cell origin (Figure 3.3). Flow cytometric analysis for T-cell markers of the 11 tumors isolated from *AP* $Mre11^{C/-}$ mice that did not stain for B-cell markers identified they were $CD4^+CD8^+$ $TCR\beta^-$ (Figure 3.2B and Figure 3.3). The one tumor excluded stained for $CD8^+$ only and the other was a solid tumor (Figure 3.3). As a result, 11/12 tumors arising in *AP* $Mre11^{C/-}$ mice were characterized as $TCR\beta^-$ thymic lymphomas developmentally blocked at antigen gene receptor assembly. (Figure 3.3 and Figure 3.4). Since CD19 Cre recombinase is only active in the B lineage, T-cells isolated from *AP* $Mre11^{C/-}$ mice should not contain Cre recombinase expression and, therefore, retain MRE11 expression and MRE11 complex activity. The distinct tumor spectrum observed in *AP* $Mre11^{C/-}$ mice was statistically significant from the tumor spectrum observed in *AP* mice ($p=0.004$; two-tailed Fisher's exact test). Taken together, my results indicate that deleting the MRE11 complex in B-cells of *AP* mice increases survival time and suppresses pro-B lymphoma.

Mutating MRE11 nuclease properties suppress pro-B lymphoma when combined with *Artemis/p53* double nullizygosity

The DNA repair activities of the MRE11 complex are associated with the error-prone aNHEJ pathway (51, 56-60). The activities of the aNHEJ pathway have been associated with chromosomal translocation formation and hypothesized to promote tumorigenesis in *cNHEJ/p53* double-deficient mice (16, 55, 61-63). A subset of reactions within the aNHEJ pathway require extensive end resection (similar to HR) prior to joining (64). The extensive end resection that ensues uncovers sequence homology on either side of the DNA ends and facilitate repair using sequence homology (microhomology) (40). The MRE11 complex is a critical factor in HR-mediated end-resection and in vitro studies identify that the nuclease activities of MRE11 can act on DNA overhangs, flaps,

loops, and hairpinned ends (52, 54, 65-67). Additionally, the MRE11 complex mediates repair of DSBs via DSB sensing and subsequent activation of the ATM kinase, a central transducer of the DNA DSB response (42). Therefore, we hypothesized that perhaps the aNHEJ-mediated events that occur in *AP* mice could be facilitated by the nuclease properties of the MRE11 complex as well as its DNA repair properties associated with ATM activation. To this end, I bred mice harboring the *Mre11*^{H129N} allele to ***A****rtemis*$^{-/-}$***p****53*$^{-/-}$ double null mice harboring the CD19 Cre transgene (referred to as *AP Mre11*$^{C/H129N}$ mice). Surprisingly, these mice also exhibited an increased survival time as compared to *AP mice* (*AP Mre11*$^{C/H129N}$ average survival time: 19 weeks vs. *AP* survival time: 15 weeks) (log rank (Mantel-Cox) test, p=0.01) (Figure 3.2A). Although, survival time of *AP Mre11*$^{C/H129N}$ mice were not statistically different from the survival time of *AP Mre11*$^{C/-}$ mice (log rank (Mantel-Cox) test, p=0.72) (Figure 3.2A).

Upon dissection of moribund *AP Mre11*$^{C/H129N}$ mice, I observed thymomegaly and splenomegaly similar to *AP Mre11*$^{C/-}$ mice. Flow cytometric analysis on dissociated enlarged lymphoid organs isolated from *AP Mre11*$^{C/H129N}$ mice identified that a majority of the enlarged lymphoid organs were B220^{-}CD43^{-} IgM^{-} indicating they were not pro-B lymphomas (Figure 3.2B). Further characterization identified that tumors isolated from *AP Mre11*$^{C/H129N}$ mice T-cell markers such as CD4^{+}CD8^{+} TCRβ^{-} (5/7) indicating they were TCRβ- thymic lymphomas that were developmentally blocked at antigen gene receptor assembly (Figure 3.3). The one tumor with a different flow cytometric analysis profile only expressed CD8^{+}. The other tumor was unable to be analyzed by flow cytometry due to precipitous death related to an enlarged thymus that filled the chest cavity. Overall, the distinct tumor spectrum observed in *AP Mre11*$^{C/H129N}$ mice was statistically significant from the tumor spectrum observed in *AP* mice (p=0.035; two-tailed Fisher's exact test).

My results suggest that mutating the nuclease properties of the MRE11 complex or deleting the MRE11 complex in AP mice increases survival time and suppresses pro-B lymphoma, thereby changing the tumor spectrum. Together,

my results suggest that promotion of pro-B lymphomas that arise in *Artemis*$^{-/-}$*p53*$^{-/-}$ mice requires activities of the MRE11 complex.

Thymic lymphomas from *AP Mre11*$^{C/-}$ and *AP Mre11*$^{C/H129N}$ mice arose independently from B lineage MRE11 mutation

The MRE11 complex plays critical roles in the repair of DNA DSBs evidenced by loss-of-function alleles and subtle partial-loss-of-function alleles associated with inherited human syndromes featuring developmental delay, neurodegeneration, cancer predisposition and immunodeficiency (52, 68). MRE11 B-cell specific mutation in *AP* mice increases survival time and suppresses pro-B lymphoma. It is plausible that the *AP Mre11*$^{C/-}$ and *AP Mre11*$^{C/H129N}$ mice tumor phenotypes were due to MRE11 mutation in the B lineage. Additionally, mutant B lymphocytes can aberrantly express T-cell markers or, it has been shown that B lineage cells can de-differentiate into T lineage cells. Therefore, we wanted to investigate if the thymic lymphomas observed in the *AP Mre11*$^{C/-}$ and *AP Mre11*$^{C/H129N}$ mice originated from MRE11 deficient (*Mre11*$^{\Delta}$) B-cells.

To this end, I employed a PCR genotyping strategy using primers that would produce amplicons including the conditional, nuclease dead, and deleted alleles (Figure 3.1, upper panel). I isolated genomic DNA from the primary tumors from *AP Mre11*$^{C/-}$ and *AP Mre11*$^{C/H129N}$ mice and identified that the tumors retained the MRE11 conditional and nuclease dead alleles (Figure 3.4A). Importantly, using this strategy I could not detect a deleted allele in tumors from *AP Mre11*$^{C/H129N}$ mice suggesting that the tumors arose independently from the B-cell specific mutation of the MRE11 complex (Figure 3.4A). We next then conducted Western analysis of MRE11 expression in thymic lymphomas isolated from *AP Mre11*$^{C/-}$ mice. Western analysis revealed that MRE11 protein levels were similar to wild type levels (Figure 3.4B compared to supplemental figure 3S14). Taken together, my results demonstrate that tumors arising in *AP Mre11*$^{C/-}$ and *AP Mre11*$^{C/H129N}$ mice retained the *Mre11* conditional allele and expressed wild type levels of MRE11. Therefore, these tumors originated from

immature mutant T-cells harboring *Artemis*$^{-/-}$*p53*$^{-/-}$ mutation or *p53*$^{-/-}$ mutation alone.

Distinct clonal V(D)J rearrangements detected in *AP Mre11*$^{C/-}$ and *AP Mre11*$^{C/H129N}$ thymic lymphomas

All of the *AP Mre11*$^{C/-}$ and *AP Mre11*$^{C/H129N}$ mice succumbed to tumorigenesis and the majority of the tumors observed were immature TCRβ^{-} thymic lymphomas (18/19) (Figure 3.3). In comparison, although *p53*$^{-/-}$ mice are predominantly predisposed to thymic lymphomas, the majority of these tumors are TCRβ^{+}, indicating they emanated from later stages of T-cell development as compared to tumors that arose in *AP Mre11*$^{C/-}$ and *AP Mre11*$^{C/H129N}$ mice (22, 25, 29, 44, 55). Solid tumors and surface IgM^{+} B-cell lymphomas can also arise in *p53*$^{-/-}$ mice. I did observed one solid tumor isolated from an *AP Mre11*$^{C/-}$ mouse. It could have arisen as an independent tumor due to p53 mutation alone.

I analyzed the rearrangement status of the TCRβ locus in thymic lymphomas that arose in *AP Mre11*$^{C/-}$ mice (8/11; data not shown for tumors M854, M941, and M964) and *AP Mre11*$^{C/H129N}$ mice (5/7) to assess the molecular events that occurred. I performed Southern blot analyses of *EcoRI*-digested genomic DNA isolated from primary tumors using a probe located 5′ of Dβ1. The majority of tumors exhibited Dβ1-Jβ1 rearrangements of one or two of the rearranging alleles evidenced by hybridization of specific bands that are distinct from the germline band (Figure 3.5). In some tumors, we did not detect a hybridization product. This could be due to a large deletion within the probe hybridization site that resulted in deletion of the genomic region that encompasses the probe hybridization site (Figure 3.5, tumor M1112). I also examined TCRβ Dβ1 to Jβ1 and Dβ2 to Jβ2 TCRβ rearrangements using a PCR strategy. I observed that 10/17 of the thymic lymphomas harbored specific Dβ1-Jβ1 rearrangements (Figure 3.6). 11/17 thymic tumors isolated from *AP Mre11*$^{C/-}$ and *AP Mre11*$^{C/H129N}$ mice exhibited detectable rearrangements involving Dβ2 to Jβ2 rearrangements similar to the control. This could be possibly due to continuous RAG expression in the thymic lymphomas (69, 70). It is unlikely that a productive Dβ2 to Jβ2 rearrangement occurred in these thymic lymphomas

because I did not detect surface expression of TCRβ in 18/19 of the tumors assayed by flow cytometric analysis (data not shown). The one tumor was a solid tumor and could not be assayed for TCRβ expression using flow cytometric analysis similarly as the other tumors.

The PCR products were subcloned and sequenced to verify they represented attempted TCRβ rearrangements and to analyze the junctional sequences. I observed several unique sequences that represented attempted TCRβ rearrangements. Sequences isolated from *AP Mre11*$^{C/-}$ (4/8) and *AP Mre11*$^{C/H129N}$ thymic lymphomas (1/7) resembled TCRβ joins that have been recovered from *Artemis*$^{-/-}$ thymocytes such as large deletions (>300 nucleotides) on either side of the junction with small P- (0-2 nucleotides) and N-nucleotide additions (0-2 nucleotides) (Figure 3.7) (32). *Artemis*$^{-/-}$ lymphocytes also exhibit "leaky" lymphocyte development and as a result, harbor TCRβ joins with minimal deletion that resemble control thymocytes. In this regard, thymic lymphomas isolated from *AP Mre11*$^{C/-}$ (4/8) and *AP Mre11*$^{C/H129N}$ mice (6/7) resembled the TCRβ joins that have been recovered from "leaky" *Artemis*$^{-/-}$ thymocytes as they also contained minimal deletion (0-13 nucleotides) with small P- (0-7 nucleotides) and N-nucleotide (0-2 nucleotides) additions (32). I also detected 1 sequence from an *AP Mre11*$^{C/-}$ thymic lymphoma that had a microhomology-mediated event with 1 nucleotide of homology. However, in this instance, I did not detect deletion on either side of the junction. In contrast, from 1 sequence from an *AP Mre11*$^{C/H129N}$ thymic lymphoma, I detected a microhomology-mediated event with 2 nucleotides of homology associated with a large deletion on the Jβ2 side (73 nucleotide deletion). From the sequences recovered, we can conclude that I was able to recover sequences that represented productive joins at the TCRβ locus that contained minimal deletions along with small P- and N- nucleotide additions. These sequences were likely processed and joined by the cNHEJ pathway. Those sequences that contained larger deletions (>300 nucleotides) with small P- and N-nucleotide addition represent unproductive joins at the TCRβ locus. These types of sequences have only been previously observed in cNHEJ deficient cells, therefore, these joins likely are a product of aNHEJ activities (32,

33, 71, 72). The one sequence observed to be joined via microhomology but lacking large deletions is difficult to ascribe to activities of the cNHEJ or aNHEJ pathway due to only one sequence recovered with only 1 nucleotide of microhomology. Obtaining more sequences from the thymic lymphomas would provide more support for the activities of microhomology-mediated end joining (MMEJ) at the TCRβ locus in thymic lymphomas arising in *AP Mre11*$^{C/-}$ and *AP Mre11*$^{C/H129N}$ mice.

One recurrent genomic event within the IgH locus observed in *Artemis/p53* double null pro-B lymphomas is amplification of regions downstream of the J_H region. Using Southern blotting analysis with probes comprised of the Cμ constant region and 3′ enhancer regulatory region located approximately 5 and 170 kb, respectively, from the rearranging J_H segments we detected genomic amplification in 4/6 *AP* pro-B lymphomas analyzed (supplementary figure 3S11). In contrast, thymic lymphomas isolated from *AP Mre11*$^{C/-}$ and *AP Mre11*$^{C/H129N}$ mice did not exhibit apparent amplification of the IgH locus (supplementary figure 3S12). I next examined the status of the *c-myc* and *n-myc* loci, as amplification of either genomic region is associated with *Artemis/p53* double null pro-B lymphomas. I detected *c-myc* or *n-myc* amplification in 5/6 *AP* tumors analyzed (supplementary figure 3S11). I did not detect genomic amplification of either *c-myc* or *n-myc* in thymic lymphomas that arose in *AP Mre11*$^{C/-}$ and *AP Mre11*$^{C/H129N}$ mice (supplementary figure 3S12).

Taken together, my results indicate that the thymic lymphomas arising in *AP Mre11*$^{C/-}$ and *AP Mre11*$^{C/H129N}$ mice emanated from clonal events within the population of developing *Artemis/p53* double deficient thymocytes (that retain the *Mre11*^{C} allele and thus, wild type levels of the MRE11 complex) and are molecularly distinct from *AP* pro-B lymphomas.

Trans-rearrangements detected in thymic lymphomas from *AP Mre11*$^{C/-}$ and *AP Mre11*$^{C/H129N}$ mice

Previous results indicating aberrant accumulation of RAG1/2-generated hairpinned coding ends in *Artemis*$^{-/-}$ mice (32) led us to hypothesize that the hairpinned coding ends, in the absence of the p53-mediated and ATM-mediated

checkpoints, may engage in aberrant rearrangements in *AP Mre11*$^{C/-}$ and *AP Mre11*$^{C/H129N}$ mice. To address this question, I determined whether interchromosomal V(D)J rearrangements between the TCRγ and TCRβ loci, which are located on chromosomes 13 and 6, respectively, were present in thymic lymphomas from *AP Mre11*$^{C/-}$ and *AP Mre11*$^{C/H129N}$ mice using a nested PCR approach (29, 73). By proxy, interchromosomal trans-rearrangement between two rearranging chromosomes, in trans, is a global predictor of chromosomal translocations and this event is elevated in lymphocytes that are mutant for genes that predispose to lymphoid neoplasia, including *Atm, Prkdc(DNA-PKcs),* the ARTEMIS C-terminal truncation mutant, *Artemis-P70* , *and Nbs1* (29, 74-76). I detected PCR products corresponding to trans-rearrangements between TCRγV3S1 and TCRβJ2 in thymic lymphomas from *AP Mre11*$^{C/-}$ mice (2/11) and *AP Mre11*$^{C/H129N}$ mice (1/7) as well as in *Atm*-null thymocytes, which has been previously observed (Figure 3.8) (29). In contrast, I did not readily observe interchromosomal trans-rearrangements in wild type thymocytes or in *a p53*$^{-/-}$ thymic lymphoma (M930; Figure 3.8)

The PCR products from the thymic lymphomas were subcloned and sequenced to verify that they represented the predicted interchromosomal events and to analyze the junctional sequences (Figure 3.9). I observed unique clones containing flanking sequences from TCRγV3S1 and TCRβJ2. Thymic lymphoma, M487, isolated from an *AP Mre11*$^{C/H129N}$ mouse contained 1 unique sequence (Figure 3.9). This sequence likely reflects the product detected in the trans-rearrangement PCR assay. The junction contained N-nucleotides (7) and small deletions (-7). Thymic lymphoma, M941, isolated from an *AP Mre11*$^{C/-}$ mouse contained 20 unique junctional sequences with N-nucleotides (1-16), P-nucleotides (1-2) small deletions (4-34), and a microhomology mediated join (1 nucleotide of microhomology) (Figure 3.9). These sequences likely represent sub-clonal events. Thymic lymphoma, M474, isolated from an *AP Mre11*$^{C/-}$ mouse contained 1 junctional sequence with a small deletion (11) and a microhomology mediated join (3 nucleotides of microhomology) (Figure 3.9). Overall, the junctional sequences from the trans-rearrangements resembled

intrachromosomal junctional sequences isolated from *AP Mre11$^{C/-}$* and *AP Mre11$^{C/H129N}$* mice due to the presence of microhomology-mediated joins (2/20), N-nucleotide addition (18/20), P-nucleotide addition (2/20) and small deletions (12/20). Therefore, I was able to detect trans-rearrangements in the thymic lymphomas. Although trans-rearrangements occur infrequently in thymic lymphomas isolated from *AP Mre11$^{C/-}$* and *AP Mre11$^{C/H129N}$* mice as I only detected trans-rearrangements in 3/18 of the thymic lymphomas.

Fluorescent in situ hybridization studies in thymic lymphomas isolated from *AP Mre11$^{C/-}$* and *AP Mre11$^{C/H129N}$* mice

Previous tumor studies of *Artemis* mutant alleles identified misrepaired RAG1/2 generated breaks using a two-color fluorescent in situ hybridization (FISH) approach (76). In this regard, FISH probes flanking a rearranging locus identified misrepaired RAG1/2 breaks evidence by separation of the FISH probes indicating a translocation event occured (76). Therefore, we wanted to investigate if thymic lymphomas arising in *AP Mre11$^{C/-}$* and *AP Mre11$^{C/H129N}$* mice harbored misrepaired RAG1/2 breaks by FISH analysis. Using this approach, I observed that 4/4 thymic lymphomas analyzed from *AP Mre11$^{C/-}$* and *AP Mre11$^{C/H129N}$* mice revealed colocalization of the TCRβ flanking probes on both alleles, indicating repair of RAG1/2-generated DSBs (supplementary figure 3S13). However, tumor M487 (*AP Mre11$^{C/H129N}$* mouse) harbored separated signals at the TCRβ locus, suggesting misrepair of RAG1/2-generated DSBs at the TCRβ locus.

Additionally, using FISH, I was also able to detect a clonal trans-rearrangement in this thymic lymphoma involving the TCRβ locus on chromosome 6, and the TCRγ locus on chromosome 13 (FISH data not shown). I was also able to detect this translocation event in thymic lymphoma, M487, using the trans-rearrangement PCR analysis (Figure 3.9). Using FISH probes flanking the TCRαδ locus, a locus that undergoes rearrangement in thymocytes, identified that 3/4 of the thymic lymphomas analyzed contained co-localized FISH probes (supplementary figure 3S15). One tumor, M487, harbored separated FISH signals suggesting misrepair of RAG1/2-generated DSBs (supplementary figure

3S15). Altogether, 1/4 thymic lymphomas analyzed exhibited breaks at the TCRβ and TCRαδ loci that were misrepaired leading to trans-rearrangements or translocations (thymic lymphoma M487). Thus, the majority of thymic lymphomas analyzed by FISH using flanking probes at the TCR loci did not harbor misrepaired RAG1/2 breaks.

Spontaneous chromosomal instability in ARTEMIS/MRE11 mutant primary MEFs

I reasoned that if mutation of the MRE11 complex suppressed pro-B lymphoma in *Artemis/p53* double mutant mice as a result of defective DNA repair, then cells doubly deficient for ARTEMIS and the MRE11 complex would exhibit accumulation of catastrophic levels of damage or additive levels of damage. To test this hypothesis, I obtained primary mouse embryonic fibroblasts (MEFs) of the following genotypes: $Mre11^{+/-}$ (functionally wild type), $Artemis^{-/-}$, $Mre11^{C/-}$ and $Artemis^{-/-}Mre11^{C/-}$ and scored spontaneous chromosomal anomalies. Preliminary investigation into overall chromosomal anomalies in primary MEFs treated with adenovirus expressing Cre recombinase (to delete the $Mre11^{C}$ allele) indicated an overall increase in chromosomal anomalies in $Artemis^{-/-}Mre11^{\Delta/-}$ primary MEFs (283 total anomalies, n=59 metaphases) as compared to $Mre11^{\Delta/-}$ (175 total anomalies, n=98 metaphase) and wild type MEFs (35 total anomalies, n=34 metaphases) (Figure 3.10). This preliminary finding suggests that combining mutation of the MRE11 complex and ARTEMIS results in additive levels of DNA due to the direct role of both ARTEMIS and the MRE11 complex in DNA repair.

Discussion

The MRE11 complex and MRE11 nuclease activities promote pro-B lymphoma in *AP* mice

In this study, I investigated the contribution of the MRE11 complex to pro-B lymphomas that arise in *Artemis/p53* double mutant mice. *AP* mice harboring a B-cell specific *Mre11* null allele had increased survival time versus the control cohort and *AP* mice. Additionally, in contrast to *Artemis/p53* double null mice that primarily succumb to pro-B lymphoma, I observed that combining the $Mre11^{\Delta}$ B-cell specific mutation in an *Artemis/p53* double null background suppressed pro-B lymphoma. The *AP* $Mre11^{C/-}$ and *AP* $Mre11^{C/H129N}$ mice primarily succumbed to $TCR\beta^{-}$ thymic lymphoma. PCR and Western analysis of the thymic lymphomas revealed they rose independently from B-cell specific, Mre11 deletion.

We hypothesized that if ATM activation and the end bridging/tethering activities of the MRE11 complex promoted pro-B lymphoma development in *AP* $Mre11^{C/H129N}$ mice, then we would observe pro-B lymphoma formation. However, if the nuclease activities are necessary for pro-B lymphoma genesis instead of ATM activation or the end bridging/tethering activities of the MRE11 complex, then we would anticipate that *AP* $Mre11^{C/H129N}$ mice would not succumb to pro-B lymphoma. In this regard, 7/7 *AP* $Mre11^{C/H129N}$ mice did not succumb to pro-B lymphoma, but rather to $TCR\beta^{-}$ thymic lymphoma. This result indicates that the nuclease activities of MRE11 are necessary to promote pro-B lymphoma in *AP* mice that are independent of the role of the MRE11 complex in ATM activation and end bridging/tethering at DNA ends.

A subset of $Artemis^{-/-}p53^{-/-}$ mice succumb to immature thymic lymphomas with TCRαδ translocations (55). If the thymic lymphomas that arose in *AP* $Mre11^{C/-}$ and *AP* $Mre11^{C/H129N}$ mice were due to *Artemis/p53* double nullizygosity rather than due to *p53* mutation alone, then I would predict that some thymic

lymphomas would harbor translocations involving the TCRαδ locus. Indeed, thymic lymphoma, M487, exhibited translocations involving the TCRαδ locus as detected by the separated FISH signals (supplementary Figure 3S15). Additionally, flow cytometric analysis identified that many of the thymic lymphomas isolated from *AP Mre11*$^{C/-}$ and *AP Mre11*$^{C/H129N}$ mice were $CD4^{+}CD8^{+}TCR\beta^{-}$ or $CD4^{-}CD8^{+}TCR\beta^{-}$ which has been previously observed in *Artemis*$^{-/-}$*p53*$^{-/-}$ thymic lymphomas, but not *p53*$^{-/-}$ thymic lymphomas (29, 77, 78). Furthermore, I detected clonal rearrangements involving the TCRβ Dβ1 to Jβ1 cluster, using Southern and PCR analysis, which has been previously observed in *Artemis/p53* double mutant tumors (29, 55, 76), but not in *p53*$^{-/-}$ thymic lymphomas (29, 78). Taken together, my results suggest that the tumors isolated from *AP Mre11*$^{C/-}$ and *AP Mre11*$^{C/H129N}$ mice arose due to *Artemis/p53* double nullizygosity rather than due to *p53* mutation alone.

The contribution of the MRE11 complex to pro-B lymphoma in *AP* mice

Nearly all cNHEJ/p53 double-deficient mice succumb to aggressive pro-B lymphoma characterized by abnormal rearrangements involving the IgH locus and *c-myc* (and *n-myc* for *Artemis/p53* double null mice). This observation suggested activity of an aberrant, alternative end joining (aNHEJ) pathway capable of forming complex chromosomal translocations and influencing proto-oncogene overexpression when cNHEJ is deficient. I hypothesized that this could be due to the role of the MRE11 complex in promoting aberrant V(D)J recombination events and/or promoting the survival of tumor cells.

The activity of the aNHEJ pathway is associated with chromosomal translocations and is likely antagonized to some degree, by the cNHEJ pathway (40, 62). The aNHEJ pathway is unique in that it relies on resection to promote joining of incompatible DNA ends increasing the possibility for chromosomal translocations. The nuclease activities of MRE11 have been implicated in end resection activities within the aNHEJ pathway (51, 58, 59). Additionally, a recent biochemical study identified an interaction between the MRE11 complex and DNA LIGASE III/XRCC1, a ligase implicated in the aNHEJ pathway (60). These

data suggest that the MRE11 complex is able to promote end joining via the aNHEJ pathway.

Studies have shown that in the absence of cNHEJ, the repair of DSBs is much slower (63, 79). This presumably will enable other factors, such as the MRE11 complex, to gain access to the DSBs, aberrantly process the ends, and recruit other factors involved in the aberrant aNHEJ pathway to promote repair. Therefore, it is possible that the MRE11 complex could promote aNHEJ-mediated joining in *Artemis/p53* double null mice (a cNHEJ-deficient system) and promote the misrepair of RAG1/2-generated DSBs involving V(D)J loci and thus, promote tumorigenesis.

In our system using CD19 Cre recombinase to delete MRE11 in the pro-B cell compartment, we were still able to detect the $Mre11^{C}$ allele using a PCR genotyping strategy. Therefore, I would have predicted that *AP* $Mre11^{C/-}$ mice would succumb to pro-B lymphomas because the B-cell compartment would essentially be that of an *AP* mouse that would succumb primarily pro-B lymphoma. However, molecular analysis of tumors isolated from *AP* $Mre11^{C/-}$ mice (11/12) identified that these mice succumbed to $TCR\beta^{-}$ thymic lymphoma and were suppressed for pro-B lymphoma. That none of the *AP* $Mre11^{C/-}$ mice analyzed succumbed to pro-B lymphoma suggests that pro-B cells mutated for the MRE11 complex may undergo cell death such as apoptosis or necrosis. This observation suggests that the MRE11 complex promotes tumor cell survival. How does the MRE11 complex promote survival of tumor cells? I hypothesize the MRE11 complex participates in DNA replication associated with DNA damage.

Previous studies have identified that the MRE11 complex can relieve S-phase related replication stress by supporting re-start of stalled replication forks and processing replication-associated DNA intermediates (80, 81). Additionally, studies have revealed that unrepaired DNA lesions and constitutive activation of oncogenes such as *C-MYC*, can lead to replication stress associated with replication fork stalling or collapse (82, 83). Nearly all *cNHEJ/p53* double null mice succumb to aggressive pro-B lymphoma harboring complex DNA rearrangements that result in C-MYC overexpression (and N-MYC

overexpression) (22, 24, 25, 42-46). These observations suggest a model in which C-MYC or N-MYC overexpression in *cNHEJ/p53* double null pro-B lymphomas, that are characterized by chromosomal translocations involving the immunoglobulin heavy chain and *c-myc* (or *n-myc* locus for *Artemis*$^{-/-}$*p53*$^{-/-}$) loci, inappropriately engage the DNA replication machinery to proceed into S-phase precipitously, and as a result induce replication stress and DNA damage. Continued cellular replication or survival may require the activities of the MRE11 complex to facilitate replication or DNA repair, respectively. In this regard, I observed additive chromosomal anomalies associated with replication defects in cells defective for DNA repair due to inactivation of ARTEMIS and the MRE11 complex (*Artemis*$^{-/-}$*Mre11*$^{\Delta/-}$ cells), as compared to *Mre11*$^{\Delta/-}$ cells and the control (Figure 3.10).

Here, these studies use the *Artemis/p53* double null mouse model as a source of spontaneous lymphomas associated with an increase in C-MYC expression, which is commonly observed in human tumors. My findings raise the possibility that in spontaneous tumors that over express C-MYC, perhaps the MRE11 complex facilitates oncogene-induced DNA damage and in its absence, the cells may be susceptible to cellular death. Future studies investigating the viability of C-MYC overexpressing tumor cells inhibited for MRE11 complex activity would be interesting as perhaps, the inhibition of the MRE11 complex would provide specificity in killing neoplastic cells, versus healthy, normal cells.

Materials and Methods

Mice.

Gene targeted *Artemis* null, *Mre11* conditional, and *Mre11*^{H129N} (129Svev/C57BL6 background) mice were previously generated. p53 (Trp53^{tm1Tyj}) mutant mice were obtained from Jackson labs. Mice were bred to mice harboring the CD19 Cre transgene (Jackson Labs). All mice were housed in a specific pathogen free facility in a room dedicated to immunocompromised animals.

Southern Blot Analysis

Southern blots of genomic DNA from control tissues, *Artemis*$^{-/-}$*p53*$^{-/-}$, AP Mre11$^{C/-}$ or AP Mre11$^{C/H129N}$ thymic or lymphnode tumor masses were enzymatically digested with EcoRI and hybridized with the following radiolabeled probes: Drd (TCRβ), JS264 (J_H), P277 (Nmyc), JS263 (HS3a), Cμ, and mycA (Cmyc), previously described (55, 76). Images were visualized by autoradiography and using a phosphoimager, signals were normalized to a non-lymphoid locus using probe JS261 (LR8) (previously described (76)) and fold induction compared to kidney.

Characterization of Tumors

All mice were regularly monitored for tumors and analyzed when moribund. Lymphoid tumors were analyzed by flow cytometry with antibodies against surface B-cells (CD43, B220, IgM) and T-cells (CD4, CD8, CD3, TCRβ, CD44, CD25) markers. Thymic and pro-B lymphomas were cultured in RPMI medium 1640 supplemented with 15% FBS, 25 units per ml IL-2 (BD Biosciences) and 25 ng/ml IL-7 (PeproTech, Rocky Hill, NJ).

Western blot analysis of MRE11 complex levels

Primary tumor lymphocytes (10,000,000 cells) were harvested in Laemmli buffer (4% sodium dodecyl sulfate, 20% glycerol, 120 mM Tris–HCl, pH 6.8). Equivalent amounts of whole-cell lysates were resolved on an 8% sodium dodecyl sulfate–polyacrylamide (SDS–PAGE) gel and transferred to a polyvinylidene fluoride membrane. Primary antibodies used were: Mre11 (1:1000, Cell Signaling, Danvers, MA, USA) and Nbs1 (1:500, Novus Biologicals; Littleton, CO, USA). The protein bands were visualized and quantified using IRDye800CW-conjugated goat anti-rabbit secondary antibody (LiCor Biosciences; Lincoln, NE, USA).

PCR analysis of TCR rearrangements

Genomic DNA was isolated from primary tumors. 200ng of genomic tumor DNA was serially diluted 1:5 such that samples consisted of 200ng, 40ng, and 8ng. The rearrangement status within each tumor was analyzed using PCR with primers to TCRγV4-TCRβJS7, V-DJβ and Dβ-Jβ as previously described (29, 33).

Chromosomal Analysis

Metaphases were either obtained from the primary lymphoma cultures on day 0 or from cultures grown for two days in the presence of IL-7 and IL-2. Day two cultures were exposed to 100ng/ml Colcemid between 1- 8 hours. Bacterial artificial chromosome (BAC) probes for fluorescent in situ hybridization (FISH) analysis were obtained from the RPCI-23 library (Children's Hospital Oakland Research Institute) and nick-translated using biotin-11-dUTP or digoxigenein-16-dUTP by standard procedures (Roche). BAC probes hybridizing to TCRα/δ are as follows: RPCI 23 204N18 (centromeric to TCRα/δ region) and RPCI 23 269E2 (telomeric to TCRα/δ region). BAC probes hybridizing to TCRβ are as follows: RPCI 23 216J19 (spans TRBD1-TRBV31), RPCI 23 216J19 (TCRβ-TCRβV31), RP23 61N4 (spans TCRDβ-TCRJβ). BAC probes hybridizing to TCRγ are as follows: RPCI-23 212N5 (within TCRγ). BAC probes hybridizing to IgH are as

follows: N-myc BAC A-10-1, Bac199 (hybridizes to Cα), Bac 207 (hybridizes to V region). BAC probes hybridizing to c-myc are as follows: myc (84).

References

1. Fisher SG, Fisher RI. The epidemiology of non-Hodgkin's lymphoma. Oncogene. 2004;23(38):6524-34.
2. Tycko B, Sklar J. Chromosomal translocations in lymphoid neoplasia: a reappraisal of the recombinase model. Cancer Cells. 1990;2(1):1-8.
3. Schatz DG, Swanson PC. V(D)J recombination: mechanisms of initiation. Annu Rev Genet. 2011;45:167-202.
4. Schlissel MS. Regulating antigen-receptor gene assembly. Nat Rev Immunol. 2003;3(11):890-9.
5. van der Burg M, van Dongen JJ, van Gent DC. DNA-PKcs deficiency in human: long predicted, finally found. Curr Opin Allergy Clin Immunol. 2009;9(6):503-9.
6. Turul T, Tezcan I, Sanal O. Cernunnos deficiency: a case report. J Investig Allergol Clin Immunol. 2011;21(4):313-6.
7. van der Burg M, Ijspeert H, Verkaik NS, Turul T, Wiegant WW, Morotomi-Yano K, et al. A DNA-PKcs mutation in a radiosensitive T-B- SCID patient inhibits Artemis activation and nonhomologous end-joining. J Clin Invest. 2009;119(1):91-8. PMCID: 2613452.
8. Xiao Z, Yannone SM, Dunn E, Cowan MJ. A novel missense RAG-1 mutation results in T-B-NK+ SCID in Athabascan-speaking Dine Indians from the Canadian Northwest Territories. Eur J Hum Genet. 2009;17(2):205-12. PMCID: 2986061.
9. Buck D, Moshous D, de Chasseval R, Ma Y, le Deist F, Cavazzana-Calvo M, et al. Severe combined immunodeficiency and microcephaly in siblings with hypomorphic mutations in DNA ligase IV. Eur J Immunol. 2006;36(1):224-35.
10. van der Burg M, van Veelen LR, Verkaik NS, Wiegant WW, Hartwig NG, Barendregt BH, et al. A new type of radiosensitive T-B-NK+ severe combined immunodeficiency caused by a LIG4 mutation. J Clin Invest. 2006;116(1):137-45. PMCID: 1312018.
11. Ege M, Ma Y, Manfras B, Kalwak K, Lu H, Lieber MR, et al. Omenn syndrome due to ARTEMIS mutations. Blood. 2005;105(11):4179-86.
12. Moshous D, Callebaut I, de Chasseval R, Corneo B, Cavazzana-Calvo M, Le Deist F, et al. Artemis, a novel DNA double-strand break repair/V(D)J recombination protein, is mutated in human severe combined immune deficiency. Cell. 2001;105(2):177-86.
13. Vera G, Rivera-Munoz P, Abramowski V, Malivert L, Lim A, Bole-Feysot C, et al. Cernunnos deficiency reduces thymocyte life span and alters the T cell repertoire in mice and humans. Mol Cell Biol. 2013;33(4):701-11. PMCID: 3571340.
14. Schwarz K, Gauss GH, Ludwig L, Pannicke U, Li Z, Lindner D, et al. RAG mutations in human B cell-negative SCID. Science. 1996;274(5284):97-9.

15. Villa A, Santagata S, Bozzi F, Imberti L, Notarangelo LD. Omenn syndrome: a disorder of Rag1 and Rag2 genes. J Clin Immunol. 1999;19(2):87-97.
16. Mills KD, Ferguson DO, Alt FW. The role of DNA breaks in genomic instability and tumorigenesis. Immunol Rev. 2003;194:77-95.
17. Chatterji M, Tsai CL, Schatz DG. New concepts in the regulation of an ancient reaction: transposition by RAG1/RAG2. Immunol Rev. 2004;200:261-71.
18. Sekiguchi J, Ferguson DO, Chen HT, Yang EM, Earle J, Frank K, et al. Genetic interactions between ATM and the nonhomologous end-joining factors in genomic stability and development. Proc Natl Acad Sci U S A. 2001;98(6):3243-8. PMCID: 30638.
19. Callen E, Jankovic M, Difilippantonio S, Daniel JA, Chen HT, Celeste A, et al. ATM prevents the persistence and propagation of chromosome breaks in lymphocytes. Cell. 2007;130(1):63-75.
20. Moshous D, Callebaut I, de Chasseval R, Poinsignon C, Villey I, Fischer A, et al. The V(D)J recombination/DNA repair factor artemis belongs to the metallo-beta-lactamase family and constitutes a critical developmental checkpoint of the lymphoid system. Ann N Y Acad Sci. 2003;987:150-7.
21. Riballo E, Critchlow SE, Teo SH, Doherty AJ, Priestley A, Broughton B, et al. Identification of a defect in DNA ligase IV in a radiosensitive leukaemia patient. Curr Biol. 1999;9(13):699-702.
22. Difilippantonio MJ, Zhu J, Chen HT, Meffre E, Nussenzweig MC, Max EE, et al. DNA repair protein Ku80 suppresses chromosomal aberrations and malignant transformation. Nature. 2000;404(6777):510-4.
23. Difilippantonio MJ, Petersen S, Chen HT, Johnson R, Jasin M, Kanaar R, et al. Evidence for replicative repair of DNA double-strand breaks leading to oncogenic translocation and gene amplification. J Exp Med. 2002;196(4):469-80. PMCID: 2196056.
24. Frank KM, Sharpless NE, Gao Y, Sekiguchi JM, Ferguson DO, Zhu C, et al. DNA ligase IV deficiency in mice leads to defective neurogenesis and embryonic lethality via the p53 pathway. Mol Cell. 2000;5(6):993-1002.
25. Gao Y, Ferguson DO, Xie W, Manis JP, Sekiguchi J, Frank KM, et al. Interplay of p53 and DNA-repair protein XRCC4 in tumorigenesis, genomic stability and development. Nature. 2000;404(6780):897-900.
26. Lim DS, Vogel H, Willerford DM, Sands AT, Platt KA, Hasty P. Analysis of ku80-mutant mice and cells with deficient levels of p53. Mol Cell Biol. 2000;20(11):3772-80. PMCID: 85695.
27. Zhu C, Mills KD, Ferguson DO, Lee C, Manis J, Fleming J, et al. Unrepaired DNA breaks in p53-deficient cells lead to oncogenic gene amplification subsequent to translocations. Cell. 2002;109(7):811-21.
28. Vanasse GJ, Halbrook J, Thomas S, Burgess A, Hoekstra MF, Disteche CM, et al. Genetic pathway to recurrent chromosome translocations in murine lymphoma involves V(D)J recombinase. J Clin Invest. 1999;103(12):1669-75. PMCID: 408389.
29. Giblin W, Chatterji M, Westfield G, Masud T, Theisen B, Cheng HL, et al. Leaky severe combined immunodeficiency and aberrant DNA rearrangements

due to a hypomorphic RAG1 mutation. Blood. 2009;113(13):2965-75. PMCID: 2662642.
30. Deriano L, Chaumeil J, Coussens M, Multani A, Chou Y, Alekseyenko AV, et al. The RAG2 C terminus suppresses genomic instability and lymphomagenesis. Nature. 2011;471(7336):119-23. PMCID: 3174233.
31. Zhu C, Bogue MA, Lim DS, Hasty P, Roth DB. Ku86-deficient mice exhibit severe combined immunodeficiency and defective processing of V(D)J recombination intermediates. Cell. 1996;86(3):379-89.
32. Rooney S, Sekiguchi J, Zhu C, Cheng HL, Manis J, Whitlow S, et al. Leaky Scid phenotype associated with defective V(D)J coding end processing in Artemis-deficient mice. Mol Cell. 2002;10(6):1379-90.
33. Huang Y, Giblin W, Kubec M, Westfield G, St Charles J, Chadde L, et al. Impact of a hypomorphic Artemis disease allele on lymphocyte development, DNA end processing, and genome stability. J Exp Med. 2009;206(4):893-908. PMCID: 2715118.
34. Blackwell TK, Malynn BA, Pollock RR, Ferrier P, Covey LR, Fulop GM, et al. Isolation of scid pre-B cells that rearrange kappa light chain genes: formation of normal signal and abnormal coding joins. EMBO J. 1989;8(3):735-42. PMCID: 400869.
35. Bogue MA, Jhappan C, Roth DB. Analysis of variable (diversity) joining recombination in DNAdependent protein kinase (DNA-PK)-deficient mice reveals DNA-PK-independent pathways for both signal and coding joint formation. Proc Natl Acad Sci U S A. 1998;95(26):15559-64. PMCID: 28082.
36. Bogue MA, Wang C, Zhu C, Roth DB. V(D)J recombination in Ku86-deficient mice: distinct effects on coding, signal, and hybrid joint formation. Immunity. 1997;7(1):37-47.
37. Malynn BA, Blackwell TK, Fulop GM, Rathbun GA, Furley AJ, Ferrier P, et al. The scid defect affects the final step of the immunoglobulin VDJ recombinase mechanism. Cell. 1988;54(4):453-60.
38. Zhang Y, Rowley JD. Chromatin structural elements and chromosomal translocations in leukemia. DNA Repair (Amst). 2006;5(9-10):1282-97.
39. Boboila C, Jankovic M, Yan CT, Wang JH, Wesemann DR, Zhang T, et al. Alternative end-joining catalyzes robust IgH locus deletions and translocations in the combined absence of ligase 4 and Ku70. Proc Natl Acad Sci U S A. 2010;107(7):3034-9. PMCID: 2840344.
40. Simsek D, Jasin M. Alternative end-joining is suppressed by the canonical NHEJ component Xrcc4-ligase IV during chromosomal translocation formation. Nat Struct Mol Biol. 2010;17(4):410-6.
41. Yoo S, Dynan WS. Geometry of a complex formed by double strand break repair proteins at a single DNA end: recruitment of DNA-PKcs induces inward translocation of Ku protein. Nucleic Acids Res. 1999;27(24):4679-86. PMCID: 148766.
42. Wang JH, Gostissa M, Yan CT, Goff P, Hickernell T, Hansen E, et al. Mechanisms promoting translocations in editing and switching peripheral B cells. Nature. 2009;460(7252):231-6. PMCID: 2907259.

43. Frank KM, Sekiguchi JM, Seidl KJ, Swat W, Rathbun GA, Cheng HL, et al. Late embryonic lethality and impaired V(D)J recombination in mice lacking DNA ligase IV. Nature. 1998;396(6707):173-7.
44. Ferguson DO, Sekiguchi JM, Chang S, Frank KM, Gao Y, DePinho RA, et al. The nonhomologous end-joining pathway of DNA repair is required for genomic stability and the suppression of translocations. Proc Natl Acad Sci U S A. 2000;97(12):6630-3. PMCID: 18682.
45. Gu Y, Sekiguchi J, Gao Y, Dikkes P, Frank K, Ferguson D, et al. Defective embryonic neurogenesis in Ku-deficient but not DNA-dependent protein kinase catalytic subunit-deficient mice. Proc Natl Acad Sci U S A. 2000;97(6):2668-73. PMCID: 15987.
46. Gao Y, Chaudhuri J, Zhu C, Davidson L, Weaver DT, Alt FW. A targeted DNA-PKcs-null mutation reveals DNA-PK-independent functions for KU in V(D)J recombination. Immunity. 1998;9(3):367-76.
47. Felsher DW, Bishop JM. Transient excess of MYC activity can elicit genomic instability and tumorigenesis. Proc Natl Acad Sci U S A. 1999;96(7):3940-4. PMCID: 22399.
48. Bartkova J, Horejsi Z, Koed K, Kramer A, Tort F, Zieger K, et al. DNA damage response as a candidate anti-cancer barrier in early human tumorigenesis. Nature. 2005;434(7035):864-70.
49. Jackson SP, Bartek J. The DNA-damage response in human biology and disease. Nature. 2009;461(7267):1071-8. PMCID: 2906700.
50. Rickert RC, Roes J, Rajewsky K. B lymphocyte-specific, Cre-mediated mutagenesis in mice. Nucleic Acids Res. 1997;25(6):1317-8. PMCID: 146582.
51. Dinkelmann M, Spehalski E, Stoneham T, Buis J, Wu Y, Sekiguchi JM, et al. Multiple functions of MRN in end-joining pathways during isotype class switching. Nat Struct Mol Biol. 2009;16(8):808-13. PMCID: 2721910.
52. Buis J, Wu Y, Deng Y, Leddon J, Westfield G, Eckersdorff M, et al. Mre11 nuclease activity has essential roles in DNA repair and genomic stability distinct from ATM activation. Cell. 2008;135(1):85-96. PMCID: 2645868.
53. Williams RS, Moncalian G, Williams JS, Yamada Y, Limbo O, Shin DS, et al. Mre11 dimers coordinate DNA end bridging and nuclease processing in double-strand-break repair. Cell. 2008;135(1):97-109. PMCID: 2681233.
54. Hopfner KP, Craig L, Moncalian G, Zinkel RA, Usui T, Owen BA, et al. The Rad50 zinc-hook is a structure joining Mre11 complexes in DNA recombination and repair. Nature. 2002;418(6897):562-6.
55. Rooney S, Sekiguchi J, Whitlow S, Eckersdorff M, Manis JP, Lee C, et al. Artemis and p53 cooperate to suppress oncogenic N-myc amplification in progenitor B cells. Proc Natl Acad Sci U S A. 2004;101(8):2410-5. PMCID: 356964.
56. McVey M, Lee SE. MMEJ repair of double-strand breaks (director's cut): deleted sequences and alternative endings. Trends Genet. 2008;24(11):529-38.
57. Bennardo N, Cheng A, Huang N, Stark JM. Alternative-NHEJ is a mechanistically distinct pathway of mammalian chromosome break repair. PLoS Genet. 2008;4(6):e1000110. PMCID: 2430616.

58. Xie A, Kwok A, Scully R. Role of mammalian Mre11 in classical and alternative nonhomologous end joining. Nat Struct Mol Biol. 2009;16(8):814-8. PMCID: 2730592.
59. Rass E, Grabarz A, Plo I, Gautier J, Bertrand P, Lopez BS. Role of Mre11 in chromosomal nonhomologous end joining in mammalian cells. Nat Struct Mol Biol. 2009;16(8):819-24.
60. Della-Maria J, Zhou Y, Tsai MS, Kuhnlein J, Carney JP, Paull TT, et al. Human Mre11/human Rad50/Nbs1 and DNA ligase IIIalpha/XRCC1 protein complexes act together in an alternative nonhomologous end joining pathway. J Biol Chem. 2011;286(39):33845-53. PMCID: 3190819.
61. Povirk LF. Biochemical mechanisms of chromosomal translocations resulting from DNA double-strand breaks. DNA Repair (Amst). 2006;5(9-10):1199-212.
62. Corneo B, Wendland RL, Deriano L, Cui X, Klein IA, Wong SY, et al. Rag mutations reveal robust alternative end joining. Nature. 2007;449(7161):483-6.
63. Yan CT, Boboila C, Souza EK, Franco S, Hickernell TR, Murphy M, et al. IgH class switching and translocations use a robust non-classical end-joining pathway. Nature. 2007;449(7161):478-82.
64. Truong LN, Li Y, Shi LZ, Hwang PY, He J, Wang H, et al. Microhomology-mediated End Joining and Homologous Recombination share the initial end resection step to repair DNA double-strand breaks in mammalian cells. Proc Natl Acad Sci U S A. 2013;110(19):7720-5. PMCID: 3651503.
65. Paull TT, Gellert M. A mechanistic basis for Mre11-directed DNA joining at microhomologies. Proc Natl Acad Sci U S A. 2000;97(12):6409-14. PMCID: 18616.
66. Hopfner KP, Karcher A, Craig L, Woo TT, Carney JP, Tainer JA. Structural biochemistry and interaction architecture of the DNA double-strand break repair Mre11 nuclease and Rad50-ATPase. Cell. 2001;105(4):473-85.
67. Shibata A, Moiani D, Arvai AS, Perry J, Harding SM, Genois MM, et al. DNA double-strand break repair pathway choice is directed by distinct MRE11 nuclease activities. Mol Cell. 2014;53(1):7-18. PMCID: 3909494.
68. Stracker TH, Petrini JH. The MRE11 complex: starting from the ends. Nat Rev Mol Cell Biol. 2011;12(2):90-103.
69. Yu W, Nagaoka H, Jankovic M, Misulovin Z, Suh H, Rolink A, et al. Continued RAG expression in late stages of B cell development and no apparent re-induction after immunization. Nature. 1999;400(6745):682-7.
70. Nagaoka H, Yu W, Nussenzweig MC. Regulation of RAG expression in developing lymphocytes. Curr Opin Immunol. 2000;12(2):187-90.
71. Rooney S, Chaudhuri J, Alt FW. The role of the non-homologous end-joining pathway in lymphocyte development. Immunol Rev. 2004;200:115-31.
72. Rooney S, Alt FW, Sekiguchi J, Manis JP. Artemis-independent functions of DNA-dependent protein kinase in Ig heavy chain class switch recombination and development. Proc Natl Acad Sci U S A. 2005;102(7):2471-5. PMCID: 548986.
73. Lista F, Bertness V, Guidos CJ, Danska JS, Kirsch IR. The absolute number of trans-rearrangements between the TCRG and TCRB loci is predictive

of lymphoma risk: a severe combined immune deficiency (SCID) murine model. Cancer Res. 1997;57(19):4408-13.
74. Kang J, Bronson RT, Xu Y. Targeted disruption of NBS1 reveals its roles in mouse development and DNA repair. EMBO J. 2002;21(6):1447-55. PMCID: 125926.
75. Kang J, Ferguson D, Song H, Bassing C, Eckersdorff M, Alt FW, et al. Functional interaction of H2AX, NBS1, and p53 in ATM-dependent DNA damage responses and tumor suppression. Mol Cell Biol. 2005;25(2):661-70. PMCID: 543410.
76. Jacobs C, Huang Y, Masud T, Lu W, Westfield G, Giblin W, et al. A hypomorphic Artemis human disease allele causes aberrant chromosomal rearrangements and tumorigenesis. Hum Mol Genet. 2011;20(4):806-19. PMCID: 3024049.
77. Yin B, Yang-Iott KS, Chao LH, Bassing CH. Cellular context-dependent effects of H2ax and p53 deletion on the development of thymic lymphoma. Blood. 2011;117(1):175-85. PMCID: 3037742.
78. Woo Y, Wright SM, Maas SA, Alley TL, Caddle LB, Kamdar S, et al. The nonhomologous end joining factor Artemis suppresses multi-tissue tumor formation and prevents loss of heterozygosity. Oncogene. 2007;26(41):6010-20.
79. Fattah F, Lee EH, Weisensel N, Wang Y, Lichter N, Hendrickson EA. Ku regulates the non-homologous end joining pathway choice of DNA double-strand break repair in human somatic cells. PLoS Genet. 2010;6(2):e1000855. PMCID: 2829059.
80. Yeo JE, Lee EH, Hendrickson E, Sobeck A. CtIP mediates replication fork recovery in a FANCD2-regulated manner. Hum Mol Genet. 2014.
81. Bruhn C, Zhou ZW, Ai H, Wang ZQ. The essential function of the MRN complex in the resolution of endogenous replication intermediates. Cell Rep. 2014;6(1):182-95.
82. Zeman MK, Cimprich KA. Causes and consequences of replication stress. Nat Cell Biol. 2014;16(1):2-9.
83. Srinivasan SV, Dominguez-Sola D, Wang LC, Hyrien O, Gautier J. Cdc45 is a critical effector of myc-dependent DNA replication stress. Cell Rep. 2013;3(5):1629-39. PMCID: 3822004.
84. Spehalski E, Kovalchuk AL, Collins JT, Liang G, Dubois W, Morse HC, 3rd, et al. Oncogenic Myc translocations are independent of chromosomal location and orientation of the immunoglobulin heavy chain locus. Proc Natl Acad Sci U S A. 2012;109(34):13728-32. PMCID: 3427096.

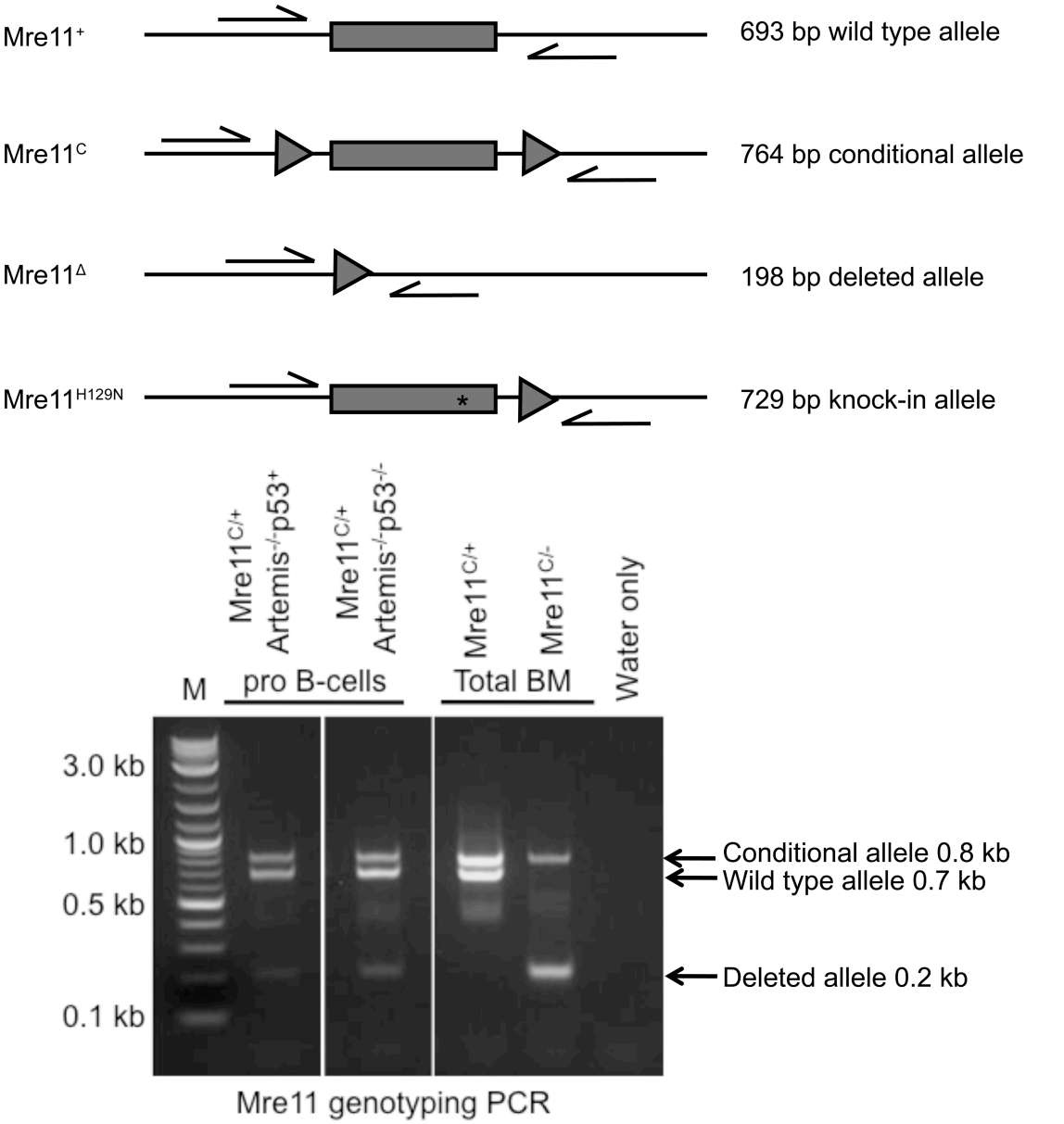

Figure 3.1 B lineage deletion of MRE11 in B-cells deficient for ARTEMIS or ARTEMIS and p53. Total bone marrow was isolated from 3-5 week old *Mre11*$^{C/+}$ *Artemis*$^{-/-}$*p53*$^{-/+}$;CD19 Cre mice or *Mre11*$^{C/+}$ *Artemis*$^{-/-}$*p53*$^{-/-}$;CD19 Cre mice and sorted into pro-B cell populations using B-cell surface stains. Total bone marrow was also isolated from 3-5 week old *Mre11*$^{C/+}$ and *Mre11*$^{C/-}$ mice (Lacking CD19 Cre). Genomic DNA was isolated and subjected to polymerase chain reaction (PCR) using primers flanking the *Mre11* locus. The upper panel of this figure represents the primer location along the *Mre11* locus and the expected product size. The lower part of the panel is the result of the PCR reaction on the selected DNAs. I am able to detect the *Mre11* deleted allele in pro-B cells harboring the CD19 Cre recombinase transgene. Arrows indicate expected *Mre11* allele sizes. M, standard lane marker (2 kb ladder); BM, bone marrow.

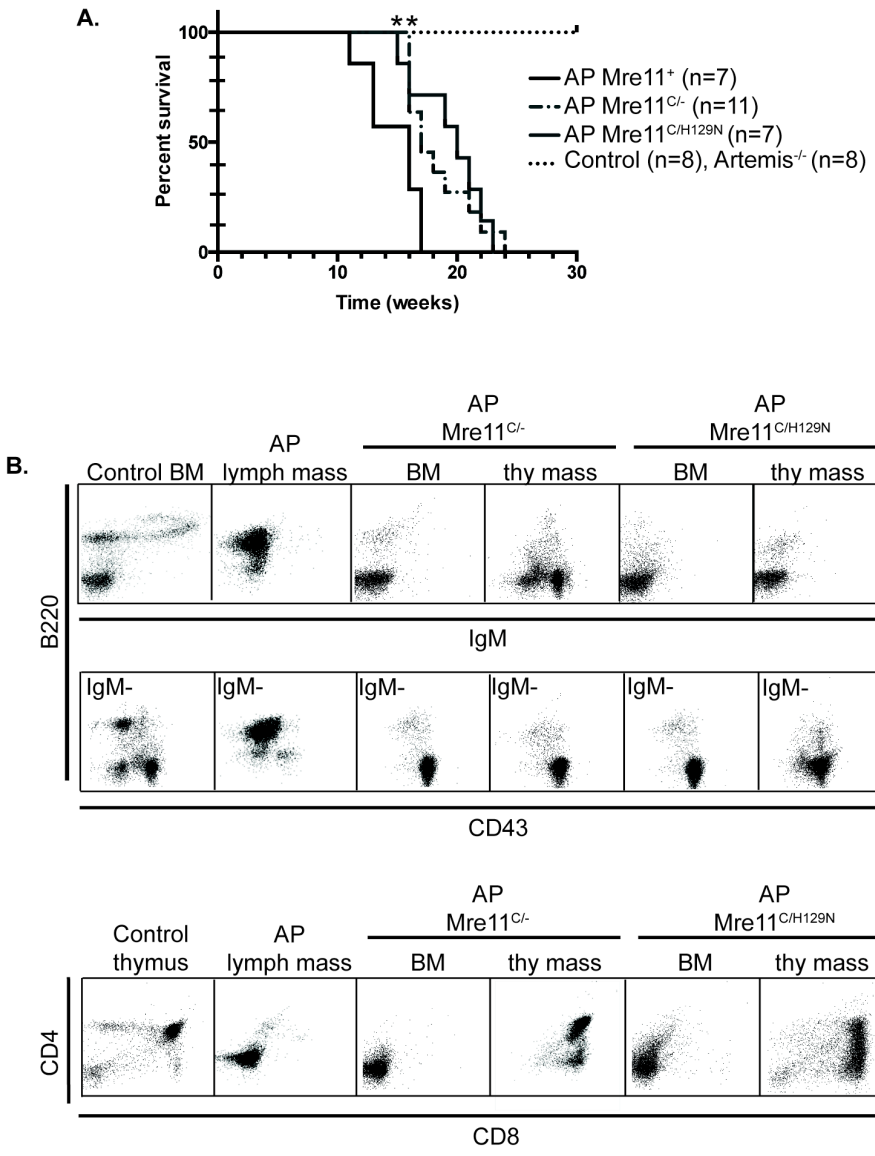

Figure 3.2. MRE11 B-cell specific mutation combined with AP mice suppresses pro B lymphoma. (**A)** Shown are Kaplan-Meier survival curves representing the percent survival of cohort mice versus age in weeks. Survival of a cohort of Control (n=8), *Artemis*$^{-/-}$ (n=8), *AP*, (n=7), *AP Mre11*$^{C/-}$ (n=11), and *AP Mre11*$^{C/H129N}$ (n=7) mice was observed for a period of 40 weeks. All mice contain the CD19 Cre transgene. Comparison of survival curves using the Log rank (Mantel-Cox) test indicate *AP Mre11*$^{C/-}$ and *AP Mre11*$^{C/H129N}$ mice survive significantly longer than *AP* mice. **(B)** Representative flow cytometric analysis of primary tumors. Tumors from *AP Mre11*$^{C/-}$ and *AP Mre11*$^{C/H129N}$ mice do not stain for B-cell markers, rather for T-cell cell markers.

Tumor spectrum in AP Mre11 mutant mice

Tumor type	Artemis$^{-/-}$	AP	AP Mre11$^{C/-}$	AP Mre11$^{C/H129N}$
pro-B lymphoma	0	6	0	0
TCRβ^{-} thymic lymphoma	0	4	11	7
Solid tumors	0	0	1	0
Total number of tumors	0	10	12	7

Figure 3.3 Tumor spectrum in *AP Mre11* mutant mice. Primary tumors were dissociated into single cells and stained for T- and B-cell surface markers and analyzed using flow cytometric analysis. The results from flow cytometry were used to characterize tumor type and the results are annotated above.

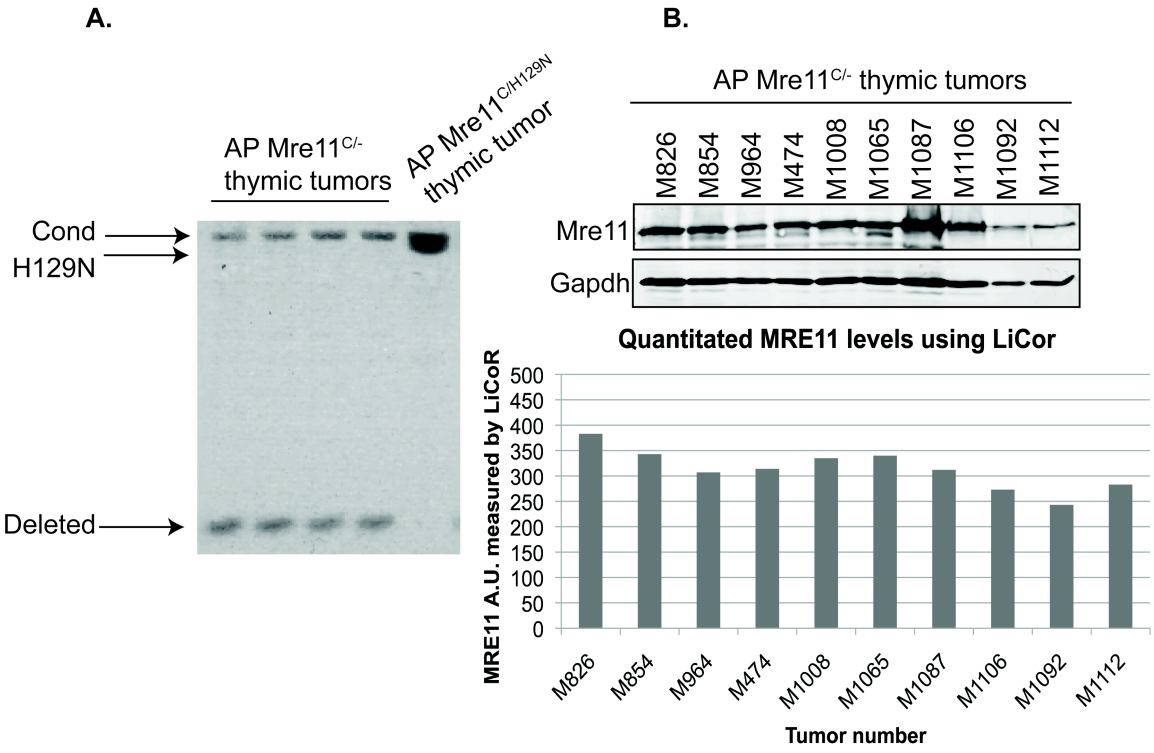

Figure 3.4 *Mre11* conditional allele retained in thymic tumors from *AP Mre11$^{C/-}$* and *AP Mre11$^{C/H129N}$* mice. (A) Representative polymerase chain reaction (PCR) of primary tumors identified the presence of the conditional allele in *AP Mre11$^{C/-}$ mice*, and in tumors isolated from *AP Mre11$^{C/H129N}$* mice, the absence of the deleted allele indicating minimal deletion of the *Mre11^{C}* allele. In *AP Mre11$^{C/H129N}$* mice the conditional and H129N allele are only separated by 50 base pairs, and on this agarose gel appear as a doublet. **(B)** Protein lysates of primary tumors were isolated and analyzed on a polyacrylamide gel (8%). Western analysis of primary tumors did not detect severely reduced levels of MRE11 in *AP Mre11$^{C/-}$* mice. Quantitation of MRE11 levels graphed below in **B**. Arbitrary units (A.U.) measured by LiCoR software.

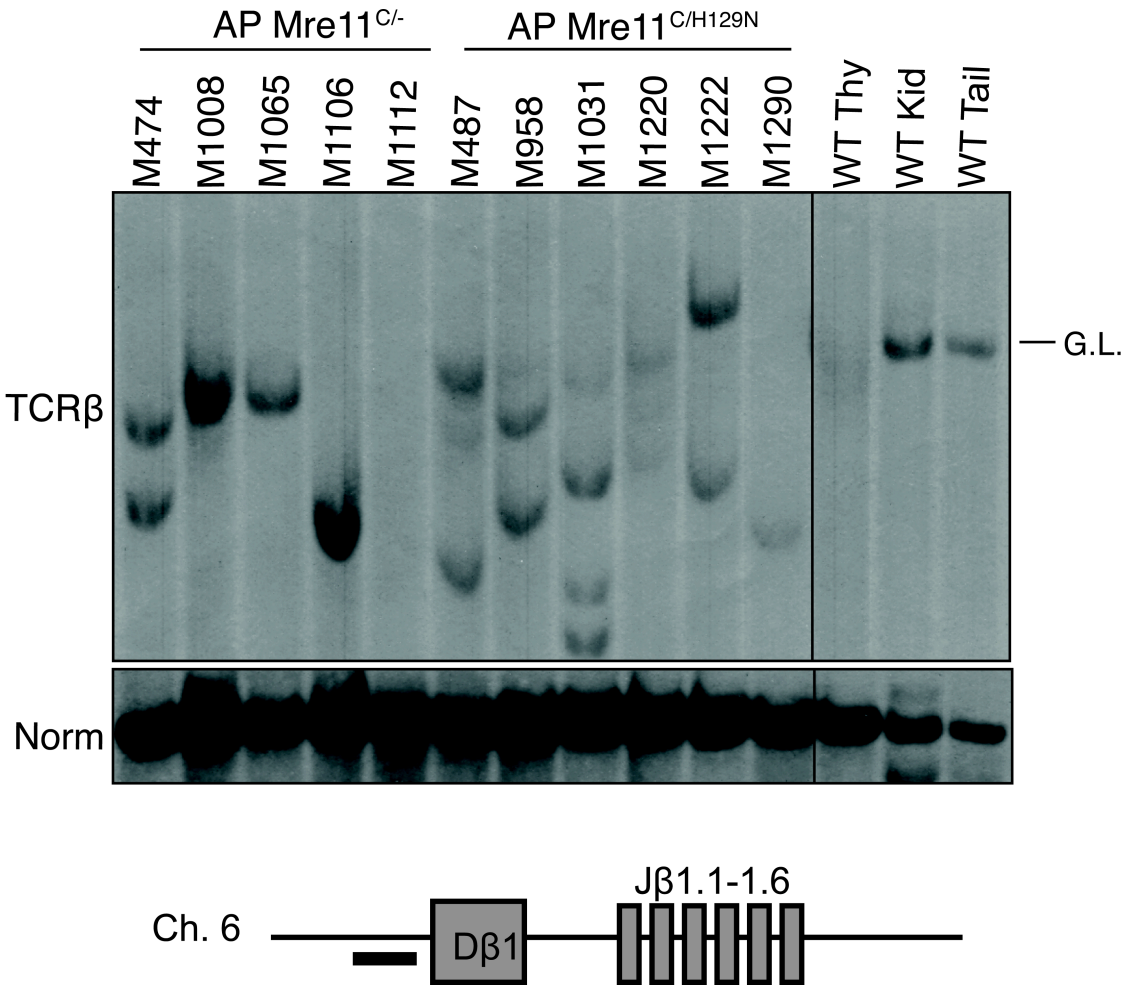

Figure 3.5. Clonal rearrangements detected at the TCRβ Dβ1-Jβ1 locus. Genomic DNA isolated from primary tumors was digested with Eco*RI* then analyzed by Southern blotting. Dβ1 to Jβ1 rearrangements were detected using a probe located 5' of the Dβ1 segment (diagrammed above). Individual tumors are indicated, top; Thymus, kidney, and bone marrow (BM), control tissues; GL, unrearranged, germline band. Amounts of input DNA were normalized to a non-rearranging locus (LR8).

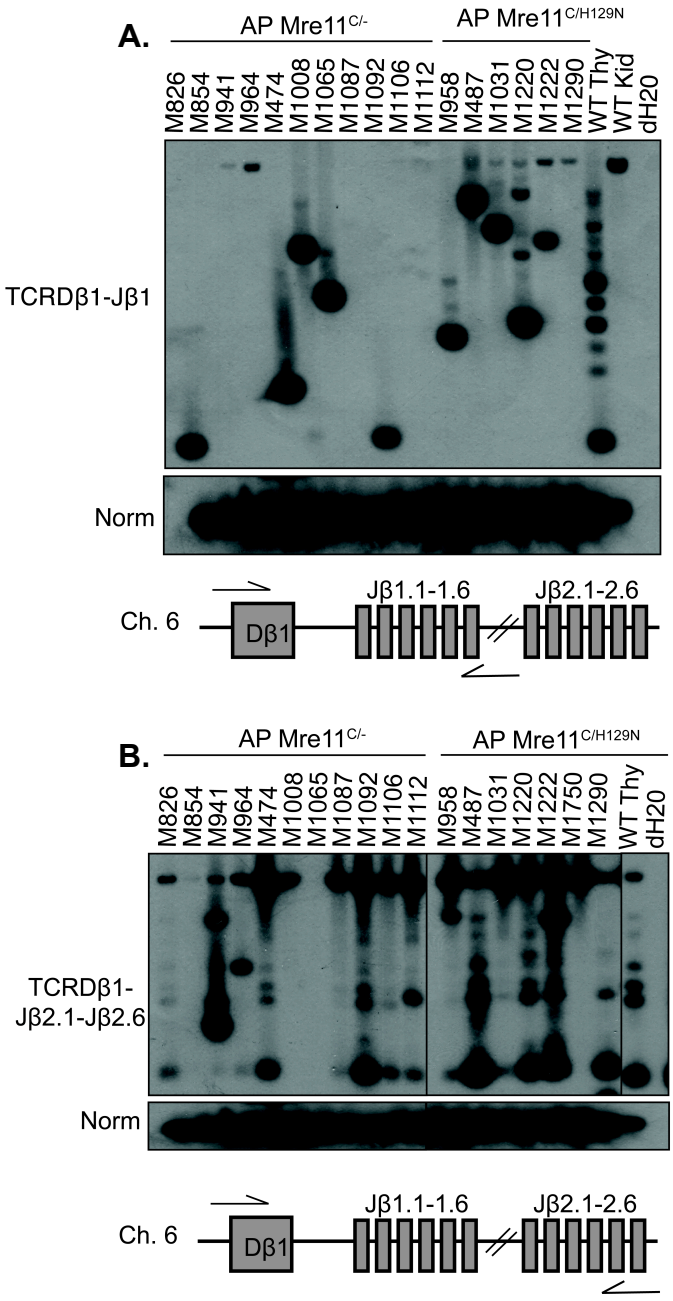

Figure 3.6 Clonal V(D)J rearrangements detected at the TCR Dβ1-Jβ1 and TCR Dβ2-Jβ2 loci. (A) Genomic DNA was isolated from primary tumors and analyzed by polymerase chain reaction (PCR) for TCRβ Dβ1-Jβ1 rearrangements on chromosome 6 using the primer scheme diagrammed. The majority of thymic tumors exhibited D-Jβ rearrangements harboring specific attempted rearrangements. **(B)** Genomic DNA was isolated from primary tumors and analyzed by polymerase chain reaction (PCR) for TCRβ Dβ2-Jβ2 rearrangements on chromosome 6 using the primer scheme diagrammed. Some tumors (M474, M1092, M487, M1220, M1222) exhibited several Dβ2-Jβ2 rearrangements suggesting multiple attempted rearrangements or polyclonality.

AP Mre11$^{C/-}$ thymic tumors: Dβ-Jβ1 PCR

Tumor#	TCRDβ1 GACAGGGGGC	N Additions	TCRJβ1.1 CAAACACAGA	Unique Seqs
M1008	GACAGGGGG**C**		CAAACACAGA	2
Tumor#	TCRDβ1 GACAGGGGGC		TCRJβ1.3 TTCTGGAAAT	Unique Seqs
M1087	GACAGGGGGCGC		(-13)CTCTA	1
Tumor#	TCRDβ1 GACAGGGGGC		TCRJβ1.4 TTTCCAACGA	Unique Seqs
M1065	GACAGGGGGCGCC		(-141)CGGGC	1
Tumor#	TCRDβ1 GACAGGGGGC		TCRJβ1.5 TAACAACCAG	Unique Seqs
M964	GACAGGGGGC	CA	(-59)GGGACA	1
M474	GACAGGGGGCG		(-313)CCCCC	1
Tumor#	TCRDβ1 GACAGGGGGC		TCRJβ1.6 TTCCTATAATT	Unique Seqs
M826	GACAGG		AATTCCTATAATT	1
M854	GACAGG		AATTCCTATAATT	1
M1008	GACAGGGG	T	(-121)CTTAG	1

Bold/underlined=microhomology
Encircled text=P-nucleotide addition

AP Mre11$^{C/H129N}$ thymic tumors: Dβ-Jβ1 PCR

Tumor#	TCRDβ1 GACAGGGGGC	N Additions	TCRJβ1.1 CAAACACAGA	Unique Seqs
M1220	GACAGGGGGCGC		(-6)CAGA	2
M487	GACAGG		(-5)ACAGA	1
Tumor#	TCRDβ1 GACAGGGGGC		TCRJβ1.3 TTCTGGAAAT	Unique Seqs
M1031	GACAGGGGGCGCCCCCT	A	AATTCTGGAAAT	1
Tumor#	TCRDβ1 GACAGGGGGC		TCRJβ1.4 TTTCCAACGA	Unique Seqs
M1112	GACAGGGGG		AAATTTCCAACGA	1
Tumor#	TCRDβ1 GACAGGGGGC		TCRJβ1.5 TAACAACCAG	Unique Seqs
M958	GACAGGG**GG**		(-73)GGGACA	1
M1220	GACAGGGGGCGCCCCCTGT		GTTATAACAACCAG	1
Tumor#	TCRDβ1 GACAGGGGGC		TCRJβ1.6 TTCCTATAATT	Unique Seqs
M1092	GACAGGGGGCGGC		CCTATAATT	1

Bold/underlined=microhomology
Encircled text=P-nucleotide addition

Figure 3.7 TCRβ D-Jβ junctional sequences of thymic lymphomas isolated from *AP Mre11*$^{C/-}$ and *AP Mre11*$^{C/H129N}$ mice. Genomic DNA was isolated from primary thymic lymphomas and TCRβ D-Jβ rearrangements amplified, subcloned, and sequenced. Many junctional sequences isolated are qualitatively similar to junctional sequences isolated from *Artemis*$^{-/-}$ thymocytes due presence of small and large deletions, P-nucleotide addition, and a few (2/15) sequences with microhomology (32). P-nucleotides denoted by circle; bold, underline indicates microhomology.

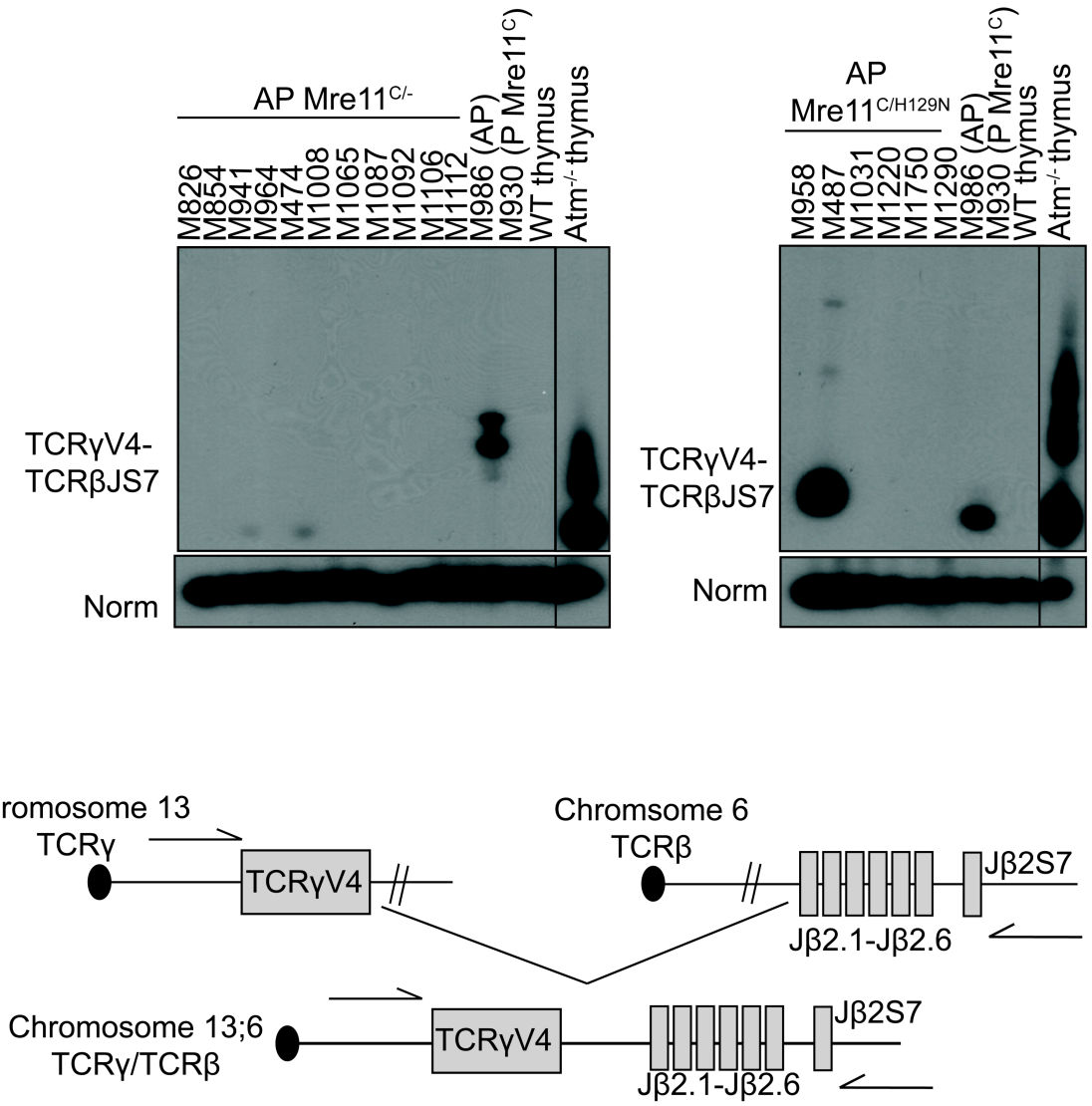

Figure 3.8 Trans-rearrangements between TCRγV3S1 and TCRβJ2 in thymic lymphomas from *AP Mre11$^{C/-}$* and *AP Mre11$^{C/H129N}$* mice. Genomic DNA was isolated from primary tumors and analyzed by polymerase chain reaction (PCR) as described previously (76). *AP Mre11$^{C/-}$* and *AP Mre11$^{C/H129N}$* mice exhibited detectable levels of trans-rearrangements. M986 is an AP pro-B lymphoma and M930 is a thymic lymphoma from a *p53$^{-/-}$Mre11$^{C/C}$*; CD19 Cre mouse.

Bold/underlined=microhomology
Encircled text=P-nucleotide addition

Mre11	Tumor#	TCRγV4 CGGCTAAAGC	N Additions	TCRβJS7 CCTCTGTGCT	# times seqs observed
$Mre11^{C/H129N}$	M487	CGGCTAAAGC	TCCTAAA	GCT	24
$Mre11^{C/+}$	M986	(-18)AG**T**		TCA(-19)	24
$Mre11^{C/\Delta}$	M474	CGG**CTA**		CTA(-11)	22
$Mre11^{C/\Delta}$	M941	CGGCT	CCCCTGTCCCGGTT	GCT	1
	M941	CGGCTAAA	TC	(-13)	2
	M941	CGGCTAAA	TGCGCCCCCCCACTTC	(-12)	1
	M941	CGGC	GCAAGGG	(-12)	1
	M941	CGGCTAAA	TTCACCCCAGG	(-14)	1
	M941	CGGCTAAA	CCCCAGG	(-14)	1
	M941	CGGCTAAAG**C**		CCTCTGTGCT	1
	M941	CGGCT	CT	(-12)	1
	M941	CG	T	(-13)	1
	M941	CGGCTAAA	TTAGGT	(-12)	2
	M941	CGGCTAA		(-12)	1

Mre11	Tumor#	TCRγV4 CGGCTAAAGC		TCRβJ2.4 AGTCAAAACA	
$Mre11^{C/\Delta}$	M941	CGGCTAAAGC	ATGGGG	CA	1
	M941	CG	TCTC	GTCAAAACA	1
	M941	CGGCTAA	ATGGCGG	CAAAACA	1
	M941	(-34)	TTC	(-15)	1

Mre11	Tumor#	TCRγV4 CGGCTAAAGC		TCRβJ2.5 AACCAAGACA	
$Mre11^{C/\Delta}$	M941	CGGC(C)	T	(TT)AACCAAGACA	1
	M941	CGGGC	GA	CAAGACA	1
	M941	CGGCT	GTCCGGG	ACA	1
	M941	CGGCTAAA	CCTC	CCAAGACA	1
	M941	(-31)(CG)		(-27)	1

Figure 3.9 Sequences of trans-rearrangements between TCRγV3S1 and TCRβJ2 in thymic lymphomas from *AP Mre11*$^{C/-}$ and *AP Mre11*$^{C/H129N}$ mice. Genomic DNA was isolated from primary tumors, analyzed by polymerase chain reaction (PCR) as described previously (76), and the products subcloned and sequenced. Sequences isolated are qualitatively similar to D to Jβ junctional sequences observed in *Artemis*$^{-/-}$ thymocytes due to small deletions, minimal P-nucleotide addition, and few (3/23) sequences with microhomology (32). P-nucleotides denoted by circle; bold, underline indicates microhomology.

A.

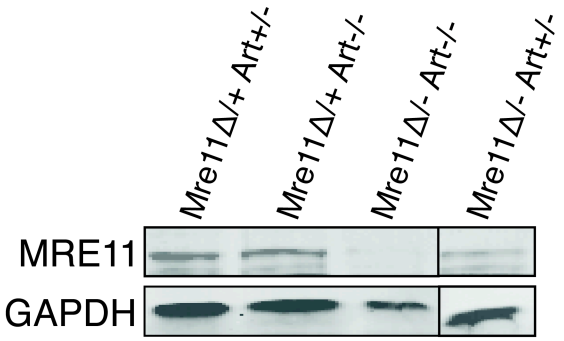

B.

Table	Mre11+/-	Mre11Δ/-	Art-/-Mre11Δ/-
Type of anomaly			
Chromatid break/gaps	18	70	206
Chromosome breaks/gaps	4	15	21
Radial structure	4	61	31
fragment	9	29	25
Total anomalies	35	175	283
Metaphase#	34	98	59

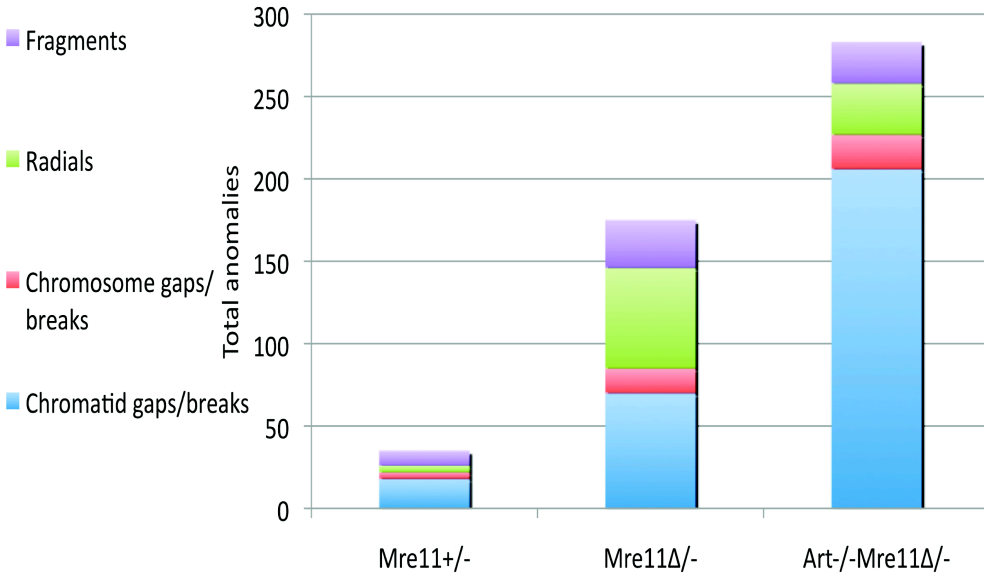

Figure 3.10 Spontaneous chromosomal aberrations in ARTEMIS/MRE11 mutant primary MEFS. (A) Primary MEFs were treated with adenovirus expressing Cre recombinase to delete the *Mre11*^{C} allele. Representative Western blot for MRE11 levels post adenovirus Cre treatment. **(B)** Metaphases were scored for chromosomal anomalies. The total number of anomalies and type of anomalies observed are listed above in a table and graph. This preliminary study suggests ARTEMIS/MRE11 mutant primary MEFs harbor additive levels of chromosomal anomalies as compared to the control and *Mre11*$^{\Delta/-}$ primary MEFs.

Supplementary Figure 3S11

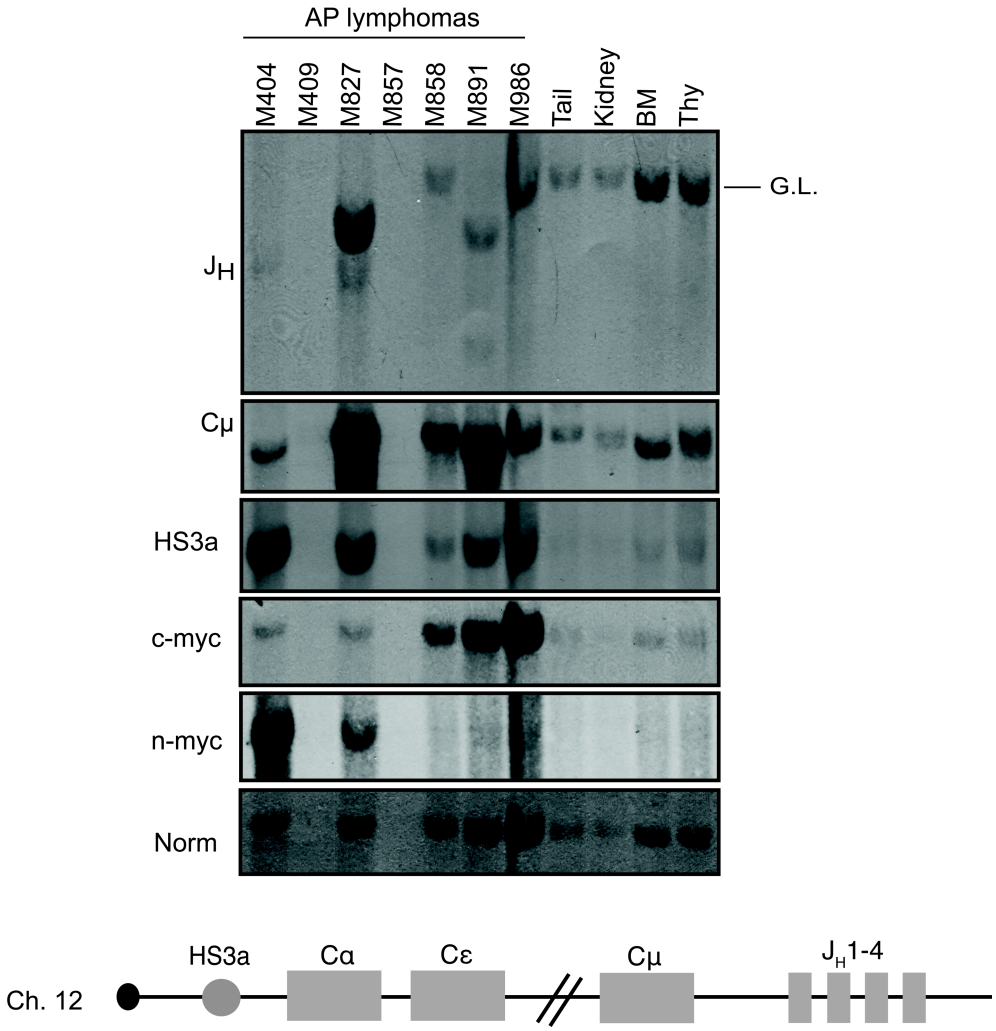

Supplementary Figure 3S11. Genomic amplification of the IgH locus and *c-myc* or *n-myc* in *AP* pro-B lymphomas. Genomic DNA was isolated from primary tumors, digested with *EcoRI* and hybridized with probes along chromosome 12, within the IgH locus (diagrammed above) or *c-myc* or *n-myc*. Characteristic amplification of the IgH locus involving the J_H cluster, Cμ, and enhancer HS3a observed in 5/7 tumors. Amplification of *c-myc* or *n-myc* observed in 5/7 tumors. Amplification was determined by comparing values to a non-rearranging locus, LR8.

Supplementary Figure 3S12

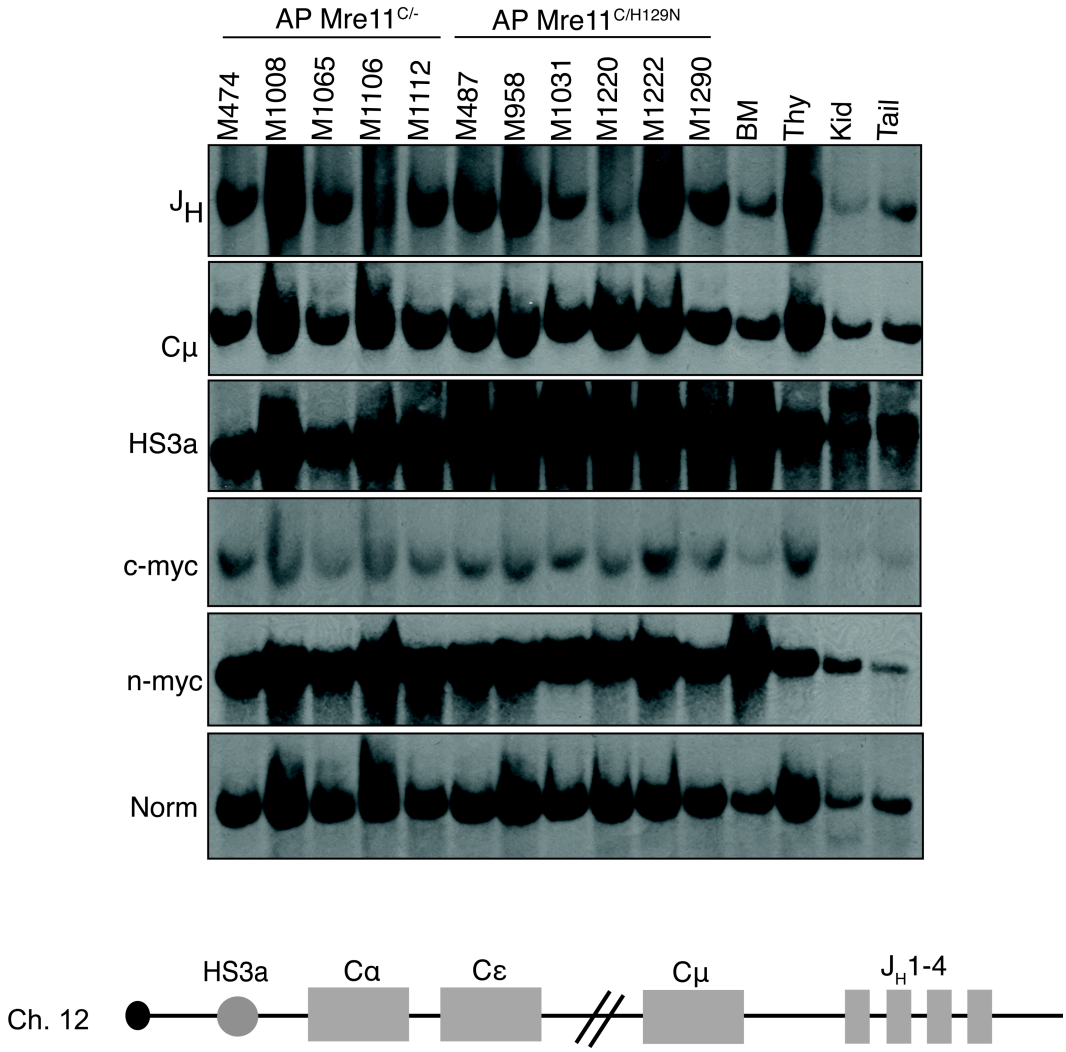

Supplementary Figure 3S12. Genomic amplification not detected within the IgH locus and *c-myc* or *n-myc* in *AP Mre11$^{C/-}$* or in *AP Mre11$^{C/H129N}$* thymic lymphomas. Genomic DNA was isolated from primary tumors, digested with *EcoR*I and hybridized with probes along chromosome 12, within the IgH locus (diagrammed above), or *c-myc* or *n-myc*. No apparent amplification of the IgH locus or *c-myc* or *n-myc* detected. Band intensities were normalized to a non-rearranging locus, LR8.

Supplementary Figure 3S13

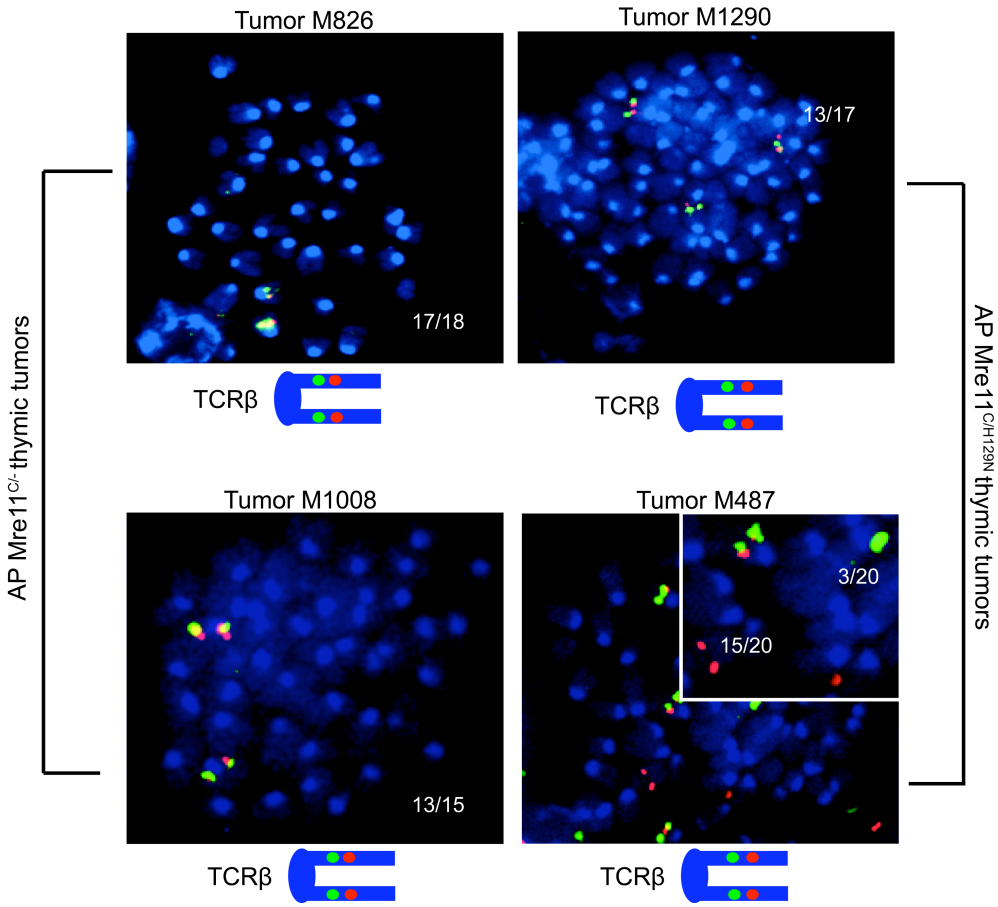

Supplementary Figure 3S13. TCRβ flanking FISH probes hybridized to thymic lymphomas from *AP Mre11$^{C/-}$* and *AP Mre11$^{C/H129N}$* mice. Metaphases were either obtained from the primary lymphoma cultures on day 0 or from cultures grown for two days in the presence of IL-7 and IL-2. BAC probes hybridizing to TCRβ are as follows: RPCI 23 216J19 (spans TRBD1-TRBV31--green) and RP23 61N4 (spans TCRDβ-TCRJβ--red) (76). Due to the location of the probes, colocalization indicates repaired RAG1/2-generated breaks while separated probe signals suggest misrepair of RAG1/2-generated breaks. Values in figures adjacent to images indicate the frequency of the observed event.

Supplementary Figure 3S14

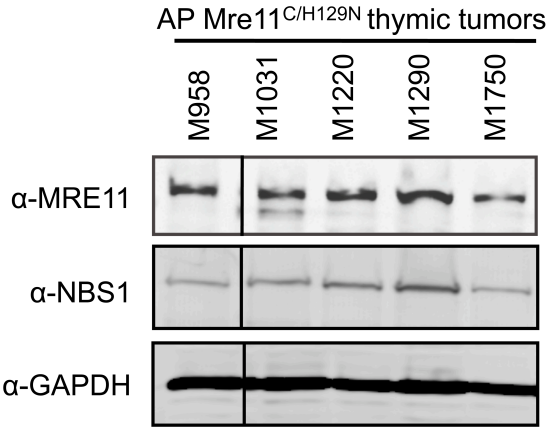

Supplementary Figure 3S14. MRE11 complex levels in *AP Mre11$^{C/H129N}$* thymic tumors. Protein lysates were isolated from primary tumors and analyzed on a polyacrylamide gel (8%). Antibodies to the MRE11 complex including MRE11 and NBS1 were used to analyze levels of the MRE11 complex (52). Previous reports indicate that the *Mre11^{H129N}* allele does not reduce MRE11 complex levels (52). I did not detect reduced levels of the MRE11 complex in thymic lymphomas from *AP Mre11$^{C/H129N}$* mice.

Supplementary Figure 3S15

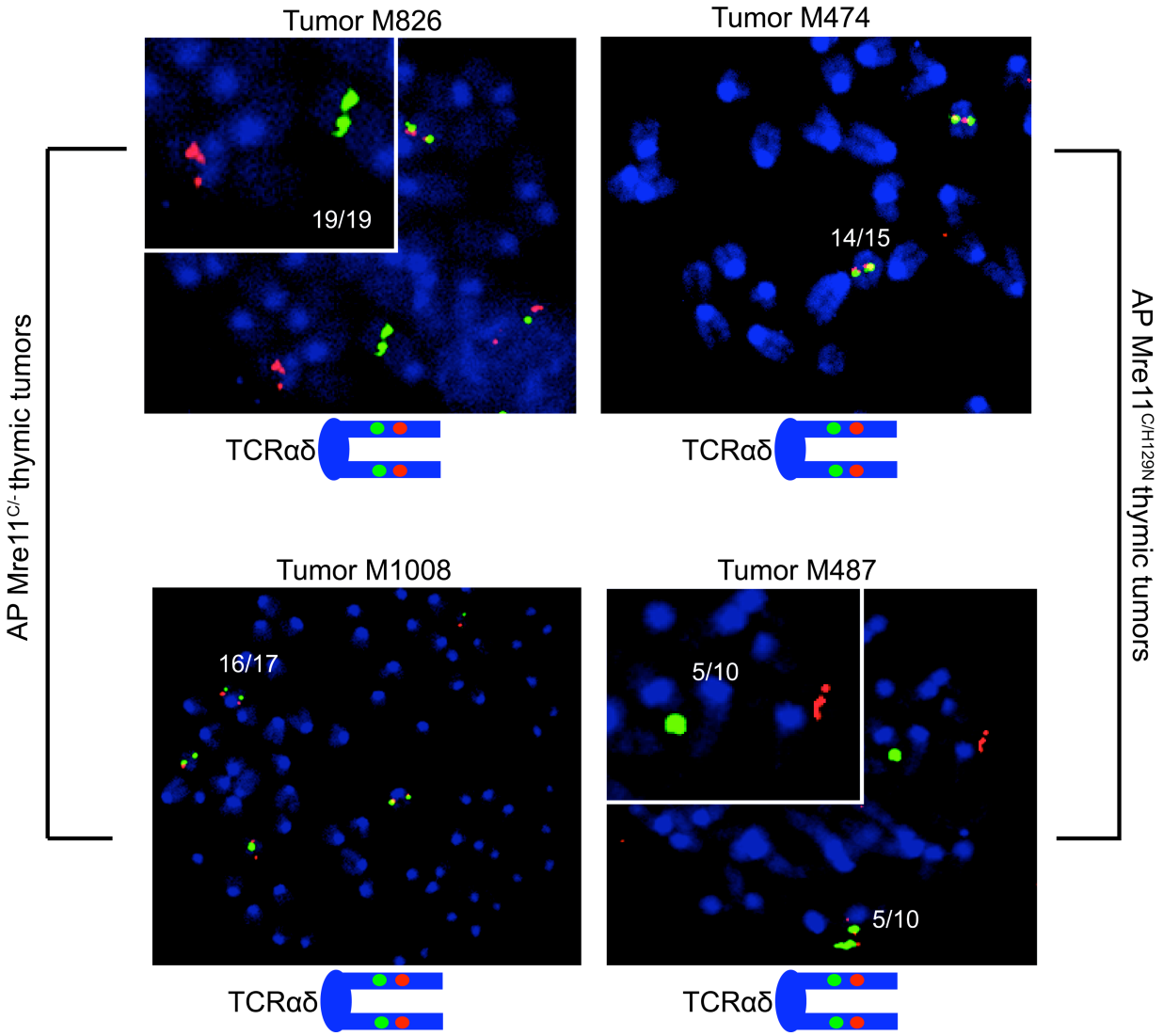

Supplementary Figure 3S15. TCRαδ flanking FISH probes hybridized to thymic lymphomas from *AP Mre11*$^{C/-}$ and *AP Mre11*$^{C/H129N}$ mice. Metaphases were either obtained from the primary lymphoma cultures on day 0 or from cultures grown for two days in the presence of IL-7 and IL-2. BAC probes hybridizing to TCRα/δ are as follows: RPCI 23 204N18 (centromeric to TCRα/δ region--green) and RPCI 23 269E2 (telomeric to TCRα/δ region--red) (76). Due to the location of the probes, colocalization indicates repaired RAG1/2-generated breaks while separated probe signals suggest misrepair of RAG1/2-generated breaks. Values in figures adjacent to images indicate the frequency of the observed event.

Supplementary Figure 3S16

Artemis$^{-/-}$p53$^{-/-}$Mre11$^{C/C}$ mutant mice			
Mouse #	Age at death (weeks)	Observation	FACs Analysis
M430	12	Enlarged thy (did not fill chest cavity) and enlarged spl; distended abd	CD4+, CD8+, TCRβ- (thy); B220+, IgM- (LN, thy, BM, spleen)
M471	14, 5 days	Enlarged thymus	CD4+ CD8+, TCRβ-
M1331	10, 3 days	Enlarged LNs	B220+, CD43+, IgM-
M1434	10, 1 day	Enlarged LNs	B220+, CD43+, IgM-
1659	13, 2 days	Enlarged LNs and spleen	B220+, CD43+, IgM-
1704	13, 2 days	Enlarge LNs and spleen; Enlarged thymus (does not fill the chest cavity); lower limb paralysis	B220+, CD43+, IgM-

No CD19 Cre Transgene			
Artemis$^{-/-}$p53$^{-/-}$Mre11C mutant mice			
Mouse #	Age at death (weeks)	Observation	FACs Analysis
M851	11, 5 days	Enlarged LNs	B220+, CD43+, IgM-
M931	14, 3 days	large LN, thymus, spleen, and liver	B220+, IgM-, +CD43
M967	12	Large LN and abdomen aceites	B220+, CD43+, IgM-
M432	8, 1 day	Large LN, spl, and liver	B220+, IgM-, CD43+
M481	10, 2 days	Enlarged LNs and spleen	B220+, CD43+, IgM-
M493	9	Enlarged LNs and spleen. Mass on rht shoulder	B220+, CD43+, IgM-
M1184	16, 2 days	Enlarged LNs, thymus and spleen	B220+, CD43+, IgM-
M1550	11, 1 day	Enlarged LNs	B220+, CD43+, IgM-

Supplementary Figure 3S16. *AP Mre11^{C}* mice, with or without CD19 Cre transgene are predisposed to pro-B lymphoma. A majority of mice succumb to pro-B lymphoma as previously described (55, 76).

IV. CHAPTER 4

Impact of Artemis and Mre11 on lymphocyte development, DNA end processing, and genome stability

Cheryl Jacobs Smith[1], Jeffrey Xie[2], and JoAnn M. Sekiguchi[1,3]

[1]Department of Human Genetics, [2]University of Michigan and [3]Internal Medicine, University of Michigan Medical School, Ann Arbor, MI 48109, USA

Smith (Jacobs) contribution: Figures 4.1-4.3

Abstract

Maintaining the integrity of the genome is crucial in ensuring cellular homeostasis. One of the most cytotoxic forms of genomic damage is the DNA double strand break (DSB). DSBs are generated as a result of exposure to exogenous and endogenous DNA damaging agents. In addition, programmed DSBs arise by highly regulated processes such as V(D)J recombination, a DNA rearrangement that is necessary for the development of mature T- and B-lymphocytes. If unrepaired or misrepaired, DSBs can lead to increased genome instability and accumulation of aberrant chromosomal rearrangements which can result in severely detrimental outcomes for cells and organisms. Classical non-homologous end-joining (cNHEJ) is one of the major DNA repair pathways and is required for both general DSB repair and V(D)J recombination.

In the cNHEJ pathway, ARTEMIS is a nuclease that plays important roles in processing broken DNA ends during DSB repair and V(D)J recombination. The intrinsic endonucleolytic activity of ARTEMIS is activated upon interaction with the DNA-PKcs protein kinase. ARTEMIS:DNA-PKcs is likely the active form of the nuclease and nicks the hairpin coding ends formed during V(D)J recombination as well as cleaves a subset of modified ends during repair of spontaneous or induced breaks. Like ARTEMIS, the MRE11 repair factor is a DNA nuclease and the intrinsic endonucleolytic and exonucleolytic activities act on hairpinned ends as well as 3' and 5' overhangs. It functions within the context of the MRE11/RAD50/NBS1 complex (MRE11 complex) that plays multiple, critical roles in DSB repair. Additionally, the MRE11 complex has been implicated in the repair of DSBs generated during a mature B lymphocyte-specific developmental process such as class switch recombination. Recent studies extend the role for the MRE11 complex in lymphocyte development outside of class switch recombination and studies suggest that the MRE11 complex may play a role in the repair of DSBs generated during V(D)J recombination.

The goals of the studies described in this chapter are to examine the genetic and functional interactions between ARTEMIS and MRE11 in V(D)J recombination and in general DSB repair.

Introduction

The efficient repair of DNA double strand breaks (DSBs) by the classical non-homologous end joining (cNHEJ) pathway requires the intricate coordination of multiple events at DNA ends. Many chromosomal DSBs have end structures that require modification prior to joining; thus, one important event that occurs during cNHEJ is the processing of the DNA ends to prepare them for ligation by the XRCC4/LIG4/XLF complex. The ARTEMIS DNA nuclease, in complex with DNA-PKcs, plays a critical role as an endonuclease and can cleave DNA substrates at single to double strand transitions, including structures such as flaps, overhangs, loops and hairpins (1, 2). Another nuclease that has critical roles during DSB repair is MRE11 which functions in the context of the MRE11/RAD50/NBS1 complex, referred to as the MRE11 complex.

Several lines of evidence suggest that ARTEMIS and the MRE11 complex may act in concert during the repair of DNA DSBs. Upon exposure of cells to DSB-inducing agents, ARTEMIS undergoes hyperphosphorylation that is dependent on the NBS1 component of the MRE11 complex and the ATM protein kinase (3-5). This hyperphosphorylated form of ARTEMIS physically interacts with the MRE11 complex (4). ARTEMIS is required to repair a subset of modified DNA ends in the context of the cNHEJ pathway during the G1 phase of the cell cycle, and likewise, the MRE11 complex also functions in G1 DSB repair events (6). In addition, recent evidence suggests that ARTEMIS has significant roles in homologous recombination during the G2 phase of the cell cycle (5). However, the functional interactions between ARTEMIS and the MRE11 complex in DSB repair remains unclear and is a focus of investigation in this chapter.

The cNHEJ pathway is not only required during general DSB repair, but also during the lymphoid specific DNA rearrangement, V(D)J recombination. This cut and paste mechanism assembles the genes encoding the variable regions of antigen receptors from numerous V, D and J coding segments that

rearrange in a multitude of combinations (7, 8). This process is initiated by the RAG1/2 endonuclease, which induces DNA DSBs adjacent to the recombining segments. Upon RAG1/2-induced cleavage, the RAG1/2 complex remains associated with the DNA ends in a postcleavage complex (PCC) and shepherds the ends to the cNHEJ pathway (9, 10) where they are subsequently processed and joined by the ubiquitously expressed cNHEJ factors (7, 11, 12).

The subsequent end processing and joining events are coordinated within the context of DNA end bound complexes, which presumably maintain the ends in proximity to facilitate postcleavage events. The stability of DNA end bound complexes are critically important in ensuring normal V(D)J rearrangements and preventing aberrant events involving RAG1/2 generated DSBs, including chromosomal translocations. Recent evidence suggests that the MRE11 complex functions to stabilize coding ends within the PCC (13). In this regard, deficiency in the MRE11 complex results in accumulation of coding ends (14), increased levels of interchromosomal trans-rearrangements (15) and increased hybrid joining, which consists of a signal end joined to a coding end resulting in a non-productive join (14, 16).

The Sekiguchi lab developed a mouse model harboring an *Artemis* hypomorphic knock-in human disease allele, *ARTEMIS-P70*, which causes a partial immunodeficiency and predisposition to B lymphoma in patients (17). We have determined that this partial loss of function allele results in a similar phenotype to MRE11 complex deficiency, such as increased coding ends, interchromosomal rearrangements and nonproductive hybrid joining. Thus, these findings suggest that ARTEMIS and the MRE11 complex function to stabilize RAG1/2-generated ends in postcleavage complexes and may also collaborate in hairpin coding end opening and processing. However, their precise functions or functional interactions in these processes are not yet known.

In this chapter, I examine the function of the MRE11 complex and the nuclease activities of MRE11 in V(D)J recombination in the context of *Artemis* mutation. I took advantage of two distinct *Mre11* alleles, which result in different phenotypic outcomes, thereby allowing the examination of multiple functions of

MRE11 and the MRE11 complex (18). A conditionally inactivatable *Mre11* null allele, which results in depletion of MRE11 as well as the entire MRE11 complex, was used in addition, to an allele containing a single amino acid change that inactivates nuclease activities, $Mre11^{H129N}$. The $Mre11^{H129N}$ allele retains MRE11 complex formation and properties such as DNA end bridging/tethering as well as ATM signaling functions, yet is deficient for direct DNA repair activities (18). Thus, I examined the function of the entire MRE11 complex and determined the mechanistic consequences of loss of a subset of MRE11 repair activities in general DSB repair and V(D)J recombination in the presence and absence of the ARTEMIS nuclease. This chapter lays important groundwork for further investigation into the coordination of DNA end processing events between ARTEMIS and the MRE11 complex in V(D)J recombination.

Results

B lymphocyte development in ARTEMIS/MRE11 double mutant B-cells

To investigate the genetic interactions between ARTEMIS and MRE11 on B-cell development, we used well-characterized mouse models containing a *Mre11* conditional allele ($Mre11^{C}$) and a *Mre11* nuclease dead allele ($Mre11^{H129N}$). When the $Mre11^{C}$ allele is in the presence of Cre recombinase, the *Mre11* conditional allele is deleted resulting in a deficiency of the MRE11 complex (18). The $Mre11^{H129N}$ allele is a nuclease dead allele, yet the MRE11 complex is retained—thus we can differentiate between the nuclease activities of MRE11 or its additional roles within the MRE11 complex such as DNA end bridging/tethering and repair. Due to embryonic lethality associated with homozygosity of the *Mre11* null and $Mre11^{H129N}$ allele (18), we decided to take a conditional allele approach and delete the *Mre11* conditional allele in B-cells to generate the $Mre11^{\Delta/-}$ and/or the $Mre11^{\Delta/H129N}$ genotypes. We generated MRE11 mutant B-cells taking advantage of the CD19 Cre transgene which drives Cre recombinase expression from the CD19 promoter early in B-cell development and throughout B-cell maturation. Thus, we can use this cre recombinase to investigate how MRE11 and ARTEMIS coordinate DNA end processing during V(D)J recombination. To this end, I interbred MRE11 mutant alleles harboring the CD19 Cre recombinase to mice with or without the *Artemis* wild type alleles to generate $Mre11^{C/-}$;CD19 Cre mice, $Mre11^{C/H129N}$;CD19 Cre mice, $Artemis^{-/-}$ $Mre11^{C/-}$;CD19 Cre mice, $Artemis^{-/-}Mre11^{C/H129N}$;CD19 Cre mice, and $Artemis^{-/-}$;CD19 Cre mice.

To characterize the immunological defects in MRE11 mutant B-cells in the presence or absence of wild type ARTEMIS, cells from spleen and bone marrow were analyzed using monoclonal antibodies specific for lymphocyte surface markers. Consistent with previous studies that did not detect a severe defect in

lymphocyte development in *Mre11*$^{\Delta/-}$;CD19 Cre mutant B-cells and *Mre11*$^{\Delta/H129N}$;CD19 Cre mutant B-cells, we also did not detect an obvious defect in lymphocyte development in progenitor B-cells (19). The average cellularity of the *Mre11*$^{C/-}$;CD19 Cre spleen (22.7 ± 17.6 x 10^6 cells; n=3 mice) and *Mre11*$^{C/H129N}$;CD19 Cre spleen (28.3 ±12.15 x10^6 cells; n=3 mice) was comparable to the average cellularity of the control (21.4 x 10^6 cells; n=2 mice) (Figure 4.1B). Additionally, we were able to detect percentages of mature B-cells expressing IgM in the spleen of both *Mre11*$^{C/-}$;CD19 Cre mice (34.2% ± 6.5; n=3 mice) and *Mre11*$^{C/H129N}$;CD19 Cre spleen (48.5% ±12.48; n=3 mice) at percentages also reflected in the control (52.8% n=2 mice) (Figure 4.1B).

Immunoglobulin heavy chain rearrangement is initiated in IgM$^-$, pro-B cells (B220$^+$CD43$^+$) in the bone marrow. Once a functional heavy chain has been expressed, the cells progress to the pre-B cell stage (B220$^+$CD43$^-$). Here, the light chain rearranges and upon successful light chain gene assembly, a cell becomes an immature B-cell that expresses a complete IgM molecule composed of the rearranged light and heavy chains. We gated on the IgM$^-$ population and detected B220$^+$CD43$^-$ pre B-cells in MRE11 mutant B-cells containing wild type ARTEMIS activity (Figure 4.1A, lower panel). We observed that pre-B cell numbers and percentages were similar between *Mre11*$^{\Delta/-}$;CD19 Cre pre B-cells (2.93 ± 1.31 x 10^6 cells; 31.1% ± 1.18; n=3 mice) and *Mre11*$^{\Delta/H129N}$;CD19 Cre pre B-cells (2.67 ± 2.14 x10^6 cells; 23.4% ± 12.23 n=3 mice). These counts and percentages were similar to those observed in the control (2.99 x10^6 cells; 29.6%; n=2 mice). These results indicate that *Mre11*$^{\Delta/-}$;CD19 Cre B-cells and *Mre11*$^{\Delta/H129N}$;CD19 Cre B-cells are quantitatively similar to the control in regards to spleen cellularity, IgM$^+$ B-cells in the spleen, and pre B-cell counts and percentages (Figure 4.1). Thus, we could not detect an obvious defect in B-cell development in *Mre11*$^{\Delta/-}$;CD19 Cre and *Mre11*$^{\Delta/H129N}$;CD19 Cre B-cells and the MRE11 mutant B-cells developed similarly to controls.

To characterize the immunological defect in *Artemis*$^{-/-}$*Mre11*$^{\Delta/-}$;CD19 Cre B-cells and *Artemis*$^{-/-}$*Mre11*$^{\Delta/H129N}$;CD19 Cre B-cells, cells from the spleen and bone marrow were analyzed using monoclonal antibodies against cell surface

markers expressed at various stages of lymphocyte development. We gated on the IgM^- B-cell population and detected that ARTEMIS/MRE11 double mutant B-cells are blocked at early precursor stages of B-cell development. B-cells were arrested at the $B220^+CD43^+$ stage indicating a block in lymphocyte development in the pro B-cell compartment. This analysis also detected a similar block in lymphocyte development in *Artemis*$^{-/-}$;CD19 Cre B-cells (Figure 4.1A) In this regard, pro B-cell cellularity and percentages for both *Artemis*$^{-/-}$*Mre11*$^{C/-}$;CD19 Cre mice (0.91 ± 2.0 x10^6; 15.1 ± 2.38%, n=4 mice) and *Artemis*$^{-/-}$ *Mre11*$^{C/H129N}$;CD19 Cre mice (0.8 ± 0.66 x10^6; 9.1 ± 0.2%, n=7 mice) increased due to a pro B-cell developmental block absent in the control (0.39 x10^6; 3.8%, n=2 mice). In contrast, pro-B cell cellularity and percentages were quantitatively similar to *Artemis*$^{-/-}$;CD19 Cre B-cells (0.6 ± 0.44 x10^6; 7.9 ± 3.42%, n=3 mice) Lymphocytes are exquisitely programmed to undergo apoptosis as a result of developmental defects. Thus, lymphocytes that are developmentally blocked have reduced lymphocyte cellularity due to cell surveillance mechanisms that induce apoptosis as a result of defective lymphocyte development. This has consistently been reported in mutant lymphocytes harboring defects in factors critical to V(D)J recombination such as *Artemis*$^{-/-}$ (20), *DNA-PKcs*$^{-/-}$ (21), *Ku80*$^{-/-}$ (22), *Ku70*$^{-/-}$ (23), and in *Xrcc4*$^{-/-}$ lymphocytes (24). Consistent with previous reports, *Artemis*$^{-/-}$*Mre11*$^{C/-}$;CD19 Cre mice and *Artemis*$^{-/-}$*Mre11*$^{C/H129N}$;CD19 Cre mice exhibited decreased cellularity of the spleen ([*Artemis*$^{-/-}$*Mre11*$^{C/-}$;CD19 Cre spleen, 0.5 ± 0.58 x10^6, n=4 mice] [*Artemis*$^{-/-}$*Mre11*$^{C/H129N}$;CD19 Cre spleen, 0.7 ± 0.76 x10^6, n=7 mice] as compared to the control, 21.4 x 10^6, n=2 mice) (Figure 4.1B). The decreased cellularity observed in *Artemis*$^{-/-}$*Mre11*$^{C/-}$;CD19 Cre and *Artemis*$^{-/-}$*Mre11*$^{C/H129N}$;CD19 Cre spleens was quantitatively similar to the spleen cellularity (2.8 ± 0.17 x10^6, n=3) observed in *Artemis*$^{-/-}$;CD19 Cre mice. Thus, we detected a defect in B-cell development in *Artemis*$^{-/-}$*Mre11*$^{\Delta/-}$;CD19 Cre and *Artemis*$^{-/-}$*Mre11*$^{\Delta/H129N}$;CD19 Cre B-cells that prevented B-cell maturation into IgM expressing B-cells and that the *Artemis*$^{-/-}$*Mre11*$^{\Delta/-}$;CD19 Cre and *Artemis*$^{-/-}$ *Mre11*$^{\Delta/H129N}$;CD19 Cre B-cells have a B-cell defect similar to what was observed in *Artemis*$^{-/-}$ B-cells.

Analysis of junctional sequences at the immunoglobulin heavy chain locus

During V(D)J recombination, coding ends undergo processing by nucleases and polymerases resulting in increased junctional diversity at coding joints (CJs) (25-28). ARTEMIS is a nuclease a part of the metallo-β-lactamase/βCASP family of nucleases (29, 30). In complex with DNA-PKcs, the ARTEMIS endonucleolytic activities are critical for nicking open hairpin intermediates that occur during V(D)J recombination as a result of RAG1/2 site-specific cleavage (1, 20). ARTEMIS endonucleolytic activities nick open hairpin coding ends ± 2-3 nucleotides from the center of the hairpin coding end apex followed by DNA polymerase fill-in resulting in P-nucleotide addition at the junction (31). Thus, sequence analysis of junctions lends insight into the impact of various mutations on DNA end processing events during V(D)J recombination. We wanted to investigate the impact of junctional diversity at the immunoglobulin heavy chain locus when nucleases ARTEMIS and MRE11 are mutated.

To this end, I analyzed the junctional sequences for D_H to J_H rearrangements initiated at the immunoglobulin heavy chain locus in *Artemis*$^{-/-}$ *Mre11*$^{\Delta/-}$;CD19 Cre B-cells and *Artemis*$^{-/-}$*Mre11*$^{\Delta/H129N}$;CD19 Cre B-cells. We were only interested in the junctional sequences involving the IgH locus, thus, we harvested genomic DNA from total bone marrow and used well-characterized polymerase chain reaction (PCR) assay to amplify specific rearrangements (17, 32). I used primers 5′ of D_{Q52}, the D segment located most proximal to J_{H1} paired with a primer 3′ of J_H4 that amplifies most D_H to J_H rearrangements and the unrearranged, germline band (Figure 4.3, see diagram). PCR products were then sub-cloned and sequenced.

Small deletions (≤21 nucleotides) and N-nucleotide additions were observed in the control B-cells (data not shown) (17, 20, 23, 33, 34). In contrast, D_{Q52} to J_H coding joins from *Artemis*$^{-/-}$;CD19 Cre B-cells (n= 2 mice, 4 unique sequences) exhibited large deletions (3/4), with >400 nt deleted from some coding flanks (Figure 4.2A). Most (3/4) *Artemis*$^{-/-}$ coding flanks also were characterized by regions of sequence homology or microhomology (>3 nucleotides of microhomology) at the junction (Figure 4.2A). Increased junctional

homology has been identified in an *Artemis* knock-out and a conditional knock-out of *Artemis* using a B-cell specific Cre, CD21, to analyze the role of ARTEMIS in DNA end processing at switch regions during class switch recombination, a mature B-cell DNA rearrangement (35-37). As a defining characteristic, *Artemis*$^{-/-}$ lymphocytes contain junctional sequences with unusually long P-nucleotide additions suggesting another nuclease can substitute for ARTEMIS hairpin opening activities (albeit inefficiently) and cleave the hairpin intermediate several nucleotides away from the apex (20, 31). However, not all coding junctions have P-nucleotide additions; if the hairpin is nicked exactly at its center, there is no self-complementary overhang (38). Or such an overhang may be resected before the ends are joined (38). In *Artemis*$^{-/-}$;CD19 Cre B-cells from our study, I did not detect P-nucleotide addition. Perhaps this was because I only subcloned a few sequences between D_{Q52} to J_H. More sequences from *Artemis*$^{-/-}$;CD19 Cre B-cells should be analyzed. The absence of P-nucleotides could also suggest that in the absence of ARTEMIS, other nuclease(s) can open the hairpin ends right at the apex rather than a few nucleotides away as has been previously suggested, or that upon hairpin opening, the ends were resected before joining (38).

Similar to *Artemis*$^{-/-}$;CD19 Cre B-cells, *Artemis*$^{-/-}$*Mre11*$^{\Delta/-}$;CD19 Cre B-cells (n=4 mice, 12 unique sequences) exhibited large deletions (4/12, ≤ 364 nucleotides) as well as small deletions (6/12; ≤ 14 nucleotides (Figure 4.2B). A subset (2/12) of junctional sequences exhibited microhomology. I did detect P-nucleotide addition in *Artemis*$^{-/-}$*Mre11*$^{\Delta/-}$;CD19 Cre B-cells (3-5 nucleotides) similar to what has been reported in *Artemis*$^{-/-}$ B-cells (Figure 4.2B) (17). Intriguingly, one sequence contained a 25, P-nucleotide addition on the D_H side of the join, followed by a 4, N-nucleotide addition, ending with a 6, P-nucleotide addition on the J_H side (Figure 4.2B). This type of sequence has not been commonly observed in *Artemis*$^{-/-}$ B-cells (17) and I did not detect this sequence in *Artemis*$^{-/-}$;CD19 Cre B-cells, *Mre11*$^{\Delta/-}$;CD19 Cre B-cells nor *Mre11*$^{\Delta/H129N}$;CD19 Cre B-cells (data not shown).

Similar to *Artemis*$^{-/-}$;CD19 Cre B-cells, *Artemis*$^{-/-}$*Mre11*$^{\Delta/H129N}$;CD19 Cre B-cells (n=2 mice, n=15 unique sequences) exhibited large deletions (7/15, 383-

390 nucleotides) but also contained small deletions (≤ 11 nucleotides) (Figure 4.2C). A subset (7/15) of junctions contained microhomology (≥ 3 nucleotides) and no sequences with P-nucleotide addition were obtained (Figure 4.2C). A few sequences had N-nucleotide addition ranging between 1-9 nucleotides—similar to what has been reported in *Artemis*$^{-/-}$ B-cells (17). Sequences recovered from *Artemis*$^{-/-}$*Mre11*$^{\Delta/H129N}$;CD19 Cre B-cells contained junctions nucleolytically processed comparable to *Artemis*$^{-/-}$;CD19 Cre B-cells. Although these findings are preliminary, the data suggests similar processing of coding ends during V(D)J recombination in *Artemis*$^{-/-}$*Mre11*$^{\Delta/H129N}$;CD19 Cre B-cells, *Artemis*$^{-/-}$ *Mre11*$^{\Delta/-}$;CD19 Cre B-cells, and *Artemis*$^{-/-}$;CD19 Cre B-cells. Intriguingly, the one sequence isolated from *Artemis*$^{-/-}$*Mre11*$^{\Delta/-}$;CD19 Cre B-cells contained a 25, P-nucleotide addition on the D_H side of the join, followed by a 4, N-nucleotide addition, ending with a 6, P-nucleotide addition on the J_H side (Figure 4.2B) and has not been reported in *Artemis*$^{-/-}$ lymphocytes and not observed in *Artemis*$^{-/-}$;CD19 Cre B-cells in this study. This sequence could indicate that in the absence of ARTEMIS and the MRE11 complex another nuclease can cleave the hairpin coding end many nucleotides away from the apex to create long P-nucleotide addition at the junction. Analyzing additional ARTEMIS/MRE11;CD19 Cre mice or using a Cre transgene that expresses earlier during B-cell development will provide insight into how nucleases ARTEMIS and MRE11 coordinate DNA end processing during V(D)J recombination.

Defective rearrangements observed in *Artemis*$^{-/-}$*Mre11*$^{\Delta/H129N}$;CD19 Cre B-cells

Quantitatively similar numbers of pro-B cells were detected in *Artemis*$^{-/-}$;CD19 Cre B-cells, *Artemis*$^{-/-}$*Mre11*$^{\Delta/-}$;CD19 Cre B-cells and *Artemis*$^{-/-}$ *Mre11*$^{\Delta/H129N}$;CD19 Cre B-cells (Figure 4.1B). Previous studies have reported that *Artemis*$^{-/-}$ lymphocytes exhibit a severe reduction in the levels of V(D)J recombination (20). Given the quantitative similarity between *Artemis*$^{-/-}$;CD19 Cre B-cells and *Artemis*$^{-/-}$*Mre11*$^{\Delta/-}$;CD19 Cre and *Artemis*$^{-/-}$*Mre11*$^{\Delta/H129N}$;CD19 Cre B-cell populations in our study, we wanted to examine levels of V(D)J rearrangement.

We extracted total bone marrow and isolated genomic DNA and assayed for D_H to J_H V(D)J rearrangements. We used 200 ng of genomic DNA isolated from bone marrow and serially diluted the DNAs 1:5 (200ng, 40ng, and 8ng). We used the same PCR approach as previously used to analyze junctional sequences between D_{Q52} to J_H and the unrearranged, germline band (Figure 4.3, see diagram). Normalization for the amount of DNA used in the reaction was performed on a non-rearranging locus (ATM) corresponding to the appropriate serial dilution.

As observed previously with this primer set, we were unable to detect rearrangements in *Artemis*$^{-/-}$ B-cell populations (n=3 mice, Figure 4.3A; 4.3B). We could detect D_{Q52} to J_H rearrangements in control (n=2 mice) and *Mre11*$^{\Delta/-}$;CD19 Cre (n=3 mice) and *Mre11*$^{\Delta/H129N}$; CD19 Cre (n=3 mice) B-cell populations involving D_{Q52} rearrangements to J_{H1}, J_{H2}, J_{H3}, and J_{H4} (data not shown). Similar to *Artemis*$^{-/-}$ B-cells, I was not able to detect rearrangements in 4/4 *Artemis*$^{-/-}$ *Mre11*$^{\Delta/-}$;CD19 Cre B-cell populations (Figure 4.3A). Surprisingly, I detected D_{Q52} to J_H rearrangements in a subset (2/7) of *Artemis*$^{-/-}$*Mre11*$^{\Delta/H129N}$;CD19 Cre B-cell populations (Figure 4.3B).

To more quantitatively assess differences in levels of D_H to J_H rearrangements in the relevant B-cell genotypes, the pro-B populations will be sorted and analyzed for levels of rearrangements. However, rearrangements are readily detectable from genomic DNA isolated from 2/7 *Artemis*$^{-/-}$*Mre11*$^{\Delta/H129N}$ bone marrow samples. This observation requires additional investigation to address how MRE11 mutation impacts levels of D_H to J_H rearrangements in the absence of ARTEMIS. This idea will be expanded upon in Chapter 5.

ARTEMIS/MRE11 mutant MEFs do not exhibit increased IR hypersensitivity

Recent studies have demonstrated a novel role for the ataxia telangiectasia mutated (ATM) and the MRE11 complex in the modulation of ARTEMIS in vivo functions (4, 13, 16, 39). ATM is a serine/threonine protein kinase and is responsible for activating the signaling pathway responding to DSBs as well as regulating direct repair events via phosphorylation of DNA repair factors (40). The MRE11 complex is involved in sensing DSBs and activates the

ATM kinase, thereby initiating the cascade of downstream events (18). Recent evidence indicates that ATM and the MRE11 complex function within a common DSB repair pathway with the ARTEMIS nuclease to process a subset of modified DNA ends (5); however, the molecular interactions between these critical repair factors in the repair of ionizing radiation (IR) –induced DSBs is not well-understood. Therefore, we investigated the functional interaction between ARTEMIS and the MRE11 complex in IR-induced DNA DSB repair.

To determine the impact of the *Mre11* null or *Mre11* knock-in mutation on *Artemis* nullizygosity on general DNA DSB repair, we examined the relative ionizing radiation (IR)-induced sensitivities of $Artemis^{+/+}Mre11^{+/+}$, $Artemis^{-/-}$, $Mre11^{C/-}$, $Mre11^{C/H129N}$, $Artemis^{-/-}Mre11^{C/-}$ and $Artemis^{-/-}Mre11^{C/H129N}$ SV40 transformed mouse embryonic fibroblasts (MEFs). Cells were treated with an adeno virus expressing Cre recombinase to delete the $Mre11^{C}$ allele in vitro. The mutant cells were exposed to increasing doses of IR, and cellular survival was determined at 5 days post IR using a colorimetric survival assay. I observed that $Mre11^{\Delta/-}$, $Artemis^{-/-}$, $Artemis^{-/-}Mre11^{H129N/\Delta}$ and $Artemis^{-/-}Mre11^{\Delta/-}$ MEFs consistently exhibited similar percent survival post-irradiation, and that the survival fractions at 250 rads and 500 rads was significantly lower from the control at those doses (Figure 4.4; $p<0.05$, Whitney-Mann t-test). These results indicate that ARTEMIS and MRE11 mutations do not have an additive impact on cellular survival post IR supporting the notion that ARTEMIS and the MRE11 complex function epistatically in the repair of IR-induced DNA damage.

Discussion

The roles of ARTEMIS and the MRE11 complex in V(D)J recombination

Efficient opening of the hairpin intermediates known as coding ends generated by site-specific RAG1/2 cleavage is dependent on the ARTEMIS nuclease (33, 41). Although other cellular nucleases have enzymatic activity that could open and resect hairpin-sealed coding ends, such as MRE11, this functional redundancy is not evident in ARTEMIS-deficient cells; as a result, ARTEMIS-deficient mice and patients are severely lymphopenic (20, 35, 42). Thus, the nucleolytic processing of broken DNA ends in lymphocytes must be tightly regulated; however, the cellular components that mediate this regulation are not known. Thus we investigated if the nucleolytic and DNA repair activities of the MRE11 complex contribute to hairpin end processing and repair in lymphocytes with and without ARTEMIS activity.

We observed that MRE11 mutated B-cells did not have an overt effect on early B-cell development associated with V(D)J recombination, as previously reported by the Ferguson lab (19). V(D)J recombination requires the generation and repair of DNA DSBs and occurs exclusively during the G1 phase of the cell cycle (43). Studies have implicated the activities of the MRE11 complex in G1-mediate repair; additionally, the MRE11 complex, along with another nuclease, CTIP, coordinate nucleolytic processing of broken DNA ends during the S- and G2-phases of the cell cycle to promote 5’ to 3’ resection of broken DNA ends and thus, initiation of homologous recombination (44). In this regard, ARTEMIS wild type activity would be sufficient to process DNA end intermediates generated by the RAG1/2 endonuclease in G1 independent of MRE11 complex activity and thus, MRE11 mutant lymphocytes would exhibit normal lymphocyte development (as previously reported and observed in our study). However, this does not exclude a role for the MRE11 complex in the repair of RAG1/2-generated DSBs.

Unopened hairpin coding ends that persist throughout phases of the cell cycle in *Artemis* null lymphocytes may become substrates for MRE11 complex activity in S- or G2- whereby the nuclease activities of MRE11 within the MRE11 complex can nick open the coding ends and in concert with the MRE11 complex and CTIP, nucleolytically process the opened hairpin intermediates to create long single strand overhangs that are poor substrates for cNHEJ repair in G1, but can be repaired using HR in G2- and S-phase (13, 45). Additionally, this resection could expose regions of microhomology, thus promoting microhomology-mediated repair oftentimes observed when critical cNHEJ factors are deficient, such as ARTEMIS (45, 46). Indeed, we did detect 3/4 *Artemis*$^{-/-}$;CD19 Cre B-cell junctional sequences harboring microhomology at the junction (≥ 3 nucleotides of microhomology; Figure 4.2A). Another not mutually exclusive hypothesis is that the MRE11 complex is able to process unopened hairpin intermediates in the G1 phase of the cell cycle, as previous studies have identified that the MRE11 complex and CTIP can promote NHEJ repair (both cNHEJ and alternative NHEJ) of extrachromosomal substrates in G1 (47-49).

We also observed that MRE11/ARTEMIS double mutant B-cells were quantitatively similar to *Artemis*$^{-/-}$ B-cells in regards to cellularity of the spleen, IgM^{+} B-cells in the spleen, and counts and percentages of pro B-cell and pre B-cell populations (Figure 4.1B). However, surprisingly, we detected D_H to J_H rearrangements in 2/7 *Artemis*$^{-/-}$*Mre11*$^{\Delta/H129N}$;CD19 Cre B-cells but not in *Artemis*$^{-/-}$*Mre11*$^{\Delta/-}$;CD19 Cre B-cells or *Artemis*$^{-/-}$ B-cells (result observed in 3 independent experiments). This preliminary finding suggests that the rearrangements we were able to detect were rare, stochastic events. Nevertheless, the frequency of rearrangements may be higher in *Artemis*$^{-/-}$*Mre11*$^{\Delta/H129N}$ cells compared to *Artemis*$^{-/-}$ as rearrangements have not been observed in *Artemis*$^{-/-}$ B-cells. To follow-up on my observations we propose to use engineered B-cell lines. Currently, in the lab, we have a system to analyze unselected V(D)J rearrangements using an extrachromosomal substrate integrated into pre-B-cell lines transformed with the v-abl kinase, each of which contain a retroviral recombination substrate (13, 39). Treatment of these cells with the v-abl kinase

inhibitor, STI571, leads to G1 cell cycle arrest, induction of RAG1/2 expression, and the generation of RAG1/2 DSBs at the endogenous immunoglobulin kappa (IgLκ) locus and at chromosomally introduced retroviral recombination substrates (13, 39). In WT G1-phase abl pre–B cells, these DSBs are rapidly repaired, whereas in cells deficient in specific DNA repair proteins these DSBs can persist unrepaired for substantial periods of time and are readily detected (13, 39). This system will allow us to extend our observations about the coordinated role of the ARTEMIS nuclease and the MRE11 complex in DNA end processing and repair of RAG1/2 generated breaks during V(D)J recombination. Additionally, this system is advantageous as we will be able to detect products from un-selected populations of lymphocytes and perhaps, this will reveal additional unique sequences previously unable to be recovered from our in vivo experiments and address the apparent stochastic rearrangements detected in *Artemis*$^{-/-}$ *Mre11*$^{\Delta/H129N}$;CD19 Cre B-cells. For future studies, we could either genetically engineer pre-B cell lines with single and double mutations of ARTEMIS and components of the MRE11 complex or combine ARTEMIS mutations with the MRE11 complex molecule inhibitor, mirin (48).

Coordinated DNA end processing events between ARTEMIS and MRE11 due to IR-induced damage

I observed that *Mre11*$^{\Delta/-}$, *Artemis*$^{-/-}$, *Artemis*$^{-/-}$*Mre11*$^{H129N/\Delta}$ and *Artemis*$^{-/-}$ *Mre11*$^{\Delta/-}$ MEFs consistently exhibited similar percent survival post-irradiation and that combining ARTEMIS and MRE11 mutation does not result in additive IR hypersensitivity. My findings provide evidence that ARTEMIS and the MRE11 complex coordinate repair of IR-induced breaks. As this observation is not surprising due to the molecular properties of both ARTEMIS and the MRE11 complex (able to nucleolytically process similar DNA substrates such as 5' and 3' overhangs, flaps, and loops) (1, 25, 44), it is surprising the mildness of sensitivity of the ARTEMIS/MRE11 double mutants to IR. The MRE11 is most notably involved in homologous recombination (HR), which favors homology-directed repair. The ARTEMIS nuclease is most notably involved in classical nonhomologous end joining (cNHEJ), a repair pathway that repairs breaks via

direct end-to-end ligation. Our observations that combining ARTEMIS and MRE11 mutation does not severely abrogate the repair of IR-induced DSBs suggests that ARTEMIS and the MRE11 complex coordinate repair of IR-induced DSBs.

Studies from the Jeggo and Lobrich laboratories identified that the ARTEMIS nuclease and ATM kinase share a similar DNA repair pathway on a subset of DNA ends that require additional end-processing prior to ligation (such as removal of 3' moieties) (5). The MRE11 complex is a sensor of DSBs that binds DNA ends in a damage-dependent manner and acts to recruit and activate the ATM kinase to propagate the DNA damage response (44). In this regard, the MRE11 complex and the ATM kinase are in a similar DNA damage repair pathway. Our observations taken together with the findings from the Jeggo and Lobrich labs suggest that ARTEMIS, MRE11, and ATM share a similar DNA repair pathway, perhaps on a subset of ends that require additional processing.

DNA damage as a result of ionizing radiation is unique in that it creates a diverse repertoire of damage including DSBs, single stranded breaks, overhangs, and DNA breaks with 3' covalently attached moities. In this regard, the activities of the ARTEMIS complex would be critical for a subset of those DSBs break requiring additional processing. In support of this notion, ARTEMIS-deficient cells are hypersensitive to DNA damaging agents that produce damage with 3' moities versus single stranded breaks (50).

Taken together, my data supports a model in which after IR-induced damage, ARTEMIS and MRE11 coordinate repair at DNA ends. This could be via their roles in NHEJ (as studies implicate MRE11 in both cNHEJ and aNHEJ) or in homologous recombination (HR). Perhaps in joining reactions that require end-tethering over many kilobases, it is appropriate for the MRE11 complex to promote end joining by bringing broken DNA ends in close proximity. Or when a DNA break necessitates additional processing, perhaps the combined nuclease activities of ARTEMIS and MRE11 are more adept at "cleaning" up the ends to promote repair. Therefore, the biochemical nature of ARTEMIS and MRE11 do

not exclude the possibility that they work together, in a very rapid fashion, to promote end joining of DSBs.

My studies explore the interplay between the two major nucleases in DSB repair, ARTEMIS and MRE11, in V(D)J recombination and in general DSB repair. The observations from these studies lay groundwork for future investigations into how ARTEMIS and MRE11 coordinate DNA end processing during V(D)J recombination and general DSB repair.

Materials and Methods

Mice.

Gene targeted *Artemis* null, *Mre11*^{C}, and *Mre11*^{H129N} (129Svev/C57Bl6 background) mice were previously generated (18, 20). Mice were bred to mice harboring CD19 Cre transgene (Jackson Labs) All mice were housed in a specific pathogen free facility in a room dedicated to immunocompromised animals.

Antibodies and flow cytometry

Single cell suspensions from thymus, bone marrow, spleen, and LNs were prepared and stained with antibodies conjugated to FITC, PE, and Cy-Chrome (CyC) according to standard procedures. Approximately 10^6 cells were stained with the appropriate antibodies and analyzed on a Accuri flow cytometer (Accuri-BD). Data were analyzed using FlowJo software (Tree Star, Inc.)

PCR analysis of IgH and TCR rearrangements

Input genomic DNA from total bone marrow (B-cells) was normalized by PCR amplification of a coding exon of the ATM gene. PCR reactions contained threefold serial dilutions of genomic DNA (from 200 ng as the starting amount in each series), 10 pmol of each primer, 0.2 mM dNTPs, 50mM KCl, 10 mM Tris-HCL, pH 8.0, 2.5 mM MgCl2, and 0.5 U Taq polymerase (QIAGEN). Amplification conditions were as follows: 94°C for 45 s, 60°C for 1 min, and 72°C for 2 min for 30–35 cycles. The PCR products were analyzed by agarose gel electrophoresis, transferred to zeta-probe membrane, and hybridized with ^{32}P 5' end-labeled oligonucleotide probes to detect the rearrangements (51, 52). PCR assays were repeated at least three times.

IR hypersensitivity assay

Mouse embryonic fibroblasts (MEFs) of indicated genotypes were isolated at e13.5 and immortalized by SV40 transfection (53). MEFs were cultured in DMEM supplemented with 10% fetal calf serum (Atlanta Biologicals), nonessential amino acids, glutamine, HEPES, sodium pyruvate, penicillin and streptomycin, and beta-mercaptoethanol. MEFs of indicated genotypes were plated in 12-well tissue culture dishes (BD Falcon) using 1000 cells for wildtype and 2000 cells for mutants. 16-18 hours later, MEFs were irradiated using a Cesium source at doses 2.5, 5, and 10 grey of ionizing radiation. When untreated controls became confluent, cells were washed with PBS, fixed in 10% methanol/10% acetic acid for 10 minutes, and subsequently stained with crystal violet. Residual crystal violet was removed and resolubilized in methanol. Crystal violet concentration was read at 595nm using a BioRad plate reader. Survival fraction was calculated comparing irradiate sample crystal violet reading to untreated. This assay was repeated at least three times.

References

1. Ma Y, Pannicke U, Schwarz K, Lieber MR. Hairpin opening and overhang processing by an Artemis/DNA-dependent protein kinase complex in nonhomologous end joining and V(D)J recombination. Cell. 2002;108(6):781-94.
2. Ma Y, Pannicke U, Lu H, Niewolik D, Schwarz K, Lieber MR. The DNA-dependent protein kinase catalytic subunit phosphorylation sites in human Artemis. J Biol Chem. 2005;280(40):33839-46.
3. Poinsignon C, de Chasseval R, Soubeyrand S, Moshous D, Fischer A, Hache RJ, et al. Phosphorylation of Artemis following irradiation-induced DNA damage. Eur J Immunol. 2004;34(11):3146-55.
4. Chen L, Morio T, Minegishi Y, Nakada S, Nagasawa M, Komatsu K, et al. Ataxia-telangiectasia-mutated dependent phosphorylation of Artemis in response to DNA damage. Cancer Sci. 2005;96(2):134-41.
5. Riballo E, Kuhne M, Rief N, Doherty A, Smith GC, Recio MJ, et al. A pathway of double-strand break rejoining dependent upon ATM, Artemis, and proteins locating to gamma-H2AX foci. Mol Cell. 2004;16(5):715-24.
6. Riballo E, Critchlow SE, Teo SH, Doherty AJ, Priestley A, Broughton B, et al. Identification of a defect in DNA ligase IV in a radiosensitive leukaemia patient. Curr Biol. 1999;9(13):699-702.
7. Sekiguchi J, Alt F.W., Oettinger M., Honjo T. Molecular Biology of B Cells. In: W. AF, editor. Elsevier Science2004. p. 57-78.
8. Schatz DG, Oettinger MA, Schlissel MS. V(D)J recombination: molecular biology and regulation. Annu Rev Immunol. 1992;10:359-83.
9. Jones JM, Gellert M. Intermediates in V(D)J recombination: a stable RAG1/2 complex sequesters cleaved RSS ends. Proc Natl Acad Sci U S A. 2001;98(23):12926-31. PMCID: 60801.
10. Lee GS, Neiditch MB, Salus SS, Roth DB. RAG proteins shepherd double-strand breaks to a specific pathway, suppressing error-prone repair, but RAG nicking initiates homologous recombination. Cell. 2004;117(2):171-84.
11. Ahnesorg P, Smith P, Jackson SP. XLF interacts with the XRCC4-DNA ligase IV complex to promote DNA nonhomologous end-joining. Cell. 2006;124(2):301-13.
12. Schatz DG, Ji Y. Recombination centres and the orchestration of V(D)J recombination. Nat Rev Immunol. 2011;11(4):251-63.
13. Helmink BA, Bredemeyer AL, Lee BS, Huang CY, Sharma GG, Walker LM, et al. MRN complex function in the repair of chromosomal Rag-mediated DNA double-strand breaks. J Exp Med. 2009;206(3):669-79. PMCID: 2699138.
14. Hendrickson EA, Schlissel MS, Weaver DT. Wild-type V(D)J recombination in scid pre-B cells. Mol Cell Biol. 1990;10(10):5397-407. PMCID: 361240.

15. Kang J, Ferguson D, Song H, Bassing C, Eckersdorff M, Alt FW, et al. Functional interaction of H2AX, NBS1, and p53 in ATM-dependent DNA damage responses and tumor suppression. Mol Cell Biol. 2005;25(2):661-70. PMCID: 543410.
16. Deriano L, Stracker TH, Baker A, Petrini JH, Roth DB. Roles for NBS1 in alternative nonhomologous end-joining of V(D)J recombination intermediates. Mol Cell. 2009;34(1):13-25. PMCID: 2704125.
17. Huang Y, Giblin W, Kubec M, Westfield G, St Charles J, Chadde L, et al. Impact of a hypomorphic Artemis disease allele on lymphocyte development, DNA end processing, and genome stability. J Exp Med. 2009;206(4):893-908. PMCID: 2715118.
18. Buis J, Wu Y, Deng Y, Leddon J, Westfield G, Eckersdorff M, et al. Mre11 nuclease activity has essential roles in DNA repair and genomic stability distinct from ATM activation. Cell. 2008;135(1):85-96. PMCID: 2645868.
19. Dinkelmann M, Spehalski E, Stoneham T, Buis J, Wu Y, Sekiguchi JM, et al. Multiple functions of MRN in end-joining pathways during isotype class switching. Nat Struct Mol Biol. 2009;16(8):808-13. PMCID: 2721910.
20. Rooney S, Sekiguchi J, Zhu C, Cheng HL, Manis J, Whitlow S, et al. Leaky Scid phenotype associated with defective V(D)J coding end processing in Artemis-deficient mice. Mol Cell. 2002;10(6):1379-90.
21. Peterson SR, Kurimasa A, Oshimura M, Dynan WS, Bradbury EM, Chen DJ. Loss of the catalytic subunit of the DNA-dependent protein kinase in DNA double-strand-break-repair mutant mammalian cells. Proc Natl Acad Sci U S A. 1995;92(8):3171-4. PMCID: 42127.
22. Lim DS, Vogel H, Willerford DM, Sands AT, Platt KA, Hasty P. Analysis of ku80-mutant mice and cells with deficient levels of p53. Mol Cell Biol. 2000;20(11):3772-80. PMCID: 85695.
23. Gu Y, Seidl KJ, Rathbun GA, Zhu C, Manis JP, van der Stoep N, et al. Growth retardation and leaky SCID phenotype of Ku70-deficient mice. Immunity. 1997;7(5):653-65.
24. Frank KM, Sekiguchi JM, Seidl KJ, Swat W, Rathbun GA, Cheng HL, et al. Late embryonic lethality and impaired V(D)J recombination in mice lacking DNA ligase IV. Nature. 1998;396(6707):173-7.
25. Ma Y, Schwarz K, Lieber MR. The Artemis:DNA-PKcs endonuclease cleaves DNA loops, flaps, and gaps. DNA Repair (Amst). 2005;4(7):845-51.
26. Mahajan KN, Gangi-Peterson L, Sorscher DH, Wang J, Gathy KN, Mahajan NP, et al. Association of terminal deoxynucleotidyl transferase with Ku. Proc Natl Acad Sci U S A. 1999;96(24):13926-31. PMCID: 24167.
27. Bertocci B, De Smet A, Weill JC, Reynaud CA. Nonoverlapping functions of DNA polymerases mu, lambda, and terminal deoxynucleotidyltransferase during immunoglobulin V(D)J recombination in vivo. Immunity. 2006;25(1):31-41.
28. Benedict CL, Gilfillan S, Thai TH, Kearney JF. Terminal deoxynucleotidyl transferase and repertoire development. Immunol Rev. 2000;175:150-7.
29. Poinsignon C, Moshous D, Callebaut I, de Chasseval R, Villey I, de Villartay JP. The metallo-beta-lactamase/beta-CASP domain of Artemis

constitutes the catalytic core for V(D)J recombination. J Exp Med. 2004;199(3):315-21. PMCID: 2211804.
30. Moshous D, Callebaut I, de Chasseval R, Poinsignon C, Villey I, Fischer A, et al. The V(D)J recombination/DNA repair factor artemis belongs to the metallo-beta-lactamase family and constitutes a critical developmental checkpoint of the lymphoid system. Ann N Y Acad Sci. 2003;987:150-7.
31. Roth DB, Menetski JP, Nakajima PB, Bosma MJ, Gellert M. V(D)J recombination: broken DNA molecules with covalently sealed (hairpin) coding ends in scid mouse thymocytes. Cell. 1992;70(6):983-91.
32. Roth DB, Wilson JH. Nonhomologous recombination in mammalian cells: role for short sequence homologies in the joining reaction. Mol Cell Biol. 1986;6(12):4295-304. PMCID: 367211.
33. Rooney S, Chaudhuri J, Alt FW. The role of the non-homologous end-joining pathway in lymphocyte development. Immunol Rev. 2004;200:115-31.
34. Zhu C, Bogue MA, Lim DS, Hasty P, Roth DB. Ku86-deficient mice exhibit severe combined immunodeficiency and defective processing of V(D)J recombination intermediates. Cell. 1996;86(3):379-89.
35. Rooney S, Alt FW, Sekiguchi J, Manis JP. Artemis-independent functions of DNA-dependent protein kinase in Ig heavy chain class switch recombination and development. Proc Natl Acad Sci U S A. 2005;102(7):2471-5. PMCID: 548986.
36. Du L, van der Burg M, Popov SW, Kotnis A, van Dongen JJ, Gennery AR, et al. Involvement of Artemis in nonhomologous end-joining during immunoglobulin class switch recombination. J Exp Med. 2008;205(13):3031-40. PMCID: 2605234.
37. Rivera-Munoz P, Soulas-Sprauel P, Le Guyader G, Abramowski V, Bruneau S, Fischer A, et al. Reduced immunoglobulin class switch recombination in the absence of Artemis. Blood. 2009;114(17):3601-9.
38. Gellert M. V(D)J recombination: RAG proteins, repair factors, and regulation. Annu Rev Biochem. 2002;71:101-32.
39. Bredemeyer AL, Sharma GG, Huang CY, Helmink BA, Walker LM, Khor KC, et al. ATM stabilizes DNA double-strand-break complexes during V(D)J recombination. Nature. 2006;442(7101):466-70.
40. Shiloh Y. ATM and related protein kinases: safeguarding genome integrity. Nat Rev Cancer. 2003;3(3):155-68.
41. Lieber MR, Yu K, Raghavan SC. Roles of nonhomologous DNA end joining, V(D)J recombination, and class switch recombination in chromosomal translocations. DNA Repair (Amst). 2006;5(9-10):1234-45.
42. Moshous D, Callebaut I, de Chasseval R, Corneo B, Cavazzana-Calvo M, Le Deist F, et al. Artemis, a novel DNA double-strand break repair/V(D)J recombination protein, is mutated in human severe combined immune deficiency. Cell. 2001;105(2):177-86.
43. Schatz DG, Swanson PC. V(D)J recombination: mechanisms of initiation. Annu Rev Genet. 2011;45:167-202.
44. Stracker TH, Petrini JH. The MRE11 complex: starting from the ends. Nat Rev Mol Cell Biol. 2011;12(2):90-103.

45. Bennardo N, Cheng A, Huang N, Stark JM. Alternative-NHEJ is a mechanistically distinct pathway of mammalian chromosome break repair. PLoS Genet. 2008;4(6):e1000110. PMCID: 2430616.
46. Lee-Theilen M, Matthews AJ, Kelly D, Zheng S, Chaudhuri J. CtIP promotes microhomology-mediated alternative end joining during class-switch recombination. Nat Struct Mol Biol. 2011;18(1):75-9. PMCID: 3471154.
47. Simsek D, Jasin M. Alternative end-joining is suppressed by the canonical NHEJ component Xrcc4-ligase IV during chromosomal translocation formation. Nat Struct Mol Biol. 2010;17(4):410-6.
48. Rass E, Grabarz A, Plo I, Gautier J, Bertrand P, Lopez BS. Role of Mre11 in chromosomal nonhomologous end joining in mammalian cells. Nat Struct Mol Biol. 2009;16(8):819-24.
49. Xie A, Kwok A, Scully R. Role of mammalian Mre11 in classical and alternative nonhomologous end joining. Nat Struct Mol Biol. 2009;16(8):814-8. PMCID: 2730592.
50. Rooney S, Alt FW, Lombard D, Whitlow S, Eckersdorff M, Fleming J, et al. Defective DNA repair and increased genomic instability in Artemis-deficient murine cells. J Exp Med. 2003;197(5):553-65. PMCID: 2193825.
51. Schlissel MS, Corcoran LM, Baltimore D. Virus-transformed pre-B cells show ordered activation but not inactivation of immunoglobulin gene rearrangement and transcription. J Exp Med. 1991;173(3):711-20. PMCID: 2118835.
52. Gartner F, Alt FW, Monroe R, Chu M, Sleckman BP, Davidson L, et al. Immature thymocytes employ distinct signaling pathways for allelic exclusion versus differentiation and expansion. Immunity. 1999;10(5):537-46.
53. Harding HP, Lackey JG, Hsu HC, Zhang Y, Deng J, Xu RM, et al. An intact unfolded protein response in Trpt1 knockout mice reveals phylogenic divergence in pathways for RNA ligation. RNA. 2008;14(2):225-32. PMCID: 2212252.

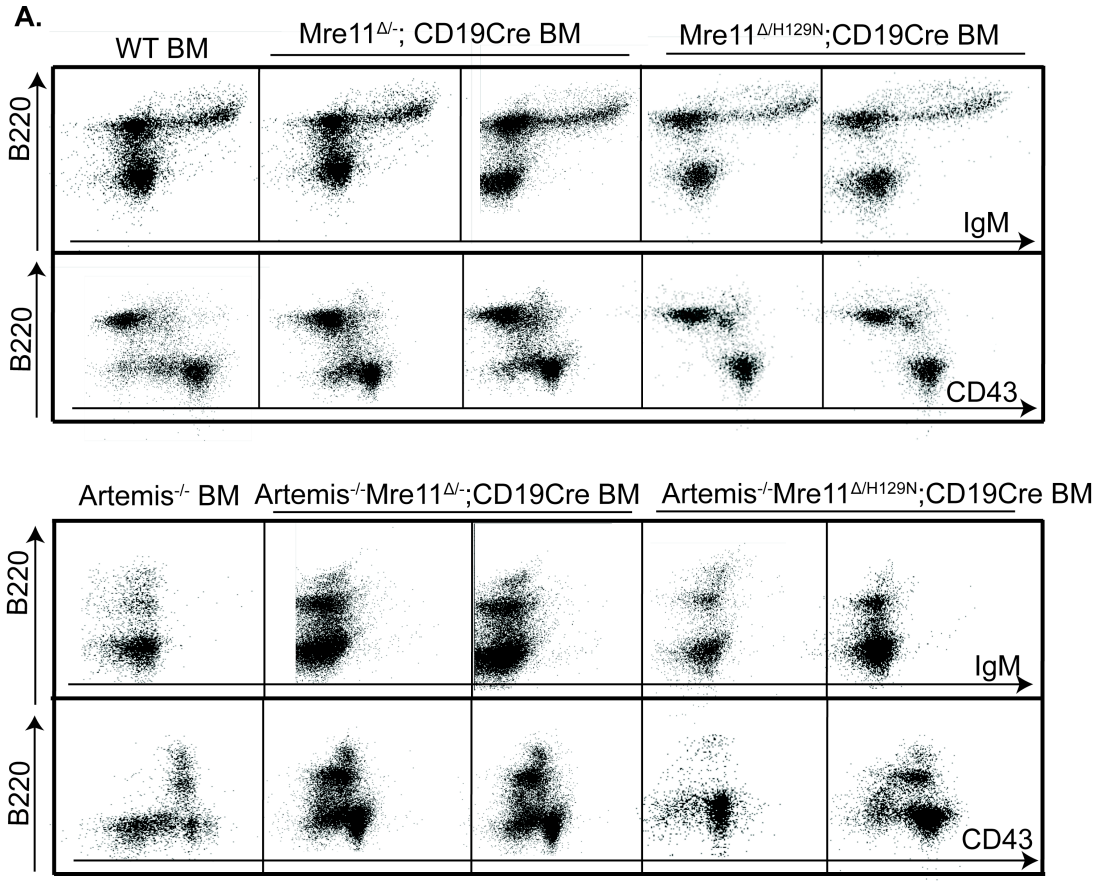

B.

B-cell genotype	Splenocytes x10^6	IgM+Splenocytes %	pro-B cells %	pro-B cells x10^6	pre-B cells %	pre-B cells x10^6
Control (n=2)	21.4	52.8	3.8	0.39	29.6	2.99
Artemis$^{-/-}$ (n=3)	2.8±0.17	0.06±0.03	7.9±3.42	0.6±0.44	4.0±0.50	0.29±0.11
Mre11$^{-/\Delta}$ (n=3)	22.7±17.6	34.2±6.5	6.6±2.0	0.57±0.14	31.1±1.18	2.93±1.31
Mre11$^{\Delta/H129N}$ (n=3)	28.3±12.15	48.5±12.48	8.58±2.5	0.95±0.42	23.4±17.23	2.67±2.14
Art-/-Mre11$^{-/\Delta}$(n=4)	2.8±0.43	0.5±0.58	15.1±2.38	0.91±0.2	3.5±2.44	0.18±0.09
Art-/-Mre11$^{\Delta/H129N}$ (n=7)	2.7±2.0	0.7±0.76	9.1±4.06	0.80±0.66	2.0±0.11	0.13±0.11

Figure 4.1 Flow cytometric analysis of lymphocyte development in control and mutant B-cells and lymphoid tissue cellularity. (A) ARTEMIS lymphocyte development is not exacerbated by combining with MRE11 mutation in B-cells and MRE11 B-cell specific mutation does not apparently result in lymphocyte developmental defects. Monocolonal antibodies conjugated to a fluorophore containing Fitc, PE, or PE-Cy5 against B-cell surface markers were used on single cells isolated from bone marrow and analyzed by flow cytometry. **(B)** Table outlining cellularity of lymphoid organs and percentage or cellular counts of B-cell populations. Single cells were isolated from bone marrow and spleen and counted using trypan blue exclusion. Shown are the averages plus or minus the standard deviation.

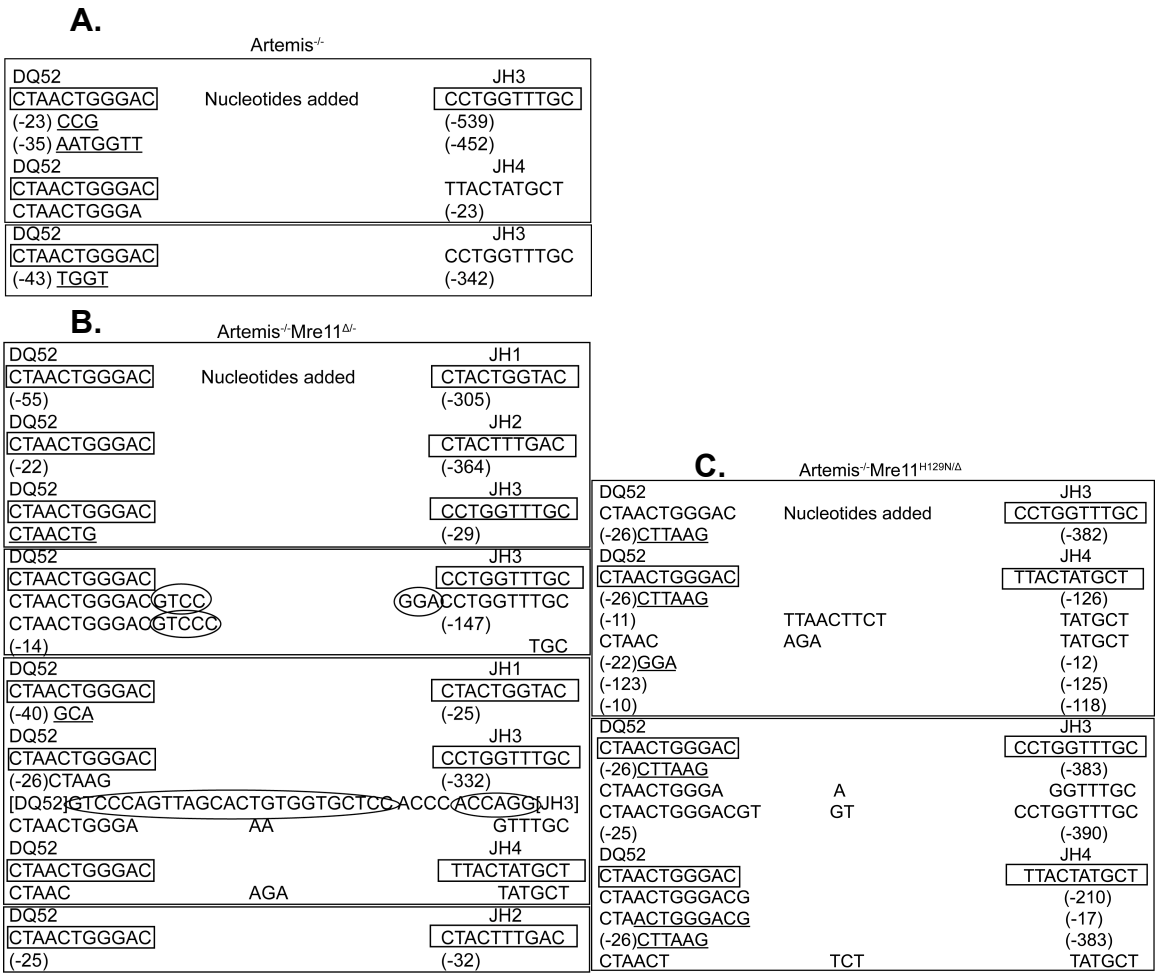

Figure 4.2 D_{Q52}-J_H junctional sequences. Total bone marrow DNA was isolated from 3-5 week old mice and D_{Q52} to J_H sequences PCR amplified using primers 5' of D_{Q52} and 3' to J_{H4}. **(A)** Sequences isolated from *Artemis*$^{-/-}$ B-cell populations. Boxed sequence indicate sequences isolated from different mice **(B)** Sequences isolated from *Artemis*$^{-/-}$*Mre11*$^{\Delta/-}$;CD19 Cre B-cell populations. Boxed sequence indicate sequences isolated from different mice **(C)** Sequences isolated from *Artemis*$^{-/-}$*Mre11*$^{\Delta/H129N}$;CD19 Cre B-cell populations. Boxed sequences indicate sequences isolated from different mice. Junctional sequence are qualitatively similar between *Artemis*$^{-/-}$ and *Artemis*$^{-/-}$*Mre11*$^{\Delta/H129N}$;CD19 Cre B-cell populations while 1/10 junctional sequence from *Artemis*$^{-/-}$*Mre11*$^{\Delta/-}$;CD19 Cre B-cell populations are distinct with long P-nucleotide addition on either side of the junction. P-nucleotides denoted by circle; bold, underline indicates microhomology.

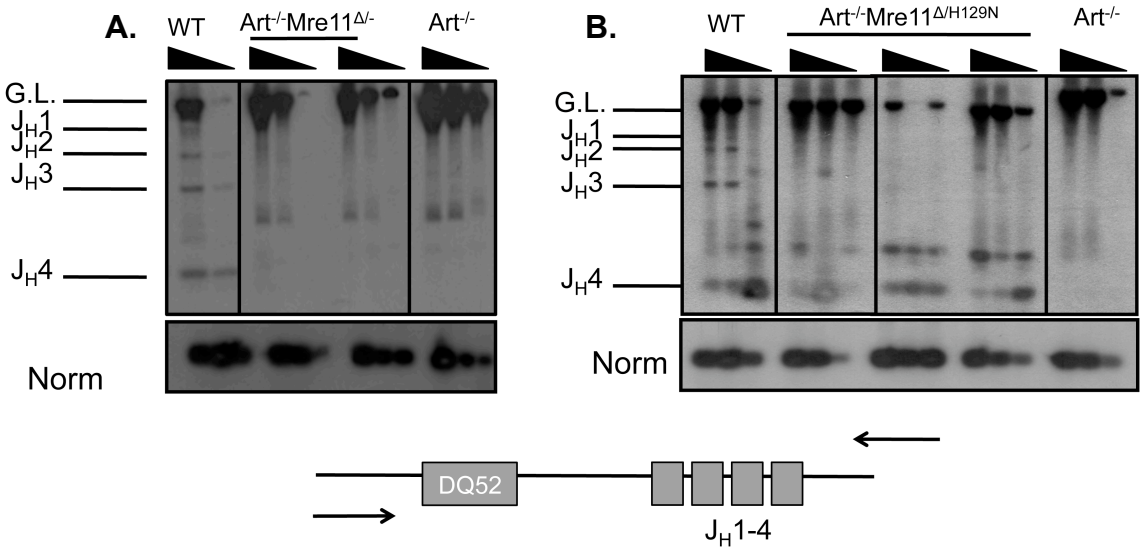

Figure 4.3 V(D)J rearrangements at the IgH locus between D_{Q52} and J_H gene segments. PCR amplification was performed on serial threefold dilutions of genomic DNA isolated from total bone marrow, and the products were detected by Southern blot hybridization. Control PCR amplification of a nonrearranging locus (ATM) was also performed to normalize levels of input genomic DNA. **(A)** D_{Q52}-J_H PCR Southern containing a wild type control (positive), *Artemis*$^{-/-}$ control (negative) and *Artemis*$^{-/-}$*Mre11*$^{\Delta/-}$;CD19 Cre B-cell populations. **(B)** D_{Q52}-J_H PCR Southern containing a wild type control (positive), *Artemis*$^{-/-}$ control (negative) and *Artemis*$^{-/-}$*Mre11*$^{\Delta/H129N}$;CD19 Cre B-cell populations.

V. CHAPTER 5

Discussion

The efficient repair of DNA double strand breaks (DSBs) by the classical nonhomologous end joining (cNHEJ) pathway requires the intricate coordination of multiple events at DNA ends. The cNHEJ pathway is not only required during general DSB repair, but also during the lymphoid specific DNA rearrangement, V(D)J recombination. This process is initiated by the RAG1/2 endonuclease that induces DNA DSBs adjacent to the recombining segments. The broken ends are subsequently processed and joined by the ubiquitously expressed cNHEJ factors (1-3). Defects during the joining phase of V(D)J recombination can lead to immunodeficiency syndromes due to impaired lymphocyte development. Furthermore, inappropriate joining of RAG1/2 generated DSBs can result in chromosomal translocations involving the juxtaposition of rearranging antigen receptor loci and cellular oncogenes which represent hallmark events associated with human lymphoid malignancies (4-6). Therefore, understanding the mechanisms of oncogenic transformation resulting from defective V(D)J recombination is important to our understanding of neoplastic transformation and genome integrity.

The cNHEJ gene, *ARTEMIS* (*DCLRE1C*, DNA crosslink repair 1C, OMIM#605988), is mutated in human immunodeficiency syndromes of varying severity (7, 8). Multiple *ARTEMIS* alleles associated with inherited combined immunodeficiency syndromes have been identified including missense, splice-site and nonsense mutations, gross exonic and smaller deletions and a small insertion (8, 9). The multiple *ARTEMIS* mutations lend themselves to genotype/phenotype correlations as most mutations located within the highly conserved metallo-β-lactamase/βCASP N-terminal domain (aa 1–385) result in inactivation of ARTEMIS activity (10). In contrast, a smaller subset of *ARTEMIS*

alleles that reside within the nonconserved C-terminus (aa 386–692), result in frameshifts followed by premature translation termination and diminished ARTEMIS activity (10).

Patients harboring null mutations suffer from an absence of lymphocytes, whereas partial loss-of-function *ARTEMIS* alleles are associated with immunodeficiency syndromes of varying severity, including $B^{-/low}T^{-/low}$ SCID, $B^{-/low}$ SCID, chronic inflammatory bowel disease and Omenn syndrome (7-22). Intriguingly, patients harboring hypomorphic, a syndrome of partial immunodeficiency and mature B lymphoma (23) characterizes C-terminal truncating ARTEMIS mutations. These lymphoid tumors were associated with Epstein-Barr virus. However, molecular analyses revealed that the lymphomas were of clonal origin, as evidenced by the rearrangement status of the immunoglobulin heavy chain locus, and also harbored chromosomal anomalies and increased genome instability (10).

These features suggest that aberrant ARTEMIS activity contributes to oncogenesis; however, before my line of investigation, it had not yet been established whether hypomorphic *ARTEMIS* mutations could predispose to tumorigenesis. The Sekiguchi lab generated a knock-in mutation of a patient hypomorphic mutation (D451fsX10, referred to as P70, herein) to investigate the in vivo impact of this mutation on V(D)J recombination and tumorigenesis (10). My studies examining the oncogenic molecular events that occurred in *Art-P70/p53* lymphomas led to the conclusion that this hypomorphic allele predisposes to lymphoid malignancies associated with clonal chromosomal anomalies. Thus, the ARTEMIS C-terminus is important in suppressing tumorigenesis and maintaining genome stability. In this regard, the ART-P70 mutant mouse provides a novel experimental system in which to elucidate the impact of aberrant V(D)J recombination events on spontaneous translocation formation in the presence of an active, albeit impaired, cNHEJ pathway.

My second line of investigation focused on the elucidation of the molecular mechanisms underlying the tumorigenesis phenotypes caused by *ARTEMIS* disease alleles and identification of factors involved in oncogenic transformation

associated with aberrant V(D)J recombination. To this end, when I interbred *Artemis*$^{-/-}$*p53*$^{-/-}$ mutant mice to MRE11 mutant alleles (that mutate the MRE11 complex in B-cells), these mice did not develop pro-B lymphomas as previously characterized, suggesting that the MRE11 complex facilitates pro-B lymphoma genesis.

My third line of investigation examined the roles of ARTEMIS and MRE11 in V(D)J recombination and in general DSB repair. To investigate how ARTEMIS and the MRE11 complex coordinate repair of RAG1/2-induced DSBs during V(D)J recombination, we mutated MRE11 in B-cells using a B-cell specific Cre and analyzed the impact of MRE11 mutation in the presence and absence of ARTEMIS. We observed that MRE11 mutated B-cells in the presence and absence of the ARTEMIS nuclease did not have an overt impact on B-cell development: MRE11 mutated B-cells in the presence of ARTEMIS exhibited normal B-cell development and MRE11 mutated B-cells in the absence of ARTEMIS exhibited impaired B lymphocyte development associated with *Artemis* nullizygosity. Additionally, we were able to detect D_H to J_H rearrangements in a subset (2/7) of *Artemis*$^{-/-}$*Mre11*$^{\Delta/H129N}$;CD19 Cre B-cells. We also observed that a subset of junctional sequences isolated from *Artemis*$^{-/-}$*Mre11*$^{\Delta/-}$;CD19 Cre B-cells exhibited unique end processing events unlike junctional sequences that had been recovered from control B-cells, MRE11 mutant B-cells, and *Artemis*$^{-/-}$ B-cells. These provocative observations raise some interesting questions about the interplay between ARTEMIS and the MRE11 complex at RAG1/2 DNA ends during V(D)J recombination and lays initial groundwork for future studies investigating the impact of ARTEMIS/MRE11 double mutation on levels of V(D)J rearrangements and quality of DNA end processing at RAG1/2 DNA ends in B-cells.

To investigate the coordination of ARTEMIS and the MRE11 complex in the repair of IR-induced DSBs, I generated murine embryonic fibroblasts (MEFs) harboring single or double mutations in ARTEMIS and MRE11. I observed that *Mre11*$^{\Delta/-}$,*Artemis*$^{-/-}$, *Artemis*$^{-/-}$*Mre11*$^{\Delta/H129N}$ and *Artemis*$^{-/-}$*Mre11*$^{\Delta/-}$ MEFs consistently exhibited similar percent survival post-irradiation, thereby indicating

that combining ARTEMIS and MRE11 mutation does not result in additive IR-sensitivity. My findings provide evidence that ARTEMIS and the MRE11 complex have overlapping roles in the repair of IR-induced breaks.

The studies of my dissertation converge on the question of the importance of ARTEMIS and the MRE11 complex on the suppression or generation of oncogenic events that lead to cellular transformation. In this chapter, I will discuss the novel findings of this dissertation and their implications with regards to our understanding DNA repair. Furthermore, future directions that will lead to a better understanding of the role of ARTEMIS and other factors in genome stability will be proposed.

The role of the ARTEMIS C-terminus in the repair of RAG1/2-generated DSBs

In chapter 2, I demonstrate that the ARTEMIS C-terminus is necessary to suppress tumorigenesis associated with aberrant V(D)J recombination and that the ART-P70 mutation combined with p53 deficiency generates a unique tumor spectrum as compared to *Artemis/p53* double null mice and other *cNHEJ/p53* double null mice (24-28).

How does the truncation of the ARTEMIS C-terminus affect the repair of RAG1/2-generated DSBs?

The ARTEMIS C-terminus is phosphorylated in a DNA damage-dependent manner by DNA-PKcs; however, the ATM kinase can also phosphorylate the ARTEMIS C-terminus in a DNA-damage dependent manner (29). In vitro studies have identified at least one ATM phosphorylation consensus cite within the Artemis C-terminus (29). Additionally, several labs have observed that DNA-PKcs and ATM can phosphorylate similar substrates in a DNA damage-dependent manner and in some cases can substitute for one another (30). Therefore, perhaps the ATM kinase phosphorylation site within the ARTEMIS C-terminus facilitates ARTEMIS functions at RAG1/2-generated DNA DSBs.

The Schatz laboratory elegantly showed that the RAG1/2 protein complex avidly binds both signal and coding ends and after cleavage, maintain the four

broken ends in a complex denoted as the post cleavage complex (PCC) (31). It is thought stabilization of the PCC facilitates the transfer of the broken DNA ends to the cNHEJ pathway for "normal," productive repair. Studies by the Sekiguchi and Sleckman laboratories identified that proteins in addition to RAG1/2, such as ATM, MRE11, NBS1, and ARTEMIS provide complex stability to the PCC (28, 32-34). Given that both ATM and ARTEMIS have been implicated in PCC stability and ATM can phosphorylate the ARTEMIS C-terminus, I hypothesize that the ATM-dependent phosphorylation of the ARTEMIS C-terminus influences the ability of ARTEMIS to provide complex stability to DNA ends within the PCC.

To test this hypothesis, I would interbreed *Atm* null mice to *Artemis*$^{P70//P70}$ mice and observe the tumor spectrum in *Artemis*$^{P70/P70}$*Atm*$^{-/-}$ mice as compared to *Atm*$^{-/-}$ mice and *Artemis-P70/p53* double mutant mice. If ATM phosphorylation of the ARTEMIS C-terminus were necessary for PCC stability, I would anticipate that *Artemis*$^{P70/P70}$*Atm*$^{-/-}$ mice would succumb to tumorigenesis associated with PCC destabilization (i.e. increase in translocations) similar to *Atm*$^{-/-}$ and *Artemis-P70/p53* double mutant mice (Figure 5.1D). However, if ATM has roles outside of PCC stability, as this is likely, then the *Artemis*$^{P70/P70}$*Atm*$^{-/-}$ mice could be devoid of tumors as a result of defective repair, likely due to a cellular overload of DNA damage (Figure 5.1E). Indeed, *Artemis*$^{-/-}$*Atm*$^{-/-}$ mice are not tumor prone suggesting that that the role of ATM in checkpoint activation and PCC stability is outweighed by its role in eliciting the DNA damage response and directing repair (35, 36). In this regard, studies have reported that ATM and ARTEMIS are epistatic in the repair of IR-induced DSBs (37). Another possibility, although not mutually exclusive, is that in the absence of ATM and ARTEMIS, perhaps additional factors can substitute for PCC stability thereby, reducing translocation frequency and tumor predisposition (Figure 5.1E).

How does the loss of the ARTEMIS C-terminus destabilize the PCC?

Protein-protein association is important for the DNA DSB response. In this regard, KU70 and KU80 directly interact to provide an appropriate scaffold for binding by DNA-PKcs. The MRE11/RAD50/NBS1 complex provides a platform

for ATM binding and kinase activation. I propose that after DNA-PKcs and ATM phosphorylate the ARTEMIS C-terminus in a DNA-damage dependent manner, the phosphorylated ARTEMIS C-terminus provides a scaffold for protein-protein interaction that in turn, recruits more proteins to the PCC to aid stabilization. To test this hypothesis, I would express a recombinant form of the phosphorylated ARTEMIS C-terminus (phosphorylated via treatment with a DNA damaging agent), and then immunoprecipitate the ARTEMIS C-terminus (anticipating interacting proteins would immunoprecipitate along with ARTEMIS) and submit for mass spec analysis to identify additional proteins that interact with the phosphorylated ARTEMIS C-terminus. To verify direct protein-protein interaction, I would use either a yeast two-hybrid approach or co-immunoprecipitation assay. Additionally, I would fine map the interactions to identify important phosphorylation sites or residues within the ARTEMIS C-terminus for protein-protein interaction.

To investigate if factors identified directly interact with the phosphorylated ARTEMIS C-terminus to aid PCC stability, I would mutate residues within ARTEMIS and observe if these mutated residues decreased PCC stability measuring inversional recombination of an extrachromosomal substrate previously used to assay PCC stability (28). Additionally, to functionally validate my observations, I could take ARTEMIS-P70 deficient cells and observe if co-expression of putative proteins increases or decreases PCC instability (i.e. increase or decrease translocations). If co-expression of the putative protein(s) and ARTEMIS-P70 results in decreased PCC stability, then it would suggest the putative protein and the ARTEMIS C-terminus coordinate PCC stability. Additional mutational analysis of the putative protein would be necessary to identify what region(s) or residue(s) are necessary to promote PCC stability via the ARTEMIS C-terminus. Overall, this additional line of investigation would provide insight into the role of the ARTEMIS C-terminus in PCC stabilization and thus, productive lymphocyte development.

Model: The ARTEMIS C-terminus provides stability to RAG1/2 DNA ends within the PCC

Putting it all together our findings suggest a model whereby after RAG1/2-induced DSBs, the ends are stabilized within the PCC to facilitate, "normal," productive repair. Destabilization of the PCC by any means (i.e. truncation of the ARTEMIS C-terminus, or mutations in ATM, NBS1, and/or MRE11) can prematurely release the broken DNA ends from the PCC making them susceptible to misrepair by an alternative pathway and increase the possibility for those ends to engage in oncogenic events and predispose to tumorigenesis.

Destabilization of the PCC by the truncation of the ARTEMIS C-terminus could occur as a result of the inability of the truncated protein to properly reach DNA ends due to 1) reduced phosphorylation by DNA-PKcs and/or ATM (29, 38) 2) or increase instability at the DNA ends. DNA-PKcs binds the KU heterodimer and facilitates synapsis of broken DNA ends (39). Evidence suggests that the KU/DNA-PKcs holoenzyme (DNA-PK) translocates away from the break to allow additional protein access (40, 41). Perhaps, the ARTEMIS C-terminus truncation mutant cannot access the break efficiently once DNA-PK translocates away from the end, and as a result, destabilizes the PCC. The mechanisms of PCC destabilization by truncation of the ARTEMIS C-terminus remains to be fully elucidated, nonetheless, our studies support an additional role for the ARTEMIS protein at DNA ends and highlights the importance of PCC stability during V(D)J recombination.

The MRE11 complex promotes pro-B lymphoma in *Artemis*$^{-/-}$*p53*$^{-/-}$ mice

In chapter 3, to investigate the contribution of the MRE11 complex to pro-B lymphomas that arise in *Artemis*$^{-/-}$*p53*$^{-/-}$ mice, I interbred *Artemis*$^{-/-}$*p53*$^{-/-}$ mice to mice harboring MRE11 mutant alleles and a B-cell specific Cre, CD19. Combining MRE11 mutation in *Artemis*$^{-/-}$*p53*$^{-/-}$ mice using a B-cell specific Cre increased survival time, suppressed pro-B lymphoma, and changed the tumor spectrum. Taken together, my data suggests that the MRE11 complex promotes tumorigenesis associated with aberrant V(D)J recombination and complex translocations in pro-B lymphomas that arise in *Artemis*$^{-/-}$*p53*$^{-/-}$ mice.

Could the MRE11 complex promote pro-B lymphoma in *Artemis*$^{-/-}$*p53*$^{-/-}$ mice via aNHEJ?

Although the MRE11 complex does not directly participate in V(D)J recombination, the MRE11 complex plays multiple roles in the repair of RAG1/2-mediated DNA DSBs. Recent evidence suggests that the MRE11 complex, as well as ATM, functions to stabilize V(D)J coding ends within the PCC (42). Indeed, deficiency of components within the MRE11 complex results in accumulation of coding ends (42, 43), increased levels of interchromosomal trans-rearrangements (a type of aberrant event that is a proxy for chromosomal translocation events) (43, 44) and hybrid joins that are non-productive V(D)J rearrangements between coding and signal ends (42, 45). Furthermore, several studies have provided compelling evidence that the MRE11 complex functions in the context of both the cNHEJ and alternative NHEJ (aNHEJ) pathways (45-48). Importantly for our proposed studies, oncogenic chromosomal translocations that are generated in *cNHEJ/p53* deficient lymphocytes are largely catalyzed by the aNHEJ pathway mediated by sequence homology at the break point junction, as the translocation breakpoints contained microhomologies of 2-8 nucleotides (24-26, 49, 50). Therefore, one possibility whereby the MRE11 complex promotes pro-B lymphoma in *Artemis*$^{-/-}$*p53*$^{-/-}$ mice could be via its activity in the aNHEJ pathway to promote chromosomal translocations and ultimately cellular transformation and oncogenesis. Indeed, recent in vitro studies have shown a coordinated effort by MRE11 and DNA LIGASE IIIα in the repair of non-compatible DNA ends utilizing end-resection and microhomology (reminiscent of in vivo aNHEJ events) (51).

To address if the MRE11 complex could support aberrant joining associated with aNHEJ (primarily between rearranging loci and C-MYC), pro-B-cell progenitors could be harvested from *Artemis*$^{-/-}$*p53*$^{-/-}$*Mre11*$^{C/-}$ murine fetal livers, the *Mre11*^{C} allele deleted, V(D)J recombination induced and over time and the cultures assayed for the generation of translocations between, in particular, the IgH locus and C-MYC using a sensitive long-range PCR technique (52). If I

am unable to detect the IgH locus and C-MYC translocations by using long-range PCR, I could use high-resolution array comparative genomic hybridization (aCGH) to investigate a global change in translocation formation. To address if the MRE11 complex supports aberrant joining associated with aNHEJ in other lymphoid malignancies, such as thymic lymphomas, I could mutate the MRE11 complex in *Artemis*$^{-/-}$*p53*$^{-/-}$ T-cells. Thymic lymphomas that arise in *Artemis*$^{-/-}$*p53*$^{-/-}$ mice also harbor translocations involving rearranging loci, such as at the TCRαδ locus, and thus, would provide a good model system to use to address if the MRE11 complex facilitates chromosomal translocations mediated by aNHEJ in other lymphoid malignancies.

Could the MRE11 complex promote pro-B lymphoma in *Artemis*$^{-/-}$*p53*$^{-/-}$ mice via its role in promoting tumor cell replication, and thus, survival?

Pro-B lymphomas from *Artemis*$^{-/-}$*p53*$^{-/-}$ mice not only contain chromosomal translocations, but also frequently overexpress C-MYC or N-MYC. In particular, C-MYC overexpression has been shown to aberrantly progress cells through the cell cycle. Initially, it was thought that C-MYC overexpression influences cell cycle progression via its role as a transcription factor; however, recent studies suggest that C-MYC directly interacts with CDC45 and the GINs complex (protein complex required for cellular replication) to bind to replication origins and travel with the replication fork after initiation (53). As a consequence of C-MYC overexpression, the fork rate is unaffected; however, fork progression becomes asymmetrical and results in fork stalling (53). Upon fork stalling, the replisome consisting of the GINs complex can dissociate and as a result, halt replication. Recent evidence implicates MRE11 in supporting replication fork progression and replication fork re-start (54-56). Taken together, in a cell that overexpresses C-MYC, perhaps the MRE11 complex is required to promote tumor cell survival by promoting DNA replication associated with C-MYC overexpression. In this regard, MRE11 complex deficiency would result in severe defects in DNA replication and eventually cell death. Therefore, the MRE11 complex may be required for tumor cell survival associated with C-MYC overexpression as an

indirect consequence of the importance of MRE11 in oncogene-induced DNA replication.

To address the role of the MRE11 complex in tumor cell survival, pro-B lymphomas (overexpressing C-MYC) isolated from *Artemis*$^{-/-}$*p53*$^{-/-}$*Mre11*$^{C/-}$ mice could be cultured and then deleted for the *Mre11*^{C} allele and assayed for cellular survival over time using an apoptosis maker such as Annexin V. To investigate if the MRE11 complex is required for tumor cell survival due to oncogene-induced replication stress (such as C-MYC overexpression), B-cells (that do not overexpress C-MYC) could be harvested from fetal liver cultures from *Artemis*$^{-/-}$ *p53*$^{-/-}$*Mre11*$^{C/-}$ mice and treated with another replication stress agent such as aphidicolin. The amount of apoptosis could be assayed using Annexin V in the presence and absence of the MRE11 complex in B-cell cultures treated with aphidicolin. If aphidicolin treatment in the absence of the MRE11 complex resulted in an increase in cellular apoptosis as compared to the control, it would provide evidence that the MRE11 complex is required for tumor cell survival associated with replication stress—as a result of C-MYC overexpression or aphidicolin treatment.

Could the MRE11 complex promote pro-B lymphoma in *Artemis*$^{-/-}$*p53*$^{-/-}$ mice via its role in the activation of the oncogene-induced damage response?

Recently, the Petrini lab generated a rodent model of ERBB2/HER2 overexpression and virally infected mammary glands of DNA repair-deficient mice to address the role of DNA repair factors in the oncogene-induced DNA damage response (57, 58). The Petrini lab identified that deficiency in the MRE11 complex (in the presence of oncogene overexpression) resulted in increased hyperplasia within the mammary gland, a muted DNA damage response, and abrogated checkpoint activation (58). Thus, the Petrini lab concluded that the activation of the oncogene-induced DNA damage response is dependent upon the activities of the MRE11 complex. Therefore, my observation that *Artemis*$^{-/-}$*p53*$^{-/-}$;CD19 Cre mice harboring the *Mre11*^{H129N} allele, associated with activation of checkpoints and ATM activity, are suppressed for pro-B

lymphoma could be due to the role of the MRE11 complex in activating an oncogene-induced DNA damage response. This observation suggests that the ATM-dependent DNA damage response, mediated by the MRE11 complex, could possibly act as a barrier to tumorigenesis, perhaps via activation of cell cycle checkpoints and the oncogene-induced DNA damage response. However, if the activity of the MRE11 complex in the oncogene-induced DNA damage response provided a barrier to tumorigenesis, we would have anticipated observing pro-B lymphoma genesis in *Artemis*$^{-/-}$*p53*$^{-/-}$ mice harboring the *Mre11*$^{\Delta}$ allele in B-cells. However, we observed that MRE11 complex deficiency resulted in pro-B suppression. Our results are in direct contrast to the studies conducted in the Petrini lab that identified an increase in tumor malignancy in the absence of components of the MRE11 complex.

A possible explanation is that in the Petrini study, they used a spontaneous mouse model of breast cancer using the ERBB2/HER2 oncogene to drive tumorigenesis in mammary glands. The etiology of different tumor types is distinct. Endothelial cells of the mammary gland that transform and become malignant are more prone to undergo oncogene-induced senescence, rather than apoptosis (59). In contrast, lymphocytes are exquisitely prone to undergo cellular apoptosis (60). Therefore, the mechanisms by which lymphocytes transform to become malignant lymphoma versus mammary endothelial cells that transform to become malignant breast cancer are distinct and could explain why we observe a contradictory role of the MRE11 complex in tumorigenesis. Additionally, the cellular responses to DNA damage as a result of different oncogenes could explain the different observed outcomes. C-MYC overexpression is well-described to drive tumor cells abruptly into S-phase resulting in increased genomic instability and chromosomal translocations (53, 61-63). ERBB2/HER2 is a tyrosine protein kinase that elicits cellular signals to promote cellular growth and differentiation (64). It is probable that the different oncogenes could elicit unique responses, and therefore, modulate the function of the MRE11 complex in tumorigenesis.

At face value, the studies conducted in our lab contradict the findings from the Petrini lab. However, both of our findings could possibly be explaining similar underlying biology of the MRE11 complex in tumorigenesis. Our observation that MRE11 mutation suppresses pro-B lymphoma (associated with C-MYC overexpression) in *Artemis*$^{-/-}$*p53*$^{-/-}$ mutant mice could be due to the role of the MRE11 complex in activating an oncogene-induced DNA damage response. In this regard, deficiency in the MRE11 complex would result in increased genome stability as a consequence of a muted DNA damage response. This has previously been reported for the *Artemis*$^{-/-}$*Atm*$^{-/-}$ mutant mice (35, 36). An apparent catastrophic overload in DNA damage in mice doubly deficient for both ATM and ARTEMIS suppressed tumorigenesis (35, 36). Strikingly, these mice survive tumor-free in contrast to *Atm*$^{-/-}$ mice that develop thymic lymphoma and *Artemis*$^{-/-}$ mice (combined with p53 deficiency, an ATM-mediated checkpoint) that are prone to progenitor lymphoid malignancies (26, 28, 36, 65). In light of these findings, I suggest that mutating the MRE11 complex in *Artemis*$^{-/-}$*p53*$^{-/-}$ mutant B-cells, results in an overwhelming amount of DNA damage as a result of additive defective DNA repair. Thus, in our tumor animal model, mutant B-cells harboring a catastrophic amount of DNA damage undergoes apoptosis and as a result, pro-B lymphoma is suppressed. In this regard, preliminary findings in *Artemis*$^{-/-}$ *Mre11*$^{\Delta/-}$ primary MEFs identified additive chromosomal anomalies as compared to the control and *Mre11*$^{\Delta/-}$ primary MEFs (Chapter 4).

To test if the MRE11 complex activates an oncogene-induced DNA damage response in pro-B lymphoma, it would be interesting to take *Artemis*$^{-/-}$ *p53*$^{-/-}$*Mre11*$^{C/-}$ pro-B lymphomas that overexpress C-MYC and measure phosphorylation levels of proteins important for the DNA damage response in the presence and absence of the MRE11 complex. Likely protein targets to measure in the DNA damage response would be those in the ATM pathway (as the MRE11 complex and ATM share a similar DNA repair pathway) such as H2AX, KAP-1, CHK2, and SMC1 that become phosphorylated in an ATM-dependent manner in the presence of DNA damage. Additionally, using an array to analyze for phosphorylation targets of ATM in pro-B lymphomas (overexpressing C-MYC)

with and without the MRE11 complex would shed light on the global consequences of the oncogene-induced DNA damage response possibly modulated by the MRE11 complex, in the context of our animal model.

Model: The MRE11 complex promotes pro-B lymphoma in *Artemis*$^{-/-}$*p53*$^{-/-}$ mice

My results suggest that the MRE11 complex facilitates pro-B lymphoma genesis in *Artemis*$^{-/-}$*p53*$^{-/-}$ B-cells perhaps via the activity of the MRE11 complex in aNHEJ or, not mutually exclusive, the role of the MRE11 complex in tumor cell survival. From my observations, I suggest the following: perhaps *Artemis*$^{-/-}$*p53*$^{-/-}$ B-cells with unrepaired RAG1/2-induced DSBs continue replicating in the presence of aberrant joins. If so, then perhaps this aberrant cycling could create additional breaks else where in the genome and the MRE11 complex could mediate chromosomal translocations that result in C-MYC overexpression and subsequent cellular transformation. Conversely, in the absence of p53, unrepaired RAG1/2 DNA ends in *Artemis*$^{-/-}$ B-cells could aberrantly progress through the cell cycle and a single such initiating event, such as a dicentric chromosome, could be amplified rapidly and inevitably by successive breakage-fusion-bridge cycles (66). Indeed, dicentric chromosomes harboring the IgH locus and *c-myc* have been reported in other *cNHEJ/p53* double deficient mice such as *Lig4/p53* double mutant mice and *Xrcc4/p53* double mutant mice that harbor IgH and *c-myc* genomic amplification as a result of breakage-fusion-bridge cycles of these intermediates (5). If C-MYC overexpression occurs as a result of dicentric chromosome amplification, then the MRE11 complex could facilitate either DNA replication in cells overexpressing C-MYC or participate in the activation of the oncogene-induced DNA damage response to promote tumor cell survival.

The functional interactions of ARTEMIS and the MRE11 complex in DNA end joining during general DSB repair

In Chapter 4, I investigate the functional interactions between ARTEMIS and the MRE11 complex that are required for DNA end processing in the context of general DSB repair. I observed that *Mre11*$^{\Delta/-}$, *Artemis*$^{-/-}$, *Artemis*$^{-/-}$*Mre11*$^{\Delta/H129N}$

and *Artemis*$^{-/-}$*Mre11*$^{\Delta/-}$ MEFs consistently exhibited similar percent survival post-irradiation, thereby demonstrating that combining ARTEMIS and MRE11 mutation does not result in additive IR-sensitivity. My dissertation lays the initial groundwork for better understanding the contribution of these two nucleases in DNA end processing events as the precise roles and functional interactions between ARTEMIS and the MRE11 complex had not been previously investigated.

How then, do ARTEMIS and the MRE11 complex coordinate their repair?

To investigate the coordination of ARTEMIS and the MRE11 complex at DNA ends I would create a system where systematic one-sided DSBs could be generated, whereby I could use chromatin immunoprecipitation (ChiP) to analyze protein:DNA interactions. I propose to investigate the coordination of ARTEMIS and the MRE11 complex by taking advantage of telomere destabilization by TRF2 depletion. Complete depletion of TRF2 uncaps telomere ends producing a one-sided break whereby the DNA damage response is activated and the uncapped telomeres are aberrantly repaired in end-to-end fusions by the cNHEJ pathway (67). As a means to bypass end-to-end fusions as a result of telomere uncapping, I propose to serially deplete TRF2 to achieve a state where the telomeres are uncapped but exist in the cell without eliciting end-to end fusions. Indeed, a group was able to achieve a level of TRF2 depletion where uncapped telomeres were able to persist throughout phases of the cell cycle and elicit the DNA damage response without detectable levels of end-to-end fusions (68). With this system, I would have the ability to introduce a one-sided DNA DSB in known regions of the genome, ChiP ARTEMIS and MRE11 molecular complexes and identify if they were bound to the damaged telomere. Additionally, with this system, I can analyze the impact of ARTEMIS and MRE11 complex depletion in the uncapped telomere-mediated DNA damage response by completing depleting TRF2 in ARTEMIS and MRE11 deficient cells and analyzing the frequency of end-to-end fusions and the junctional sequences within the fusions. Additionally, I can elucidate what phases of the cell cycle ARTEMIS and the

MRE11 complex coordinate repair via cell cycle synchronization or taking advantage of well-established cell cycle markers to sort cells in different phases of the cell cycle. I could then subject the cells to my TRF2 depletion system and ChiP ARTEMIS and the MRE11 complex to identify if cell cycle phases impact their binding of uncapped, damaged telomeres or affect the frequency of end-to-end fusions.

Model: ARTEMIS and the MRE11 complex coordinate repair of DNA ends

My findings provide evidence that ARTEMIS and the MRE11 complex have overlapping roles in the repair of IR-induced breaks. This observation is not surprising due to the molecular properties of ARTEMIS and MRE11 (i.e. nuclease activities prefer similar DNA substrate: loops, flaps, 5' and 3' overhangs). However, it is surprising the mildness of sensitivity of the ARTEMIS/MRE11 double mutants in response to IR in SV40 MEFs. The MRE11 complex is predominantly involved in homologous recombination (HR), which favors homology-directed repair. ARTEMIS is primarily involved in the cNHEJ pathway that repairs breaks via direct end-to-end ligation, with modification at the junction. These two DNA repair pathways repair the bulk of DSBs and deficiencies in either pathway results in cellular sensitivity to DNA damaging agents (69, 70). That the combination of ARTEMIS and MRE11 deficiencies does not result in additive sensitivity to IR-induced breaks provides strong evidence for the importance of ARTEMIS in repair pathways outside of cNHEJ and for MRE11 in repair pathways outside of HR.

Taken together, my data supports a model in which after DNA damage, ARTEMIS and MRE11 coordinate repair at DNA ends. This could be via their roles in NHEJ (as studies implicate MRE11 in both cNHEJ and aNHEJ) or in HR (45-48, 51). Although the studies for ARTEMIS in HR do not suggest that ARTEMIS repairs the bulk of DSBs, the studies do suggest that ARTEMIS nuclease activities are important for the removal of lesions or secondary structures, which act to inhibit HR-mediated DNA resection essential for HR (71). Indeed a nuclease deficient mutation of ARTEMIS could not compliment *ARTEMIS* null cells defective in G2-mediated end resection suggesting the

endonucleolytic activities of ARTEMIS are important for G2-mediated end resection to promote HR (71). Therefore, it is possible that ARTEMIS and the MRE11 complex coordinate repair to remove moieties from DNA DSBs to promote HR-mediated resection and thus, resolution of the break.

There is a growing amount of evidence that implicates MRE11 in the repair of DNA damage utilizing an end joining pathway. The MRE11 complex recruits and activates the ATM kinase in a DNA damage-dependent manner. Therefore, the MRE11 complex and the ATM kinase share a similar DNA repair pathway. Interestingly, studies have implicated ATM and ARTEMIS in a similar DNA repair pathway for a subset of breaks that require additional DNA end processing (37). Extending these observations suggest that ARTEMIS and the MRE11 complex could potentially work together (perhaps via ATM) to promote NHEJ on a subset of breaks that require additional processing.

The functional interactions of ARTEMIS and the MRE11 complex in DNA end joining during V(D)J recombination

In Chapter 4, I investigate the functional interactions between ARTEMIS and the MRE11 complex that are required for DNA end processing in the context of V(D)J recombination, a lymphocyte specific somatic rearrangement. We observed that MRE11 mutated B-cells did not have an overt impact on B-cell development and that *Artemis*$^{-/-}$*Mre11*$^{\Delta/-}$;CD19 Cre B-cells and *Artemis*$^{-/-}$ *Mre11*$^{\Delta/H129N}$;CD19 Cre B-cells resembled *Artemis*$^{-/-}$ B-cells in regards to lymphocyte development, lymphocyte ceullarity and percentage of B-cell populations associated with different developmental stages of V(D)J recombination. Interestingly, we could detect D_H to J_H rearrangements in a subset (2/7) of *Artemis*$^{-/-}$*Mre11*$^{\Delta/H129N}$;CD19 Cre B-cells. In contrast, I did not detect D_H to J_H rearrangements in *Artemis*$^{-/-}$ B-cells. This result implicates a structural role for the MRE11 complex at DNA ends. This data suggests that in the absence of ARTEMIS, the MRE11 complex can bind RAG1/2-generated ends and potentially promote D_H to J_H joining. My observation is consistent with previous studies that identified that MRE11 can directly bind DNA ends to

facilitate DNA end bridging, and through its interaction with RAD50, tether DNA ends over long distances to promote repair (72-74).

What is the role of the MRE11 complex at RAG1/2-induced breaks in *Artemis*$^{-/-}$ B-cells?

While there is lacking evidence to support a role for the nuclease activities of the MRE11 complex in cNHEJ, my evidence does possibly provide support for a role for the nuclease activities of the MRE11 complex in a back-up end joining pathway or a alternative end joining pathway (aNHEJ). I propose that in *Artemis*$^{-/-}$ lymphocytes, the MRE11 complex is present and via its DNA end binding or end tethering capabilities, can bind RAG1/2-generated ends and stabilize the PCC. As a result of ARTEMIS-deficiency, the hairpin coding ends accumulate (with the MRE11 complex bound at the ends) and the nuclease properties of the MRE11 complex may process a subset of ends to be repaired via aNHEJ. Why did I not detect robust products in my PCR assay for D_H to J_H rearrangements in *Artemis*$^{-/-}$ lymphocytes? Perhaps the RAG1/2 ends bound by the MRE11 complex, once opened by the MRE11 complex, were shuttled to an aNHEJ pathway that utilized robust resection and chewed back the DNA ends so far that I was not able to detect those products in my PCR based assay. I could address this caveat by using well-established pre-B cells lines that contain an extrachromosomal V(D)J recombination substrate. The extrachromosomal substrate allows investigation of coding end joining by genomic Southern, thus, I could analyze coding join fidelity associated with large deletions that may have been excluded using PCR analysis.

Artemis$^{-/-}$*Mre11*$^{\Delta/H129N}$ B lymphocytes contain detectable rearrangement products of D_H to J_H rearrangements, albeit in a subset of mice. In this scenario, the MRE11 complex is present and maintains ends in the PCC; however, since the nuclease properties of the MRE11 complex are hampered, another nuclease could be recruited where only minimal resection occurs and allows for an aNHEJ repair event (associated with minimal deletion) to occur whereby we can detect these products in the PCR based assay. In support of this model, we are unable

to detect rearrangements in *Artemis*$^{-/-}$*Mre11*$^{\Delta/-}$ lymphocytes, as there is an absence of hairpin opening, PCC stabilization, and repair pathways.

How does the MRE11 complex facilitate V(D)J recombination?

To better address this question, it would be useful to use an early hematopoietic Cre expresser, such as the mb1 Cre transgene, where expression begins early in lymphocyte progenitors so that more of the lymphocyte population would be doubly deficient at the initiation of V(D)J recombination. As my present study suggests a role for the MRE11 complex in aNHEJ, it is worth addressing the role of the MRE11 complex in cNHEJ during V(D)J recombination. 53BP1 has recently been identified to support cNHEJ during general DSB repair and V(D)J recombination, even though *53bp1*$^{-/-}$ mice do not have an overt V(D)J recombination defect (75, 76). 53BP1 and the MRE11 complex directly interact to amplify the DNA damage response (77). Therefore, perhaps similarly to 53BP1, the MRE11 complex may have a limited role during V(D)J recombination at DNA ends that require specific mechanisms of joining during cNHEJ repair of RAG1/2 breaks.

Initial characterization of *53bp1*$^{-/-}$ lymphocytes indicated that 53BP1 was dispensable for V(D)J rearrangements but required for class switch recombination (75). Interestingly, upon further investigation of *53bp1*$^{-/-}$ lymphocytes it was observed using quantitative polymerase chain reactions (Q-PCR) at the TCRα/δ locus that 53BP1 deficiency decreased “long-range” joining between Vδ-DJδ but “short-range” joining between Dδ2-Jδ2 was unaffected (76). Perhaps the MRE11 complex possesses requirements in end joining, similar to 53BP1, to facilitate repair or RAG1/2 DNA ends during “long-range” joining. It would be interesting to investigate the contribution of the MRE11 complex to “long-range” and “short-range” recombination in B and T lymphocytes using the mb1 Cre transgene.

Model: The MRE11 complex facilitates aberrant V(D)J recombination

Taken together, my results suggest that the MRE11 complex facilitates repair of RAG1/2 DSBs when cNHEJ is deficient. Therefore, from my

observations, I suggest that the MRE11 complex promotes aberrant V(D)J recombination. There are several lines of evidence to support my observations. The MRE11 complex has been implicated in aNHEJ joining events in cNHEJ-deficient cells and mice (46-48). Furthermore, biochemical studies identified a functional interaction between MRE11 and the prominent ligase in aNHEJ, DNA LIGASE IIIα/XRCC1 (51). Therefore, this suggests that the MRE11 complex can promote repair via the aNHEJ pathway and it is possible that the MRE11 complex contributes to 'leaky' lymphocyte development in cNHEJ-deficient mice.

Summary

Chromosomal translocations linking cellular oncogenes to the loci undergoing V(D)J rearrangements are hallmarks of a number of human lymphoid neoplasias (78). Defective V(D)J recombination represents one mechanism by which these oncogenic chromosomal anomalies arise and can lead to oncogene overexpression (78). The majority of translocations associated with human lymphoid malignancies are catalyzed by microhomologies, which are hypothesized to facilitate the alignment and joining of broken DNA ends. The studies conducted in this dissertation are aimed at gaining a better understanding of the DNA repair pathways that function to prevent and/or mediate aberrant V(D)J recombination events that lead to tumorigenesis.

My studies of the ARTEMIS-P70 C-terminal truncation mutant revealed important functions of the ARTEMIS C-terminus in providing stability to RAG1/2-generated DSBs within the PCC and in turn, suppressing aberrant V(D)J rearrangements that can lead to oncogenic transformation. These findings have important implications for the diagnosis and treatment of other ARTEMIS C-terminal truncating mutations and of other factors involved in lymphocyte development that reduce, but not severely abrogate, lymphocyte development.

My dissertation work defining critical roles for the MRE11 complex in promoting pro-B lymphoma in *Artemis/p53* double mutant mice provides novel observations to the role of the MRE11 complex in pro-B lymphoma genesis. My studies implicate the MRE11 complex either in promoting aberrant DNA rearrangements that arise in *Artemis/p53* double mutant and predispose to

tumorigenesis or, not mutually exclusive, promote tumor cell survival. My findings provide a platform to investigate the roles of the MRE11 complex in promoting other malignancies and thus, implicate the MRE11 complex as a potential chemotherapeutic.

Furthermore, my dissertation provides novel observations about the complex functional interactions between the DNA repair factors that control cellular responses to DNA DSBs, ATM and MRE11, and the ARTEMIS nuclease. The compound mutant cell lines and mice I have generated represent unique and valuable reagents to address these important questions. My dissertation not only contributes to our understanding of the molecular mechanisms of V(D)J recombination, DNA DSB repair and maintenance of genome stability, but also provides insights into the underlying causes of human immunodeficiency and cancer predisposition syndromes, which may ultimately provide direct insights into targets for improved treatment of these diseases.

References

1. Bassing CH, Suh H, Ferguson DO, Chua KF, Manis J, Eckersdorff M, et al. Histone H2AX: a dosage-dependent suppressor of oncogenic translocations and tumors. Cell. 2003;114(3):359-70.
2. Sekiguchi J, Alt F.W., Oettinger M., Honjo T. Molecular Biology of B Cells. In: W. AF, editor. Elsevier Science2004. p. 57-78.
3. Ahnesorg P, Smith P, Jackson SP. XLF interacts with the XRCC4-DNA ligase IV complex to promote DNA nonhomologous end-joining. Cell. 2006;124(2):301-13.
4. Tycko B, Sklar J. Chromosomal translocations in lymphoid neoplasia: a reappraisal of the recombinase model. Cancer Cells. 1990;2(1):1-8.
5. Mills KD, Ferguson DO, Alt FW. The role of DNA breaks in genomic instability and tumorigenesis. Immunol Rev. 2003;194:77-95.
6. Chatterji M, Tsai CL, Schatz DG. New concepts in the regulation of an ancient reaction: transposition by RAG1/RAG2. Immunol Rev. 2004;200:261-71.
7. Moshous D, Callebaut I, de Chasseval R, Corneo B, Cavazzana-Calvo M, Le Deist F, et al. Artemis, a novel DNA double-strand break repair/V(D)J recombination protein, is mutated in human severe combined immune deficiency. Cell. 2001;105(2):177-86.
8. Le Deist F, Poinsignon C, Moshous D, Fischer A, de Villartay JP. Artemis sheds new light on V(D)J recombination. Immunol Rev. 2004;200:142-55.
9. Pannicke U, Honig M, Schulze I, Rohr J, Heinz GA, Braun S, et al. The most frequent DCLRE1C (ARTEMIS) mutations are based on homologous recombination events. Hum Mutat. 2010;31(2):197-207.
10. Moshous D, Pannetier C, Chasseval Rd R, Deist Fl F, Cavazzana-Calvo M, Romana S, et al. Partial T and B lymphocyte immunodeficiency and predisposition to lymphoma in patients with hypomorphic mutations in Artemis. J Clin Invest. 2003;111(3):381-7. PMCID: 151863.
11. Ege M, Ma Y, Manfras B, Kalwak K, Lu H, Lieber MR, et al. Omenn syndrome due to ARTEMIS mutations. Blood. 2005;105(11):4179-86.
12. van der Burg M, Verkaik NS, den Dekker AT, Barendregt BH, Pico-Knijnenburg I, Tezcan I, et al. Defective Artemis nuclease is characterized by coding joints with microhomology in long palindromic-nucleotide stretches. Eur J Immunol. 2007;37(12):3522-8.
13. Musio A, Marrella V, Sobacchi C, Rucci F, Fariselli L, Giliani S, et al. Damaging-agent sensitivity of Artemis-deficient cell lines. Eur J Immunol. 2005;35(4):1250-6.
14. de Villartay JP, Shimazaki N, Charbonnier JB, Fischer A, Mornon JP, Lieber MR, et al. A histidine in the beta-CASP domain of Artemis is critical for its full in vitro and in vivo functions. DNA Repair (Amst). 2009;8(2):202-8.

15. Darroudi F, Wiegant W, Meijers M, Friedl AA, van der Burg M, Fomina J, et al. Role of Artemis in DSB repair and guarding chromosomal stability following exposure to ionizing radiation at different stages of cell cycle. Mutat Res. 2007;615(1-2):111-24.
16. Lagresle-Peyrou C, Benjelloun F, Hue C, Andre-Schmutz I, Bonhomme D, Forveille M, et al. Restoration of human B-cell differentiation into NOD-SCID mice engrafted with gene-corrected CD34+ cells isolated from Artemis or RAG1-deficient patients. Mol Ther. 2008;16(2):396-403.
17. Evans PM, Woodbine L, Riballo E, Gennery AR, Hubank M, Jeggo PA. Radiation-induced delayed cell death in a hypomorphic Artemis cell line. Hum Mol Genet. 2006;15(8):1303-11.
18. Kobayashi N, Agematsu K, Sugita K, Sako M, Nonoyama S, Yachie A, et al. Novel Artemis gene mutations of radiosensitive severe combined immunodeficiency in Japanese families. Hum Genet. 2003;112(4):348-52.
19. Li L, Moshous D, Zhou Y, Wang J, Xie G, Salido E, et al. A founder mutation in Artemis, an SNM1-like protein, causes SCID in Athabascan-speaking Native Americans. J Immunol. 2002;168(12):6323-9.
20. Noordzij JG, Verkaik NS, van der Burg M, van Veelen LR, de Bruin-Versteeg S, Wiegant W, et al. Radiosensitive SCID patients with Artemis gene mutations show a complete B-cell differentiation arrest at the pre-B-cell receptor checkpoint in bone marrow. Blood. 2003;101(4):1446-52.
21. van Zelm MC, Geertsema C, Nieuwenhuis N, de Ridder D, Conley ME, Schiff C, et al. Gross deletions involving IGHM, BTK, or Artemis: a model for genomic lesions mediated by transposable elements. Am J Hum Genet. 2008;82(2):320-32. PMCID: 2427306.
22. Rohr J, Pannicke U, Doring M, Schmitt-Graeff A, Wiech E, Busch A, et al. Chronic inflammatory bowel disease as key manifestation of atypical ARTEMIS deficiency. J Clin Immunol. 2010;30(2):314-20.
23. Moshous D, Callebaut I, de Chasseval R, Poinsignon C, Villey I, Fischer A, et al. The V(D)J recombination/DNA repair factor artemis belongs to the metallo-beta-lactamase family and constitutes a critical developmental checkpoint of the lymphoid system. Ann N Y Acad Sci. 2003;987:150-7.
24. Difilippantonio MJ, Zhu J, Chen HT, Meffre E, Nussenzweig MC, Max EE, et al. DNA repair protein Ku80 suppresses chromosomal aberrations and malignant transformation. Nature. 2000;404(6777):510-4.
25. Nacht M, Strasser A, Chan YR, Harris AW, Schlissel M, Bronson RT, et al. Mutations in the p53 and SCID genes cooperate in tumorigenesis. Genes Dev. 1996;10(16):2055-66.
26. Rooney S, Sekiguchi J, Whitlow S, Eckersdorff M, Manis JP, Lee C, et al. Artemis and p53 cooperate to suppress oncogenic N-myc amplification in progenitor B cells. Proc Natl Acad Sci U S A. 2004;101(8):2410-5. PMCID: 356964.
27. Zhu C, Mills KD, Ferguson DO, Lee C, Manis J, Fleming J, et al. Unrepaired DNA breaks in p53-deficient cells lead to oncogenic gene amplification subsequent to translocations. Cell. 2002;109(7):811-21.

28. Jacobs C, Huang Y, Masud T, Lu W, Westfield G, Giblin W, et al. A hypomorphic Artemis human disease allele causes aberrant chromosomal rearrangements and tumorigenesis. Hum Mol Genet. 2011;20(4):806-19. PMCID: 3024049.
29. Chen L, Morio T, Minegishi Y, Nakada S, Nagasawa M, Komatsu K, et al. Ataxia-telangiectasia-mutated dependent phosphorylation of Artemis in response to DNA damage. Cancer Sci. 2005;96(2):134-41.
30. Stiff T, O'Driscoll M, Rief N, Iwabuchi K, Lobrich M, Jeggo PA. ATM and DNA-PK function redundantly to phosphorylate H2AX after exposure to ionizing radiation. Cancer Res. 2004;64(7):2390-6.
31. Agrawal A, Schatz DG. RAG1 and RAG2 form a stable postcleavage synaptic complex with DNA containing signal ends in V(D)J recombination. Cell. 1997;89(1):43-53.
32. Tsai CL, Drejer AH, Schatz DG. Evidence of a critical architectural function for the RAG proteins in end processing, protection, and joining in V(D)J recombination. Genes Dev. 2002;16(15):1934-49. PMCID: 186421.
33. Giblin W, Chatterji M, Westfield G, Masud T, Theisen B, Cheng HL, et al. Leaky severe combined immunodeficiency and aberrant DNA rearrangements due to a hypomorphic RAG1 mutation. Blood. 2009;113(13):2965-75. PMCID: 2662642.
34. Bredemeyer AL, Sharma GG, Huang CY, Helmink BA, Walker LM, Khor KC, et al. ATM stabilizes DNA double-strand-break complexes during V(D)J recombination. Nature. 2006;442(7101):466-70.
35. Rooney S, Alt FW, Sekiguchi J, Manis JP. Artemis-independent functions of DNA-dependent protein kinase in Ig heavy chain class switch recombination and development. Proc Natl Acad Sci U S A. 2005;102(7):2471-5. PMCID: 548986.
36. Sekiguchi J, Ferguson DO, Chen HT, Yang EM, Earle J, Frank K, et al. Genetic interactions between ATM and the nonhomologous end-joining factors in genomic stability and development. Proc Natl Acad Sci U S A. 2001;98(6):3243-8. PMCID: 30638.
37. Riballo E, Kuhne M, Rief N, Doherty A, Smith GC, Recio MJ, et al. A pathway of double-strand break rejoining dependent upon ATM, Artemis, and proteins locating to gamma-H2AX foci. Mol Cell. 2004;16(5):715-24.
38. Poinsignon C, de Chasseval R, Soubeyrand S, Moshous D, Fischer A, Hache RJ, et al. Phosphorylation of Artemis following irradiation-induced DNA damage. Eur J Immunol. 2004;34(11):3146-55.
39. Weterings E, Verkaik NS, Bruggenwirth HT, Hoeijmakers JH, van Gent DC. The role of DNA dependent protein kinase in synapsis of DNA ends. Nucleic Acids Res. 2003;31(24):7238-46. PMCID: 291856.
40. Gottlieb TM, Jackson SP. The DNA-dependent protein kinase: requirement for DNA ends and association with Ku antigen. Cell. 1993;72(1):131-42.
41. Meek K, Dang V, Lees-Miller SP. DNA-PK: the means to justify the ends? Adv Immunol. 2008;99:33-58.

42. Helmink BA, Bredemeyer AL, Lee BS, Huang CY, Sharma GG, Walker LM, et al. MRN complex function in the repair of chromosomal Rag-mediated DNA double-strand breaks. J Exp Med. 2009;206(3):669-79. PMCID: 2699138.
43. Theunissen JW, Kaplan MI, Hunt PA, Williams BR, Ferguson DO, Alt FW, et al. Checkpoint failure and chromosomal instability without lymphomagenesis in Mre11(ATLD1/ATLD1) mice. Mol Cell. 2003;12(6):1511-23.
44. Kang J, Ferguson D, Song H, Bassing C, Eckersdorff M, Alt FW, et al. Functional interaction of H2AX, NBS1, and p53 in ATM-dependent DNA damage responses and tumor suppression. Mol Cell Biol. 2005;25(2):661-70. PMCID: 543410.
45. Deriano L, Stracker TH, Baker A, Petrini JH, Roth DB. Roles for NBS1 in alternative nonhomologous end-joining of V(D)J recombination intermediates. Mol Cell. 2009;34(1):13-25. PMCID: 2704125.
46. Dinkelmann M, Spehalski E, Stoneham T, Buis J, Wu Y, Sekiguchi JM, et al. Multiple functions of MRN in end-joining pathways during isotype class switching. Nat Struct Mol Biol. 2009;16(8):808-13. PMCID: 2721910.
47. Rass E, Grabarz A, Plo I, Gautier J, Bertrand P, Lopez BS. Role of Mre11 in chromosomal nonhomologous end joining in mammalian cells. Nat Struct Mol Biol. 2009;16(8):819-24.
48. Xie A, Kwok A, Scully R. Role of mammalian Mre11 in classical and alternative nonhomologous end joining. Nat Struct Mol Biol. 2009;16(8):814-8. PMCID: 2730592.
49. Gao Y, Sun Y, Frank KM, Dikkes P, Fujiwara Y, Seidl KJ, et al. A critical role for DNA end-joining proteins in both lymphogenesis and neurogenesis. Cell. 1998;95(7):891-902.
50. Gao Y, Ferguson DO, Xie W, Manis JP, Sekiguchi J, Frank KM, et al. Interplay of p53 and DNA-repair protein XRCC4 in tumorigenesis, genomic stability and development. Nature. 2000;404(6780):897-900.
51. Della-Maria J, Zhou Y, Tsai MS, Kuhnlein J, Carney JP, Paull TT, et al. Human Mre11/human Rad50/Nbs1 and DNA ligase IIIalpha/XRCC1 protein complexes act together in an alternative nonhomologous end joining pathway. J Biol Chem. 2011;286(39):33845-53. PMCID: 3190819.
52. Wang JH, Gostissa M, Yan CT, Goff P, Hickernell T, Hansen E, et al. Mechanisms promoting translocations in editing and switching peripheral B cells. Nature. 2009;460(7252):231-6. PMCID: 2907259.
53. Dominguez-Sola D, Ying CY, Grandori C, Ruggiero L, Chen B, Li M, et al. Non-transcriptional control of DNA replication by c-Myc. Nature. 2007;448(7152):445-51.
54. Petermann E, Helleday T. Pathways of mammalian replication fork restart. Nat Rev Mol Cell Biol. 2010;11(10):683-7.
55. Yeo JE, Lee EH, Hendrickson E, Sobeck A. CtIP mediates replication fork recovery in a FANCD2-regulated manner. Hum Mol Genet. 2014.
56. Bruhn C, Zhou ZW, Ai H, Wang ZQ. The essential function of the MRN complex in the resolution of endogenous replication intermediates. Cell Rep. 2014;6(1):182-95.

57. Bartkova J, Horejsi Z, Koed K, Kramer A, Tort F, Zieger K, et al. DNA damage response as a candidate anti-cancer barrier in early human tumorigenesis. Nature. 2005;434(7035):864-70.
58. Gupta GP, Vanness K, Barlas A, Manova-Todorova KO, Wen YH, Petrini JH. The Mre11 complex suppresses oncogene-driven breast tumorigenesis and metastasis. Mol Cell. 2013;52(3):353-65. PMCID: 3902959.
59. Powell E, Piwnica-Worms D, Piwnica-Worms H. Contribution of p53 to Metastasis. Cancer Discov. 2014;4(4):405-14.
60. Kenneth Murphy PT, Mark Walport. Janeway's Immunobiology. Lawrence E, editor: Garland Science, Taylor & Francis Group; 2008.
61. Osborne CS, Chakalova L, Mitchell JA, Horton A, Wood AL, Bolland DJ, et al. Myc dynamically and preferentially relocates to a transcription factory occupied by Igh. PLoS Biol. 2007;5(8):e192. PMCID: 1945077.
62. Lin CY, Loven J, Rahl PB, Paranal RM, Burge CB, Bradner JE, et al. Transcriptional amplification in tumor cells with elevated c-Myc. Cell. 2012;151(1):56-67. PMCID: 3462372.
63. Valovka T, Schonfeld M, Raffeiner P, Breuker K, Dunzendorfer-Matt T, Hartl M, et al. Transcriptional control of DNA replication licensing by Myc. Sci Rep. 2013;3:3444. PMCID: 3853707.
64. Lobke C, Laible M, Rappl C, Ruschhaupt M, Sahin O, Arlt D, et al. Contact spotting of protein microarrays coupled with spike-in of normalizer protein permits time-resolved analysis of ERBB receptor signaling. Proteomics. 2008;8(8):1586-94.
65. Liyanage M, Weaver Z, Barlow C, Coleman A, Pankratz DG, Anderson S, et al. Abnormal rearrangement within the alpha/delta T-cell receptor locus in lymphomas from Atm-deficient mice. Blood. 2000;96(5):1940-6.
66. Stark GR, Wahl GM. Gene amplification. Annu Rev Biochem. 1984;53:447-91.
67. Celli GB, Denchi EL, de Lange T. Ku70 stimulates fusion of dysfunctional telomeres yet protects chromosome ends from homologous recombination. Nat Cell Biol. 2006;8(8):885-90.
68. Cesare AJ, Hayashi MT, Crabbe L, Karlseder J. The telomere deprotection response is functionally distinct from the genomic DNA damage response. Mol Cell. 2013;51(2):141-55. PMCID: 3721072.
69. Takata M, Sasaki MS, Sonoda E, Morrison C, Hashimoto M, Utsumi H, et al. Homologous recombination and non-homologous end-joining pathways of DNA double-strand break repair have overlapping roles in the maintenance of chromosomal integrity in vertebrate cells. EMBO J. 1998;17(18):5497-508. PMCID: 1170875.
70. King JS, Valcarcel ER, Rufer JT, Phillips JW, Morgan WF. Noncomplementary DNA double-strand-break rejoining in bacterial and human cells. Nucleic Acids Res. 1993;21(5):1055-9. PMCID: 309262.
71. Beucher A, Birraux J, Tchouandong L, Barton O, Shibata A, Conrad S, et al. ATM and Artemis promote homologous recombination of radiation-induced DNA double-strand breaks in G2. EMBO J. 2009;28(21):3413-27. PMCID: 2752027.

72. Williams RS, Moncalian G, Williams JS, Yamada Y, Limbo O, Shin DS, et al. Mre11 dimers coordinate DNA end bridging and nuclease processing in double-strand-break repair. Cell. 2008;135(1):97-109. PMCID: 2681233.
73. Hopfner KP, Craig L, Moncalian G, Zinkel RA, Usui T, Owen BA, et al. The Rad50 zinc-hook is a structure joining Mre11 complexes in DNA recombination and repair. Nature. 2002;418(6897):562-6.
74. Hopfner KP, Karcher A, Craig L, Woo TT, Carney JP, Tainer JA. Structural biochemistry and interaction architecture of the DNA double-strand break repair Mre11 nuclease and Rad50-ATPase. Cell. 2001;105(4):473-85.
75. Manis JP, Morales JC, Xia Z, Kutok JL, Alt FW, Carpenter PB. 53BP1 links DNA damage-response pathways to immunoglobulin heavy chain class-switch recombination. Nat Immunol. 2004;5(5):481-7.
76. Difilippantonio S, Gapud E, Wong N, Huang CY, Mahowald G, Chen HT, et al. 53BP1 facilitates long-range DNA end-joining during V(D)J recombination. Nature. 2008;456(7221):529-33. PMCID: 3596817.
77. Lee JH, Goodarzi AA, Jeggo PA, Paull TT. 53BP1 promotes ATM activity through direct interactions with the MRN complex. EMBO J. 2010;29(3):574-85. PMCID: 2830698.
78. Kuppers R, Dalla-Favera R. Mechanisms of chromosomal translocations in B cell lymphomas. Oncogene. 2001;20(40):5580-94.

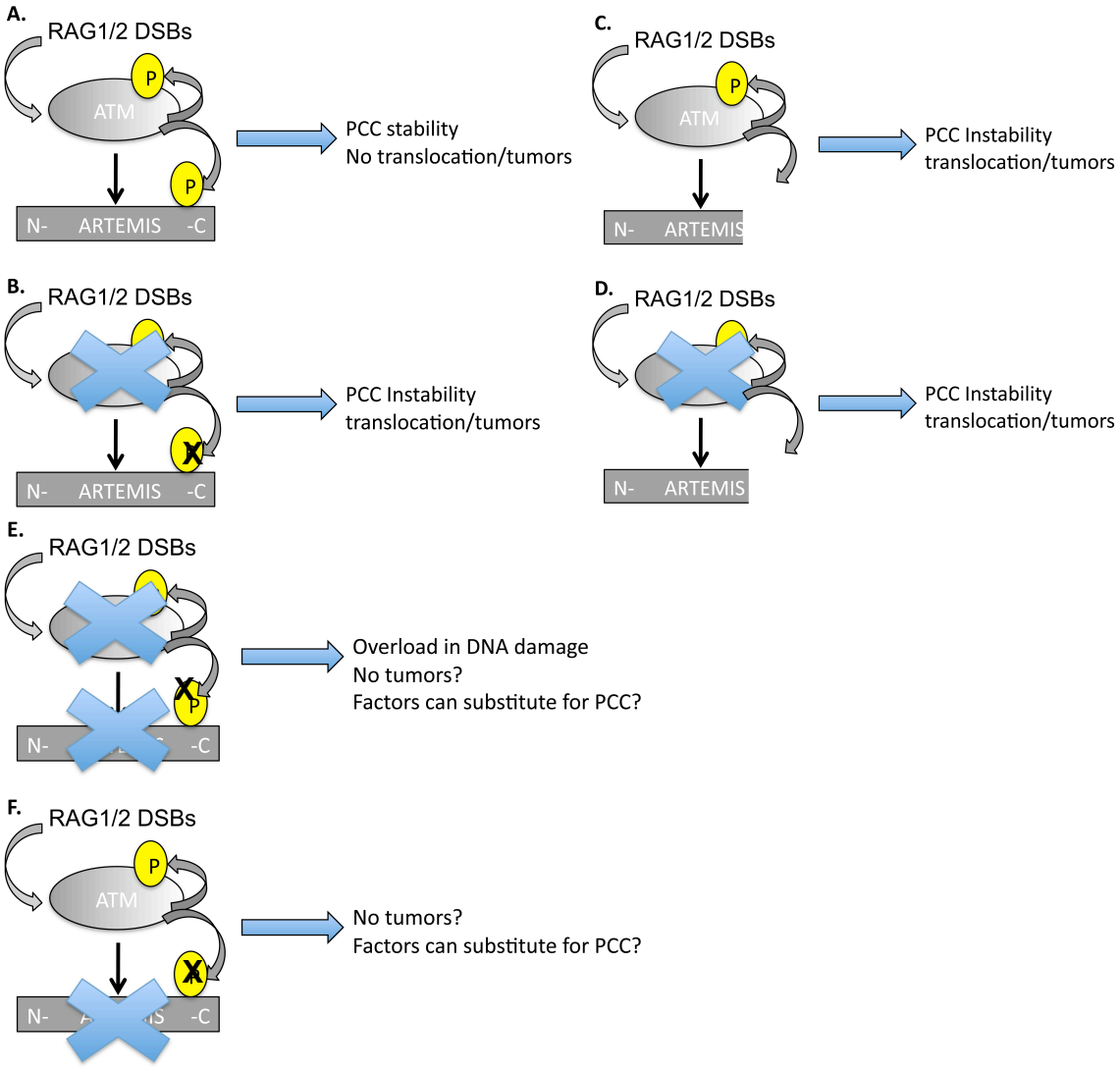

Figure 5.1 Schematic representations of possible outcomes due to ATM or combined ART-P70/ATM mutations. Diagrammed above are my anticipated results if ATM-mediated phosphorylation of ARTEMIS facilitates PCC stability. **(A)** PCC is stabilized due to WT activity of ARTEMIS and ATM **(B)** ATM kinase activity is abrogated and results in destabilization of the PCC and I hypothesize this is due, in part, to abrogated phosphorylation of the ARTEMIS C-terminus by ATM **(C)** Situation when the ARTEMIS C-terminus is truncated (P70 mutation) and results in PCC destabilization and I hypothesize this is due to the absence of the ATM-dependent phosphorylation site necessary to support PCC stabilization **(D)** ATM/ART-P70 double mutation situation that would result in PCC destabilization implicating ATM and the ARTEMIS C-terminus in PCC stabilization (perhaps via ATM-dependent phosphorylation of the ARTEMIS C-terminus) **(E)** ATM/ART-P70 double mutation situation where an additional factor(s) can substitute for PCC stability and the double mutation does not result in PCC destabilization, perhaps due to DNA damage overload **(F)** *Artemis*$^{-/-}$

situation where I hypothesize *Artemis*$^{-/-}$ cells do not exhibit PCC destabilization because additional factors can substitute.